Thermal Modeling of Phase Change Solidification in Thermal Control Devices Including Natural Convection Effects

CSM-CPR-R372

(NASA-CR-129910) THERMAL MODELING OF PHASE CHANGE SOLIDIFICATION IN THERMAL CONTROL DEVICES INCLUDING NATURAL A.O. Ukanwa, et al (Colorado School of Mines) 26 Jan. 1972 119 p CSCL 07D

N73-13132

Unclas G3/06 16588

Chemical and Petroleum-Refining Engineering Department
Colorado School of Mines
Golden, Colorado 80401

Preface

This work was prepared by Colorado School of Mines, Golden, Colorado, under Contract NAS 8-30511, Mod. 2, "Research in Phase Change Thermal Control Technology" and under Colorado School of Mines Foundation Contracts F-6911 and F-6915. The work was administered under the direction of the Space Sciences Laboratory, George C. Marshall Space Flight Center, with Miss Barbara Richard acting as the contracting officers' technical representative.

This report covers work from 21 Nov. 1970 to 31 Dec. 1971.

The work at Colorado School of Mines was carried out by A. O. Ukanwa under the direction of F. J. Stermole and J. O. Golden, principle investigators.

ABSTRACT

The goal of this investigation was to contribute to the understanding of natural convection effects in phase change thermal control devices. This goal was accomplished by developing a mathematical model to evaluate natural convection effects in a phase change test cell undergoing solidification and then evaluating the model against experimental data. Although natural convection effects would be minimized in flight spacecraft, all phase change devices would be ground tested and thus understanding the effect of natural convection on such devices and the ability to predict ground-based system thermal performance become quite important.

The mathematical approach to the problem was to first develop a transient two-dimensional conduction heat transfer model for the solidification of a normal paraffin of finite geometry. Next, a transient two-dimensional model was developed for the solidification of the same paraffin by a combined conduction-natural-convection heat transfer model. Throughout the study, n-hexadecane ($n\text{-}C_{16}H_{34}$) was used as the phase-change material in both the theoretical and the experimental work. The models were based on the transient two-dimensional finite difference solutions of the energy, continuity, and momentum equations. The convection model

assumed incompressible flow except as modified in the gravity terms in the equations of motion.

An experimental system was set up to verify the theoretical analyses and results. The system consisted of a closed rectangular box inclined at various angles from the horizontal plane, and cooled from below. The box was completely filled with n-hexadecane ($n\text{-}C_{16}H_{34}$), a long-chain paraffin.

Gravity levels were calculated, depending on the angle of inclination of the test cell. Temperatures in various parts of the cell were recorded by 24 thermocouples as functions of elapsed time from the start of the experiments. Comparisons were made between experimental results and computer-calculated theoretical results.

Heat transfer when the cell was in the horizontal plane was by conduction. With the cell inclined at various angles, the heat transfer rate was increased due to combined conduction-convection heat transfer. The cell was generally cooled below the conduction temperatures, when convection was also present. The shape of the phase interface between the liquid and the solid phases was also changed from a flat plane to a curved surface by convection. One half of the test cell was cooled faster than the other half, during convective cooling. Convection was found to be an important parameter in the solidification process.

Remarkably good agreement was obtained between experimental data for solidification with conduction heat transfer and calculated results from the theoretical transient two-dimensional conduction-heat-transfer model. Close agreement was also obtained between experimental data for solidification with the test cell inclined at various angles and the theoretical results from the transient two-dimensional conduction-natural-convection heat transfer model. The trend of the effect of convection on the system was clearly revealed by both the experimental and the theoretical results.

Stability problems were encountered in the finite-difference solutions of the theoretical heat-transfer models. Central differences were used to eliminate the dependence of the finite-difference time step on the unknown velocity components in the convection equations which would have occurred if forward or backward differences had been used. Maximum allowable velocities were severely restricted by stability requirements of the finite differences, so that we could not use as high velocities as we would have liked to in the solutions of the convection-temperature equations. In addition to these restrictions, more severe restrictions on the magnitude of a time step were imposed by the need to minimize errors due to numerical dispersion on the theoretical results from the natural convection model. Numerical dispersion error terms, introduced by the neglect of second-order time derivatives in the central difference approximations of the boundary layer energy equations, could not be eliminated entirely, but they were minimized to less than 10 percent by the use of very small time-steps.

This study is a first attempt to model the effects of natural convection on a solidifying system with moving boundaries. It is also a good basis for further, more rigorous analyses in which the energy, momentum and continuity equations may be solved completely.

CONTENTS

LIST OF TABLES

LIST OF FIGURES

INTRODUCTION

Phase-change phenomena have received wide scientific attention for some time and are of significant importance in many technical problems such as solidification of a billet, formation of snow, solidification of an asphalt layer, melting of alloys and growth of crystals. Recently, phase-change materials have been seriously considered for spacecraft thermal control. In concept, such materials would be used in passive systems employing the process of melting or solidification to remove or add themal energy from or to a system. Thermal control systems based on solid-liquid phase change have many advantages which make them useful for certain applications. They are light, easy to handle, and easily used as wall-lining elements around electronic equipment.

When a phase-change thermal control material goes from the solid to the liquid phase or vice versa, convection currents may be set up in the liquid phase by temperature gradients in the system. These temperature gradients affect the density of the material and hence the force of gravity on it. Thus, the resultant convection is known as gravity-induced or natural convection. It is not a forced convection since no initial bulk flow is forced on the system.

The present investigation was aimed at studying the effect and importance of such natural convection currents on the rate of solidification, temperature profiles and the shape of the interface of a phase-change material, n-hexadecane ($n\text{-}C_{16}H_{34}$), a normal long-chain paraffin that is liquid at normal room temperatures. It was hoped that the investigation would help reveal any influence of natural convection on the ability of such a phase-change material to control the temperature of an instrument around which it is packaged. If convection increased heat transfer remarkably, a decision would have to be made as to the suitability of using such a material in the liquid phase for thermal control.

LITERATURE SURVEY

Much theoretical work has been presented in the literature dealing with problems which are related to physical change of state. The basic feature of such problems is the existence of a moving boundary or surface between phases. Therefore, the problem that is most often considered is how to determine the way in which this surface or boundary moves. Heat may be liberated or absorbed on the boundary; there may be a volume change accompanying the change of state, and the thermal properties of the phases on either side of the interface may be different for the phases and may vary as the change of state proceeds. Therefore, the problem is non-linear in nature and general analytical solutions for it are not available. Some exact solutions for models that mathematically approximate the real problems have been obtained, mostly for infinite or semi-infinite geometry.

Carslaw and Jaeger[1] were among the first to give in-depth treatment of melting and solidification problems. They commented on the need to use numerical and finite-difference methods in solving many of the complex problems that arise in finite geometric configurations.

Many of the solutions presented in the literature of phase-change problems are valid only if the material

under study is initially at its equilibrium temperature for change of state. They ignore the most frequently encountered case in which the material under study is initially at a temperature quite different from the phase-change temperature.

Stefan[2] was the first to give a published discussion of a one-dimensional transient conduction problem with phase change, for a single component or eutectic composition with constant properties. Thus, the term "Stefan's Problem" came to be used to describe a one-dimensional conduction problem in which a semi-infinite slab initially at a constant non-zero temperature, has one face maintained at zero temperature for time greater than zero. The solution to the problem entailed the assumption that the time-dependent interface position was proportional to the square root of the product of time and the thermal diffusivity of the material of the slab.

Danckwerts[3], Booth[4], and Kreith and Romie[5] have all presented analytical or semi-analytical solutions to phase-change problems under various boundary and initial conditions. Chao and Weiner[6] investigated the temperature in a solid-liquid system while the liquid was being poured. The latent heat of phase change was treated as a "pseudo"-specific heat and the solution, obtained by a Laplace transform technique was an integral that was solved numerically.

Many authors used the variational technique to solve heat transfer problems, with or without a phase change. Chambers[7], Biot and Daughaday[8] used this approach. Biot and Daughaday studied an ablation problem in which the melt was removed as it was formed.

The heat-balance-integral technique, an analytical method that gives approximate solutions to a wide variety of heat transfer problems, is used in many papers in the literature. It is mostly used to solve non-linear problems that must be solved numerically or approximately. Its big advantage is that it changes an energy equation from a partial differential equation to an ordinary differential equation. One disadvantage of this method is that the solutions obtained satisfy the differential equations only on the average. Goodman[9] and Poots[10] have used this method to study heat transfer problems. Poots studied the two-dimensional inward solidification of a uniform prism initially at the fusion temperature.

In the study of more general cases of phase-change problems, numerical analysis may be the only feasible technique available. Dusinberre[11], Pujado[12], Ukanwa, Stermole and Golden[13] have all used finite-difference techniques to study phase-change problems in which the heat transfer mode is by conduction only.

Miller[14] used the "surplus temperature" technique

in an attempt to improve the predictions of the phase front. To account for the heat absorbed at the phase front, the calculated temperature was permitted to exceed the actual melting temperature until an arbitrarily selected temperature was reached. When this temperature was reached, the grid element containing this particular nodal point was considered to have changed phase, and the phase front was shifted to the next node.

Ehrlich[15] gave the implicit finite-difference equations for the one-dimensional melting problem with a variable heat input specified as a function of time. The implicit equations were then put into tridiagonal matrix forms for easy solution by Gauss elimination and by back-substitution. Special modified equations were given for nodes near the freezing front.

The Northrop Corporation reports[16, 17] presented a survey of the phase-change problems involving selection of the proper compounds for phase-change thermal control devices, evaluation of properties, and experimental study of different test cells. Some of the physical properties used in the present study on n-hexadecane have been taken from these reports.

Other works on phase-change phenomena include Bannister and Bentilla[18], Grodzka and Fan[19], and Chambre[20]. A survey of many papers on phase-change phenomena has been

presented by Muehlbauer and Sunderland.[21]

Convection in enclosed fluids has been studied extensively. Unfortunately, most of the studies have been either only experimental with no attempt at theoretical modeling or only theoretical with no experimental corroboration. In addition, the majority of the studies on convection deal with flat or parallel plates and on gases. The works that do deal with completely-enclosed liquids often have theoretical solutions that hardly, if ever, approximate real situations closely.

Some good texts for theoretical references on heat transfer and fluid flow are Rohsenow and Choi[22], Schlichting[23], Longwell[24], and Bird, Stewart and Lightfoot[25]. The last two references were used as the references for developing the basic boundary-layer equations for gravity-induced convection in the present study.

Wilkes and Churchill[26] studied temperature profiles in an enclosed rectangular cavity subject to adverse temperature gradients. Their equations for gravity-induced free convection were developed from the basic equations of continuity, motion and energy. The resultant system of equations was solved by an implicit alternating-direction technique developed by Peaceman and Rachford.[27]

Chandrasekhar[28] gave an extensive treatment of stability and instability in fluids subject to adverse

temperature, gravity and magnetic effects. The method used by Pellew and Southwell[29] to linearize temperature and velocity equations was also discussed. It involved the solution by the separation-of-variables technique, the equations of continuity, momentum and energy in order to determine the critical Rayleigh number ($gh^3\Delta d_L/\lambda_L \nu \bar{d}_L$) necessary to initiate free convection in a fluid heated from below. The method assumed that motion in fluids heated from below was cellular and involved finite numbers of rolls corresponding to particular wave numbers.

Leont'ev and Kirdyashkin[30] studied convection in fluids of large volumes. They assumed that, except in the boundary layer which was very small relative to the dimensions of the fluid, motion was by ideal flow. However, the maximum velocity occurred in the boundary layer, near the walls, where the temperature gradient or heat flux was largest. This ideal-flow approximation for natural convection in completely enclosed fluids has been used by other authors. The velocity profiles used in the present study assumed ideal flow profiles similar to their models. This approach was necessitated by the difficulty in satisfying all no-slip conditions on rigid boundaries of completely enclosed fluids.

Bain[31] performed a two-dimensional experimental study of gravity-induced convection in an enclosed liquid

in a rectangular cavity inclined at an angle from the horizontal plane. Solid-liquid phase change was also involved. Personal communication with Mr. Bain has revealed that he is presently involved in providing theoretical ideal-flow models to predict his experimental data.

THEORETICAL ANALYSIS

Formulation of the Problem

The physical problem to be studied is the solidification of normal hexadecane enclosed in a cell cavity of height h (initial height h_o) and constant square cross-sectional area of lateral dimension W. The cell is inclined at angle α degrees measured from the horizontal plane. The coordinate axes and their origin are located as shown in Figure 1 with x along the cold bottom plate and y perpendicular to it.

Some physical properties of the test material, n-hexadecane (n-$C_{16}H_{34}$), were taken from Reference 17:

Density

Solid n-hexadecane: $d_S = 1.0772 - 8.41 \times 10^{-4}\ T\ gm/cm^3$

for $T \leq 290.0^oK$

Liquid n-hexadecane: $d_L = 0.9726 - 6.813 \times 10^{-4}\ T\ gm/cm^3$

for $290.0^oK \leq T \leq 400.0^oK$

Specific Heat

Solid n-hexadeane: $c_{pS} = 0.505\ cal/(gm-^oK)$

for $T \leq 290.0^oK$

Liquid n-hexadecane: $c_{pL} = 0.1626 + 1.164 \times 10^{-3}\ T\ cal/(gm-^oK)$

for $290.0^oK \leq T \leq 480.0^oK$

Thermal Conductivity

Solid: $k_S = 2.390 \times 10^{-3} - 3.047 \times 10^{-6}\ T\ watt/(cm-^oK)$

FIGURE 1. A SECTION OF THE TEST CELL WITH COORDINATE SYSTEM INDICATED.

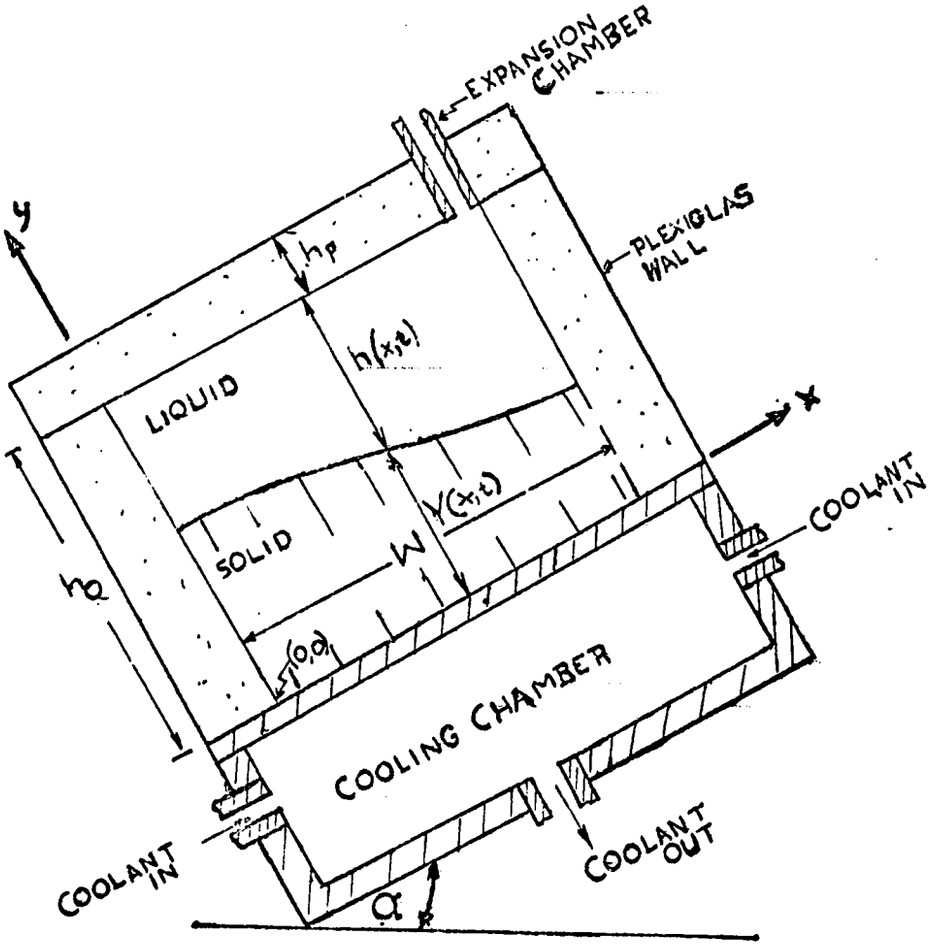

Liquid: $k_L = 2.390 \times 10^{-3} - 3.047 \times 10^{-6}$ T watt/(cm-°K)

for $250^{\circ}K \leq T \leq 425^{\circ}K$

Solidification temperature: $T_f = 290.0^{\circ}K = 16.7^{\circ}C$

Latent heat of solidification: $H_f = 56.67$ cal/gm

The cold bottom plate is maintained at temperature, $T(x,0,t) = f(t)$. The effects of natural convection, induced by density and temperature changes, on the solidification rate and the temperature profiles of the paraffin are to be studied as functions of time and angle (equivalent to changing gravity levels). By changing angle α, one may vary the components of the force of gravity acting on the system. Only density changes affecting the gravity term in the equations of motion are considered.

For this investigation, temperature-averaged properties are used. The following properties, obtained by experiment and from References 17, 32 and 33 are used:

$T_f = 290.66^{\circ}K$ (experiment)

$d_S = 0.833$ gm/cm^3 (experiment at $268.2^{\circ}K$)

$d_L = 0.755$ gm/cm^3 (experiment at $294.7^{\circ}K$)

d_P = density of plexiglas (material of cell wall)

$= 1.155$ gm/cm^3 (experiment at $298^{\circ}K$)

From Reference 17:

$\beta = -6.813 \times 10^{-4}$ gm/(cm^3-°K) (from $d_L = d_{Lo} + \beta T$)

$c_{pL} = 0.506$ cal/(gm-°K) (at $296.0^{\circ}K$, the average temperature encountered in the liquid phase)

c_{pS}= 0.505 cal/(gm-^{o}K)

k_S = 3.720 x 10^{-4} cal/(sec-cm-^{o}K) (at 280.2^{o}K, the average temperature encountered in the solid phase)

k_L = 3.555 x 10^{-4} cal/(sec-cm-^{o}K) (at 296.0^{o}K)

From Reference 32:

k_p = plexiglas thermal conductivity = 4.960 x 10^{-4} cal/(sec-cm-^{o}K)

c_{pp}= plexiglas specific heat = 0.35 cal/(gm-^{o}K)

From Reference 33:

ν = kinematic viscosity of n-hexadecane = 0.04 cm^2/sec

Prediction of the rate of solidification and the temperature profile of the test paraffin under a given set of initial and boundary conditions are to be made using (1) a conduction model and (2) a combined conduction-convection heat-transfer model. The following definitions are used: For a function f(x,y,t),

$$\delta f/\delta t = f_t \; ; \; \delta^2 f/\delta t^2 = f_{tt} \; ; \; \delta f/\delta x = f_x \; ; \; \delta^2 f/\delta x^2 = f_{xx} ;$$
$$\delta f/\delta y = f_y \; ; \; \delta^2 f/\delta y^2 = f_{yy} \; ; \; \delta^2 f/\delta x \delta y = f_{xy} \qquad (1)$$

$$Df/Dt = f_t + uf_x + vf_y \qquad (2)$$

With these definitions, we have

(1) Conduction Model ; temperature equations:

Liquid phase

$$T_t = \lambda_L (T_{xx} + T_{yy}) \text{ for } Y(x,t) < y \leq h_o \qquad (3)$$

$$T(x,Y,t) = T_f \qquad (i)$$

$$T(x,h_o+h_p,t) = T_a \qquad \text{(ii)}$$

$$T_x(0,y,t) = T_x(W,y,t) = 0 \qquad \text{(iii)}$$

$$T(x,y,0) = T_a \qquad \text{(iv)}$$

Solid phase

$$T_t = \lambda_S \ (T_{xx} + T_{yy}) \text{ for } 0 < y < Y(x,t) \qquad (4)$$

$$T(x,Y,t) = T_f \qquad \text{(i)}$$

$$T(x,0,t) = f(t) \qquad \text{(ii)}$$

$$T_x(0,y,t) = T_x(W,y,t) = 0 \qquad \text{(iii)}$$

$$T(x,y,0) = T_a \qquad \text{(iv)}$$

In Equations (3) and (4), T_a is ambient temperature, h_p is the thickness of the plexiglas wall of the test cell and $\lambda = k/(dc_p)$ is the thermal diffusivity of the test material. No equations of motion are involved in the conduction model.

(2) Combined Conduction-Convection Model

Temperature equations:

Solid phase:- Equations (4) apply.

Liquid phase

$$DT/Dt = \lambda_L \ (T_{xx} + T_{yy}) \qquad (5)$$

Viscous heating is negligible. The boundary conditions (i) to (iv) of Equation (3) apply here also.

Equation of Continuity:

$$u_x + v_y = 0 \qquad (6)$$

for an incompressible fluid.

Equations of Motion:-

The Navier-Stokes' equations of motion for an incompressible fluid are

$$d_L \, Du/Dt = d_L \nu \, (u_{xx} + u_{yy}) - P_x - d_L g \sin \alpha \qquad (7a)$$

$$d_L \, Dv/Dt = d_L \nu \, (v_{xx} + v_{yy}) - P_y - d_L g \cos \alpha \qquad (7b)$$

Velocity components u and v are each zero at each of the walls, $x = 0$, $x = W$, $y = 0$, and $y = h_o$. At time $t = 0$, velocities are also equal to zero.

The temperature equations for both liquid and solid phases are coupled by an interface equation for phase change involving enthalpy change during solidification. This is true for both models: conduction and combined conduction-convection models. The proper phase-change equation will be discussed later.

Equations (7) may be modified as follows. Let $P = \bar{P} + p$, where $\bar{P}$ is the value of the pressure in the test cell when there is no motion. Also, $\bar{T}$ and $\bar{d}_L$ are the values of temperature and the density of the test material (liquid) when there is no motion. When there is no motion, Equations (7) become

$$0 = - \bar{P}_x - \bar{d}_L g \sin \alpha \qquad (7'a)$$

$$0 = - \bar{P}_y - \bar{d}_L g \cos \alpha \qquad (7'b)$$

When Equation (7'a) is subtracted from Equation (7a), and

(7'b) from (7b), the following modified equations are obtained for gravity-induced natural convection as a result of temperature-caused density variations in the test material.

$$Du/Dt = \nu (u_{xx} + u_{yy}) - p_x/\bar{d}_L - \frac{\beta g (T-\bar{T})}{\bar{d}_L} \sin \alpha \qquad (8a)$$

$$Dv/Dt = \nu (v_{xx} + v_{yy}) - p_y/\bar{d}_L - \frac{\beta g (T-\bar{T})}{\bar{d}_L} \cos \alpha \qquad (8b)$$

where $\beta(T-\bar{T}) = d_L - \bar{d}_L$. Equations (8) include the effect of the angle of inclination of the test cell from the horizontal plane. Thus the normal gravity level is modified by the angle, α.

Equations (8) may be further modified as follows: Let a stream function, $\varphi(x,y,t)$, be defined by the two equations

$$u = -\varphi_y \qquad (9a)$$

$$v = \varphi_x \qquad (9b)$$

Thus, Equations (9) automatically satisfy the continuity equation (6). Define a vorticity, $\omega(x,y,t)$, by the two identical equations

$$\omega = v_x - u_y \qquad (10a)$$

$$\omega = \varphi_{xx} + \varphi_{yy} \qquad (10b)$$

Differentiate Equation (8b) with respect to x and Equation (8a) with respect to y, and subtract the result of the later operation from the result of the former. The resultant

equation becomes, on the application of Equation (6) and Equation (10):

$$D\omega/Dt = \nu(\omega_{xx} + \omega_{yy}) + \frac{\beta g}{\bar{d}_L}\left((T-\bar{T})_y \sin\alpha - (T-\bar{T})_x \cos\alpha\right) \quad (11)$$

Thus, Equation (11) replaces Equations (8) as the equation of motion. The pressure terms drop out of the equations.

As is shown in Appendix C, limitations imposed by stability criteria for stable solutions by finite-difference approximations of Equations (5) and (11) or (5) and (8) simultaneously could not be satisfied within the limitations of digital-computer time and memory available to us. In order to get meaningful results from these full equations of motion and temperature, one would have to use very small time and space grid elements, values that are too small to allow for the acquisition of meaningful theoretical data within the time and memory limitations permitted to these investigators by the university computer center.

Therefore, the approach to be used to obtain approximate solutions of Equations (5) and (8) is to use approximate velocity profiles obtained by combining an ideal-flow model with a viscous-flow model.

Approximate Velocity Profiles

Assume that $(T-\bar{T})_x$ is negligible, compared to $(T-\bar{T})_y$.

(a) Ideal-flow Model (Maintained Convection)

Let $T-\bar{T} = c\,u(x,y,t)$ where c is a constant, and let $\omega = -q\,\varphi(x,y,t)$ where q is a characteristic constant. Also, assume that $\varphi(x,y,t)$ is separable into a product of functions of x, y and t. From Equation (11), we get

$$\varphi_t = \nu(\varphi_{xx} + \varphi_{yy}) + \frac{\beta g c}{q\bar{d}_L}\,\varphi_{yy}\sin\alpha \qquad (12)$$

with initial and boundary conditions,

$$\varphi(0,y,t) = \varphi(W,y,t) = \varphi(x,0,t) = \varphi(x,h,t) \qquad (13)$$

When Equation (12) is solved by the separation-of-variables method, we get

$$\varphi_{n,m} = A_{n,m}\sin\frac{(2n+1)\pi x}{W}\sin\frac{(2m+1)\pi y}{h}\,e^{-\nu t\left(q+\frac{\pi^2(2m+1)^2\beta g c}{q\bar{d}_L\nu h^2}\right)}$$

where $q = \pi^2\left(\frac{(2n+1)^2}{W^2} + \frac{(2m+1)^2}{h^2}\right)$, $m=0,1,2,\ldots$; $n=0,1,2,\ldots$ (14)

For maintained motion (independent of time), the exponent in the exponential term is zero, that is

$$c = -\frac{\bar{d}_L\,\nu\,q^2h^2}{\pi^2(2m+1)^2\beta g} \qquad (15)$$

When Equation (15) is put into Equation (14), we get

$$\varphi_{n,m} = A_{n,m}\sin\frac{(2n+1)\pi x}{W}\sin\frac{(2m+1)\pi y}{h}, \qquad (16)$$

$$m=0,1,2,\ldots..;\ n=0,1,2,\ldots..$$

Equation (16) is analogous to the equation for the vibrations of a string in which q (Equation 14) gives the characteristic numbers corresponding to the modes. If n = m = 0, we

get a single circulation flow (one finite roll) in the test cell. If either n or m or both are not equal to zero, multiple rolls result. Figure 2 shows sketches of the rolls that would result for various values of m and n.

(b) Viscous-flow Model (First-order Kantorovich profile approximation by variational method).

Assume that $T-\bar{T} = y\Delta T_o/h$, where ΔT_o is the temperature difference between the hot plate at y = h and the cold plate at y = 0. Also, assume a steady-state solution and negligible pressure variation in Equation (8a). Therefore, Equation (8a), as modified, becomes

$$u_{xx} + u_{yy} - \frac{\beta g y \Delta T_o}{\bar{d}_L \nu h} \sin \alpha = 0 \qquad (17)$$

Assume a profile, $\varphi = h(y/h - 2y^3/h^3 + y^4/h^4)\ X(x)$ (18)

where the profile has been made to satisfy in the y-direction the boundary conditions of Equation (13) for a stream function. From Equations (9a) and (18), we get

$$u = (1 - 6y^2/h^2 + 4y^3/h^3)\ X(x) \qquad (19)$$

The function X(x) is to be determined by variational technique and should satisfy the boundary conditions

$$X(0) = X(W) = 0 \qquad (20)$$

The appropriate equation for X(x) by variational method is

FIGURE 2. SKETCHES OF STREAMLINES $\varphi = A \sin\frac{(2m+1)\pi x}{w} \sin\frac{(2n+1)\pi y}{h}$ = CONSTANT

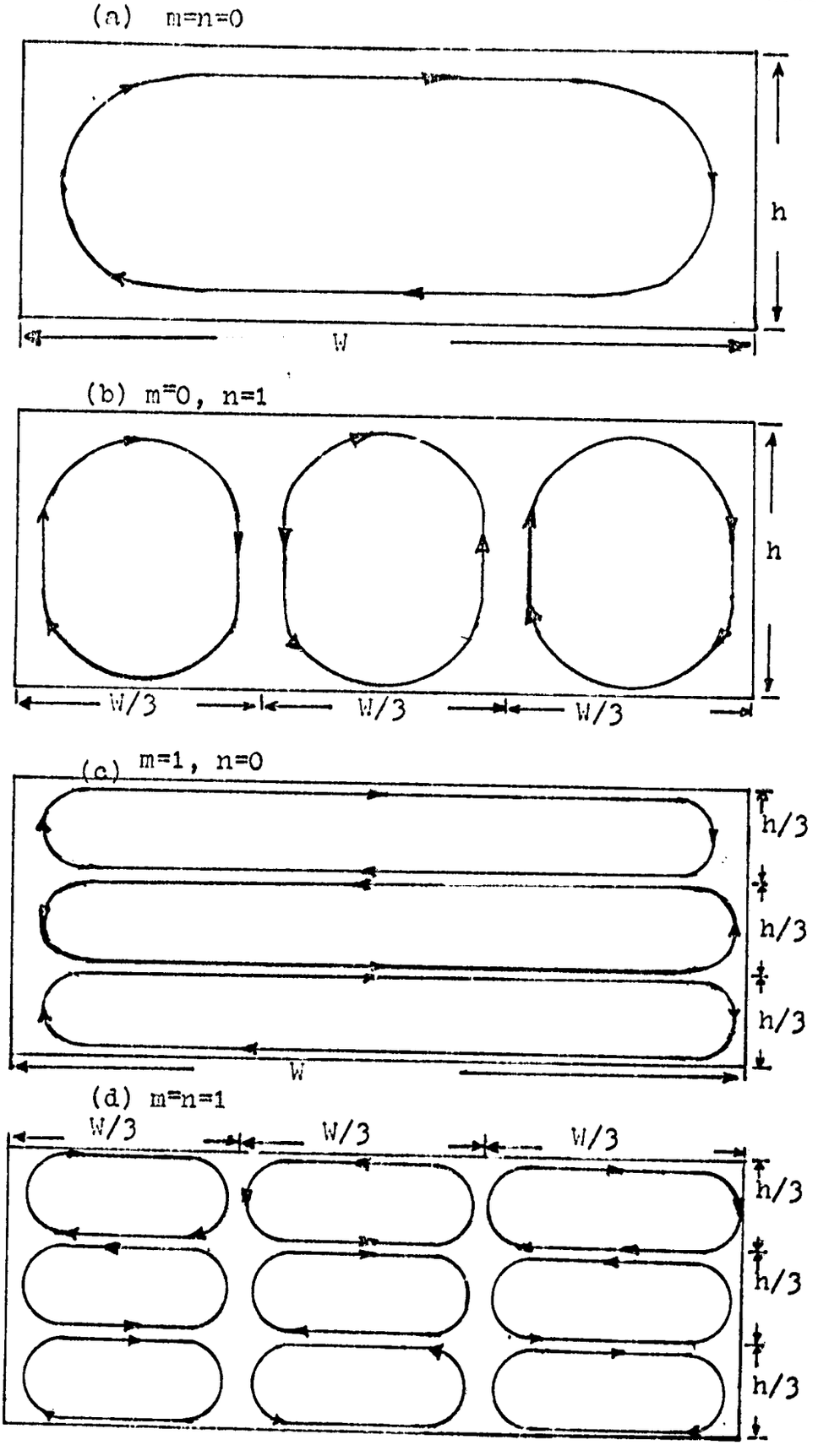

obtained by integrating the product of $1-6y^2/h^2+4y^3/h^3$ and Equation (17) with respect to y between y = 0 and y = h. The definition of Equation (19) for u is employed in the integration. The resulting equation for X(x) is

$$d^2X/dx^2 - (168/17h^2)\,X + \frac{7\beta g\Delta T_o}{17\,\bar{d}_L}\sin\alpha = 0 \qquad (21)$$

On solving Equation (21) with the boundary conditions of Equation (20), we get

$$X = \frac{\beta g h^2 \Delta T_o}{24\nu\bar{d}_L}\sin\alpha\left(1 - \frac{\sinh\gamma(W-x)+\sinh\gamma x}{\sinh\gamma W}\right) \qquad (22)$$

where $\gamma = \sqrt{(168/17)}\,/h$ (23)

Therefor, the first-order Kantorovich profiles are

$$u = -B(1-6y^2/h^2+4y^3/h^3)\left(1-\frac{\sinh\gamma(W-x)+\sinh\gamma x}{\sinh\gamma W}\right) \qquad (24a)$$

$$v = B\gamma h(y/h-2y^3/h^3+y^4/h^4)\left(\frac{\cosh\gamma(W-x)-\cosh\gamma x}{\sinh\gamma W}\right) \qquad (24b)$$

$$\varphi = Bh(y/h-2y^3/h^3+y^4/h^4)\left(1-\frac{\sinh\gamma(W-x)+\sinh\gamma x}{\sinh\gamma W}\right) \qquad (24c)$$

where $B = -\beta g h^2\Delta T_o \sin\alpha/(24\nu\bar{d}_L)$.

The stream function of Equation (24c) gives one finite roll (singlet flow). As it turned out, however, a single symmetric roll could not predict the experimental data in all

sections of the test cell. It could predict only one half of the test cell ($0<x<W/2$). Multiple rolls given by Equation (16) when at least one of m and n is not zero, do not predict the entire cell performance either.

Hence, a modified profile involving a combination of Equation (24c) and Equation (16) for $n = m = 0$ was used to get a single roll, non-symmetric in the x-direction, but symmetric in the y-direction. Equation (16), for $n = m = 0$, was allowed to apply for $0 \leq x \leq W'/2$, so that at $x = W'/2$,

$$v = 0; \text{ and } u = -A_{0,0}\frac{\pi}{h} \cos \frac{\pi}{h}y \qquad (25)$$

Equation (25) was obtained by applying Equation (9a) on Equation (16) and letting $x = W/2$. $W'/2$ must satisfy the relationship $2h \leq W'/2 \leq W$. The second portion of the stream function profile was obtained by using Equation (24c) in the range $W'/2 \leq x \leq W$. In addition, v from this profile was set equal to zero at $x = W'/2$ so that u for this part became

$$u = -B(1-6y^2/h^2+4y^3/h^3) \text{ at } x=W'/2 \qquad (26)$$

Equations (25) and (26) should yield the same values for u at $x=W'/2$. They both go to a maximum, a minimum and zero at the same points: $y/h = 1, 0, \frac{1}{2}$, respectively. Thus, the maximum value given by Equation (25) was set equal to the

maximum value given by Equation (26) to get $A_{0,C}=Bh/\pi$. Thus, the complete stream function that was used was

$$\varphi = \begin{cases} \frac{Bh}{\pi}\sin\frac{\pi x}{W'}\sin\frac{\pi y}{h}, & \text{for } 0 \leq x \leq W'/2 \\ Bh(y/h-2y^3/h^3+y^4/h^4)\left(1-\frac{\sinh \gamma(W-x)+\sinh \gamma(W+x-W')}{\sinh \gamma(2W-W')}\right), & \text{for } W'/2 \leq x \leq W \end{cases} \qquad (27)$$

Figure 3 shows graphs of u from Equation (25) and u from Equation (26) at the merging of the two portions of the stream function in Equation (27), that is, at $x = W'/2$.

For the present study, $W'/2$ was chosen as $0.95\ W$. So, the final form of the resultant stream function profile that was used in this study is

$$\varphi = \begin{cases} \frac{Bh}{\pi}\sin\frac{\pi x}{1.9W}\sin\frac{\pi y}{h}, & \text{for } 0 \leq x \leq 0.95\ W \\ Bh(y/h-2y^3/h^3+y^4/h^4)\left(1-\frac{\sinh \gamma(W-x)+\sinh \gamma(x-0.9\ W)}{\sinh 0.1\gamma W}\right), & \text{for } 0.95\ W \leq x \leq W \end{cases} \qquad (28)$$

The introduction of the definitions in Equation (9) into Equation (28) gives u and v. Hence, Equation (28) is used in the finite-difference solution of Equation (5) to obtain the convection temperature profiles in the liquid phase. Since the angle, α, appears only in the term B, Equation (28) indicates that the angle of inclination, α, affects

FIGURE 3. HORIZONTAL VELOCITIES, -u/B, AT COUPLING POINT, x=W'/2.

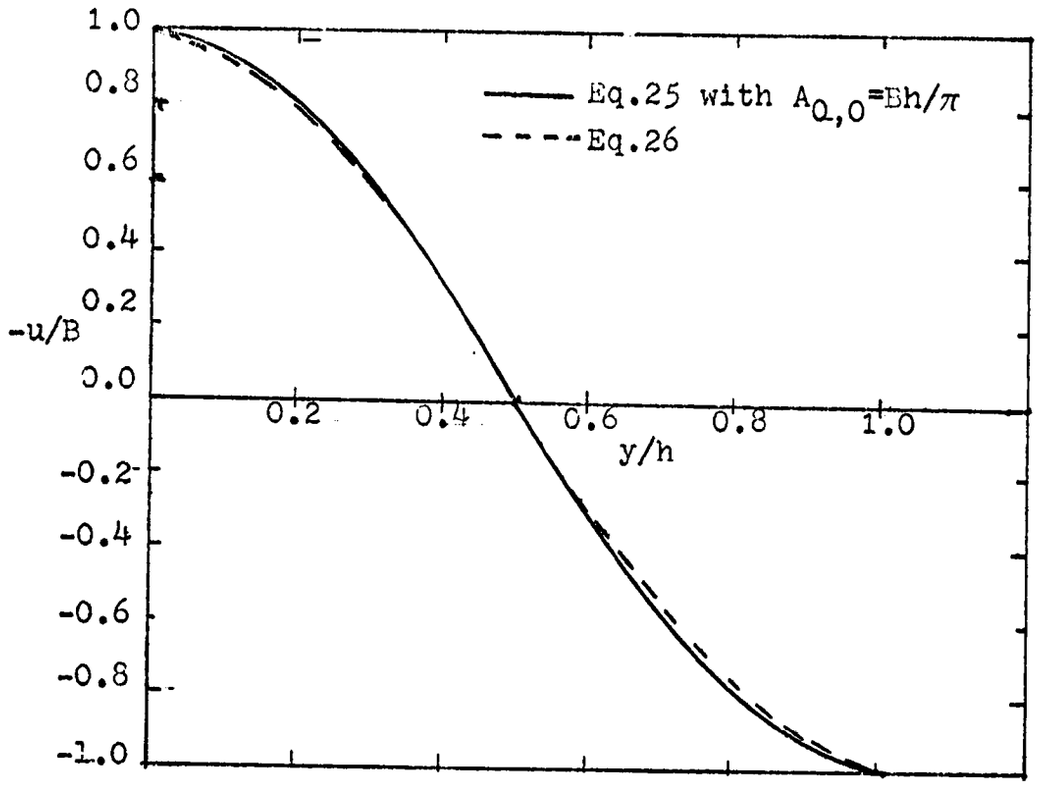

FIGURE 4. FINITE-DIFFERENCE GRID AND NODAL ARRANGEMENT

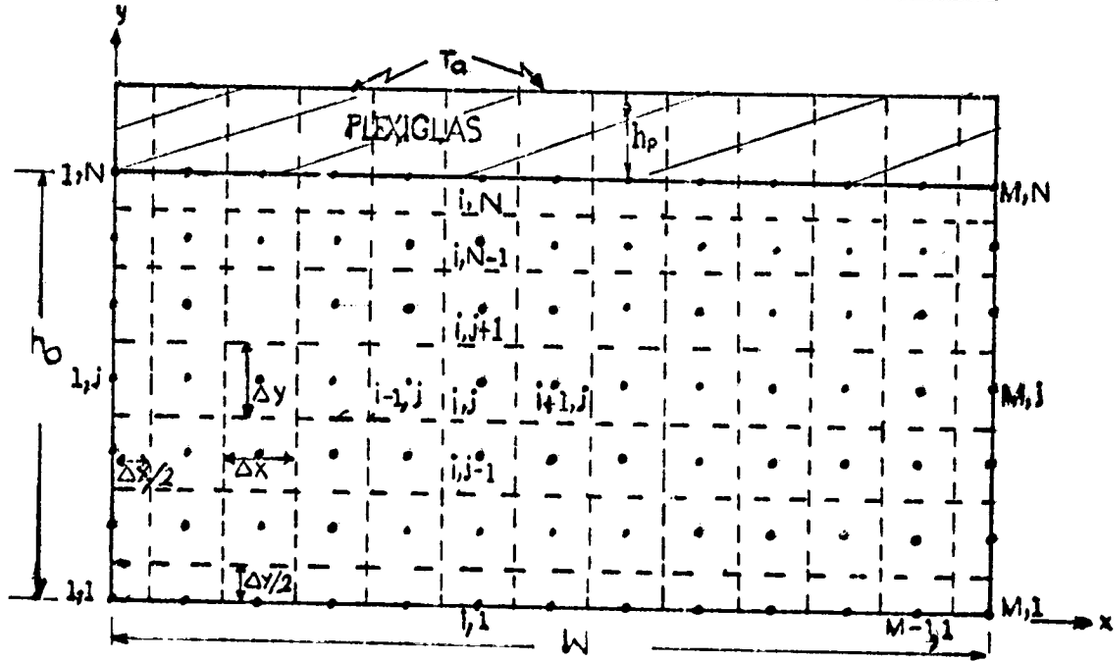

the magnitude of the velocities but not their shape. In Equation (28), h is the time-dependent height of the liquid phase which becomes smaller than the height h_o of the test cell cavity as solidification continues.

Finite-Difference Approximations of Governing Temperature Equations

The following definitions are used. Ignore third-order derivatives. Figure 4 explains the space-grid arrangement.

Central-difference approximations

$$\frac{T(i+1,j) - T(i-1,j)}{2\,\Delta x} = T_x \qquad (29i)$$

$$\frac{T(i,j+1) - T(i,j-1)}{2\,\Delta y} = T_y \qquad (29ii)$$

$$\frac{T(i+1,j) - 2T(i,j) + T(i-1,j)}{(\Delta x)^2} = T_{xx} \qquad (29iii)$$

$$\frac{T(i,j+1) - 2T(i,j) + T(i,j-1)}{(\Delta y)^2} = T_{yy} \qquad (29iv)$$

Forward-difference approximations

$$\frac{T'(i,j) - T(i,j)}{\Delta t} = T_t + \tfrac{1}{2}\Delta t T_{tt} \qquad (29v)$$

$$\frac{T(i+1,j) - T(i,j)}{\Delta x} = T_x + \tfrac{1}{2}\Delta x T_{xx} \qquad (29vi)$$

$$\frac{T(i,j+1) - T(i,j)}{\Delta y} = T_y + \tfrac{1}{2}\Delta y T_{yy} \qquad (29vii)$$

Backward-difference approximations

$$\frac{T(i,j) - T(i-1,j)}{\Delta x} = T_x - \tfrac{1}{2}\Delta x T_{xx} \qquad (29viii)$$

$$\frac{T(i,j) - T(i,j-1)}{\Delta y} = T_y - \tfrac{1}{2}\Delta y T_{yy} \qquad (29ix)$$

Coefficients:

$$G_1 = 1 - 2\lambda\Delta t(1/(\Delta x)^2 + 1/(\Delta y)^2) \qquad (30i)$$

$$G_2 = \lambda\Delta t/(\Delta x)^2 \qquad (30ii)$$

$$G_3 = \lambda\Delta t/(\Delta y)^2 \qquad (30iii)$$

$$C_1 = 2d_p c_{pp} h_p + d_L c_{pL}\Delta y \qquad (30iv)$$

$$C_2 = k_L\Delta y + 2k_p h_p \qquad (30v)$$

$$G_4 = 1 - \frac{2\Delta t}{C_1}(C_2/(\Delta x)^2 + k_L/\Delta y + k_p/h_p) \qquad (30vi)$$

$$G_5 = \Delta t C_2/(C_1(\Delta x)^2) \qquad (30vii)$$

$$G_6 = 2\Delta t k_L/C_1\Delta y \qquad (30viii)$$

$$G_7 = 2\Delta t k_p/C_1 h_p \qquad (30ix)$$

$$G_8 = G_2 + u(i,j)\Delta t/2\Delta x \qquad (31i)$$

$$G_9 = G_2 - u(i,j)\Delta t/2\Delta x \qquad (31ii)$$

$$G_{10} = G_3 + v(i,j)\Delta t/2\Delta y \qquad (31iii)$$

$$G_{11} = G_3 - v(i,j)\Delta t/2\Delta y \qquad (31iv)$$

On the application of the central-difference space definitions and the time-forward-difference definitions to Equations (3), (4) and (5), we get the following sets of equations. Second-order time derivative is ignored.

(1) Conduction Model

Liquid phase

$$T'(i,j) = G_{1L}T(i,j) + G_{2L}(T(i+1,j) + T(i-1,j)) + G_{3L}(T(i,j+1) + T(i,j-1)), \text{ for } 2 \leq i \leq M-1 \text{ and } NS(i)+1 \leq j \leq N-1 \quad (32i)$$

$$T'(1,j) = G_{1L}T(1,j) + 2G_{2L}T(2,j) + G_{3L}(T(1,j+1) + T(1,j-1)), \text{ for } NS(1)+1 \leq j \leq N-1 \quad (32ii)$$

$$T'(M,j) = G_{1L}T(M,j) + 2G_{2L}T(M-1,j) + G_{3L}(T(M,j+1) + T(M,j-1)), \quad NS(M)+1 \leq j \leq N-1 \quad (32iii)$$

$$T'(i,N) = G_4T(i,N) + G_5(T(i+1,N) + T(i-1,N)) + G_7T_a + G_6T(i,N-1), \text{ for } 2 \leq i \leq M-1 \quad (32iv)$$

$$T'(1,N) = G_4T(1,N) + 2G_5T(2,N) + G_6T(1,N-1) + G_7T_a \quad (32v)$$

$$T'(M,N) = G_4T(M,N) + 2G_5T(M-1,N) + G_6T(M,N-1) + G_7T_a \quad (32vi)$$

Solid phase

$$T'(i,j) = G_{1S}T(i,j) + G_{2S}(T(i+1,j) + T(i-1,j)) + G_{3S}(T(i,j+1) + T(i,j-1)), \text{ for } 2 \leq i \leq M-1, \ 2 \leq j \leq NS(i) \quad (33i)$$

$$T'(1,j) = G_{1S}T(1,j) + 2G_{2S}T(2,j) + G_{3S}(T(1,j+1) + T(1,j-1)), \text{ for } 2 \leq j \leq NS(1) \quad (33ii)$$

$$T'(M,j) = G_{1S}T(M,j) + 2G_{2S}T(M-1,j) + G_{3S}(T(M,j+1) + T(M,j-1)), \text{ for } 2 \leq j \leq NS(M) \quad (32iii)$$

$$T'(i,1) = f(t), \text{ for } 1 \leq i \leq M \quad (33iv)$$

(2) Combined Conduction-Convection Model

Solid phase:- The solid-phase Equations (33i) to (33iv) of the conduction model apply here in their entirety.

Liquid phase

$$T'(i,j) = G_{1L}T(i,j) + G_{8L}T(i-1,j) + G_{9L}T(i+1,j) + G_{10L}T(i,j-1) + G_{11L}T(i,j+1), \text{ for } 2 \leq i \leq M-1,\ NS(i)+1 \leq j \leq N-1 \quad (34i)$$

Equations (32ii) to (32vi) also apply here in their entirety.

In Equation (32) to Equation (34), subscripts L and S on a coefficint imply that the properties of liquid and solid test material are to be used respectively.

Calculation of the Phase-change Rate and the Height of the Solid Phase

In Equations (32) to (34), NS(i) is the number of y-nodes in the solid phase given as a function of horizontal location x (that is, $i\Delta x$). Thus, the height of the solid phase at any time t is given by the equation

$$Y(i,t) = \Delta y(NS(i)-0.5), \text{ for } 1 \leq i \leq M \text{ and } NS(i) \geq 2 \quad (35)$$

If NS(i) = 1, then Y(i,t) is on the cold bottom plate and is equal to $\Delta y/2$. NS(i) and Y(i,t) must satisfy, at any time, the following inequations.

$$1 \leq NS(i) \leq N, \text{ for } 1 \leq i \leq M \quad \text{---} \quad \text{---} \quad (36i)$$

$$0 \leq Y(i,t) \leq h, \text{ for } 1 \leq i \leq M \quad (36ii)$$

At any time t, NS(i) is evaluated as follows. Firstly, $T(i,1,t) = f(t)$ is checked to see if $f(t) \leq T_f$. The first time that $f(t) \leq T_f$, NS(i) is set equal to 1 for all $1 \leq i \leq M$ to see if $T(i,NS(i)_{old}+1) \leq T_f$. If it is, then a new NS(i) is obtained from the equation $NS(i) = NS(i)_{old} + 1$ for that particular i, and thenceforth, that node is treated as a node in the solid phase.

The latent heat of solidification is used to modify the specific heat of the solid phase so as to incorporate the effect of change of phase. It is assumed that, since the rate of change of phase is so slow and the solid phase is at a much lower temperature than the liquid phase, most of the heat liberated by solidification goes to warm up the solid phase in the form of sensible heat. Thus, an effective heat capacity c^*_{pS}, based on a lumped average temperature, $T_{av} = \frac{1}{2}(T_f+T(x,0,t)) = \frac{1}{2}(T_f+f(t))$, of the solid phase is defined to include the phase-change enthalpy change:

$$\underset{\text{per gram}}{\text{Enthalpy change}} = \underset{\text{per gram}}{\text{Latent heat}} + \underset{\text{per gram}}{\text{Sensible heat gain}} \quad (37i)$$

Thus, $c^{*}_{pS}(T_f-T_{av}) = H_f + c_{pS}(T_f-T_{av})$ (37ii)

So, we obtain an equation for the effective specific heat c^{*}_{pS} :

$$c^{*}_{pS} = c_{pS} + 2H_f/(T_f-f(t)) \cdot \quad (38)$$

c^{*}_{pS}, instead of c_{pS}, is used in the calculations of the temperature profiles of the solid phase in Equation (30) and Equation (33). No separate interface equation is now needed.

Therefore, to summarize, when the temperature of a node in the liquid phase equals or drops below the solidification temperature, T_f, the node is henceforth treated as a node in the solid phase, and c^{*}_{pS}, instead of c_{pS}, is used to calculate solid-phase temperatures so long as solidification is in progress. Thus, Equation (28) to Equation (38) are sufficient to determine the temperature profile, the rate of solidification, and the streamlines in the test cell at any time t.

Stability Criteria for the Finite-Difference Approximations

(1) Conduction Model

The stability criteria for this model are

$$G_1 \geq 0 \; ; \; G_4 \geq 0 \quad (39)$$

for both liquid and solid phases. From Equation (39), maximum

allowable Δt for given Δx and Δy are evaluated. Whichever Δt from Equation (39) is smaller is the controlling Δt for a stable solution. It is recommended that a smaller value of Δt than the maximum allowable Δt be used. The smaller the value of Δt, the smaller the error in the finite-difference approximation gets. For our system, G_1 controls the allowable Δt.

(2) Conduction-Convection Model

The stability criteria of Equation (39) also apply here. Other criteria are imposed on velocity, thus:

$$G_8 \geq 0;\ G_9 \geq 0;\ G_{10} \geq 0;\ \text{and}\ G_{11} \geq 0 \qquad (40)$$

These inequalities yield the following restrictions on u and v:

$$|u(i,j)| \leq 2\lambda_L/\Delta x\ ,\ |v(i,j)| \leq 2\lambda_L/\Delta y \qquad (41)$$

Thus, for a given Δx or Δy, a maximum allowable absolute value of u or v may be determined. The resultant velocities evaluated for our test material are small, a fact that caused the difficulty in finding any stable finite-difference solutions for the full-blown coupled equations of energy and motion so long as the gravity term remained in the velocity equations.

The velocities obtained by differentiating Equation (28) with respect to x or y must satisfy Equation (41).

With the experimentally-observed temperature difference between the hot and the cold plates, we could not use the full magnitude of Equation (28) without violating Equations (41). So, we restricted the maximum velocities that we used to be 95 percent of the maximum velocities permitted by Equations (41), and the constant B in Equation (28) was modified accordingly. If the maximum permitted velocities, in stead of some slightly lower values were used, our solution would be in the critical region where a small round-off error from the digital computer could make the solution unstable and meaningless. Table 1 gives the time elements and velocities permitted by stability restrictions and the actual values used in our calculations.

Table 1: TIME INCREMENTS AND VELOCITIES ALLOWABLE BY STABILITY CRITERIA

$\Delta x = \Delta y$; $\lambda_L = 9.306 \times 10^{-4}$ cm^2/sec

Space Element Δx(cm)	Time Element Δt(sec)	u(max) (cm/sec)	v(max) (cm/sec)
0.254	17.33	7.32×10^{-3}	2.75×10^{-3}
0.127	4.33	14.65×10^{-3}	5.49×10^{-3}
0.0635	1.08	29.31×10^{-3}	10.99×10^{-3}

Actual values used:

$\Delta x = 0.127$ cm; $\Delta t = 1.0$ sec; u(max) = 13.92×10^{-3} cm/sec; v(max) = 5.22×10^{-3} cm/sec

Error Analysis of the Central Difference Method Used

(1) Conduction Model

The terms ignored in the finite-difference approximations are of the order of $(\Delta x)^2 T_{xx}/6$, $(\Delta y)^2 T_{yy}/6$, and $\frac{1}{2}\Delta t T_{tt}$. These terms are assumed to be small provided Δx, Δy and Δt are small. We ran our digital-computer programs for a square-grid system ($\Delta x = \Delta y$) for different values of Δx and Δt. We found that a solution at $\Delta x = 0.127$ cm, $\Delta t = 2.0$ sec was not much different from a solution at $\Delta x = 0.0635$ cm, $\Delta t = 1.0$ sec (see Table 2), but involved quite a large difference in computation time. Hence, we assumed that the solution had converged at $\Delta x = 0.137$ cm and $\Delta t = 2.0$ sec, and therefore, used $\Delta t = 1.0$ sec and $\Delta x = 0.127$ cm for computation.

Table 2: CHECK FOR CONVERGENCE OF FINITE-DIFFERENCE SOLUTION OF THE CONDUCTION MODEL

Time (1000 sec)	^oK* $\Delta x = 0.127$ cm $\Delta t = 2.0$ sec	^oK* $\Delta x = 0.0635$ cm $\Delta t = 1.0$ sec
0.36	299.636	299.638
1.44	293.139	293.150
2.16	291.272	291.277
2.52	290.622	290.660
2.88	290.185	290.205
3.60	289.472	289.500
3.96	289.233	289.260
4.68	288.766	288.614
5.04	287.557	287.606
5.76	286.361	286.161
6.48	285.226	285.202
7.20	284.161	284.112

* Calculated temperature

(2) Conduction-Convection Model

The errors inherent in the finite-difference approximations of the conduction model are also present in the combined conduction-convection model. But the most important source of error is due to hidden numerical dispersion terms. These are terms that are introduced inadvertently into the original temperature equations (Equation 5), when finite-difference approximations that ignore second-order derivatives are used. In the backward- and the forward-difference approximations both the second-order space derivatives and the second-order time derivatives contribute to these dispersion error terms. In the central-difference method, only the second-order time derivative introduces the numerical dispersion error terms. This kind of error cannot be avoided by using time-implicit finite-difference techniques. The numerical dispersion errors are revealed in the central-difference method as follows:-

If Equation (34i) is rewritten in terms of derivatives by using Equation (29) without ignoring the second-order time derivative, the resulting equation is:

$$\tfrac{1}{2}\Delta t T_{tt} + DT/Dt = \lambda_L(T_{xx} + T_{yy}) \qquad (42)$$

By comparing Equation (42) and Equation (5), we find that an extra term $\tfrac{1}{2}\Delta t T_{tt}$ has been introduced into the original Equation (5) by the finite-difference approximation that ignored second-order time derivative T_{tt}. By differentiat-

ing Equation (5) with respect to t, ignoring third- and higher order derivatives, and introducing the result into Equation (42) we get, on further rearrangement:

$$DT/Dt = (\lambda_L - \tfrac{1}{2}u^2\Delta t)T_{xx} + (\lambda_L - \tfrac{1}{2}v^2\Delta t)T_{yy} - uv\Delta t T_{xy} \qquad (43)$$

Thus, the finite-difference (central-difference) approximation has introduced the extra terms $-\frac{1}{2}u^2\Delta t T_{xx}$, $-\frac{1}{2}v^2 T_{xx}\Delta t$ and $-uvT_{xy}\Delta t$ into the original Equation (5). These are the numerical-dispersion terms. The numerical-dispersion coefficients $-\frac{1}{2}u^2\Delta t$, $-\frac{1}{2}v^2\Delta t$ and $-uv\Delta t$ must be compared against λ_L to see how much error is introduced. They could introduce devastatingly significant errors. Errors due to dispersion terms do not arise in the conduction model but in models involving the boundary-layer equations of energy and motion. These errors can be reduced but not eliminated by including higher-order derivatives of time in the difference approximations or by reducing the magnitudes of the velocity components and/or time step. Table 3 gives the magnitude of the dispersion coefficients evaluated for our problem in which $\lambda_L = 9.306 \times 10^{-4}$ cm^2/sec, $u_{max} = 13.92 \times 10^{-3}$ cm/sec, and $v_{max} = 5.2 \times 10^{-3}$ cm/sec.

Note that, although it is desirable to decrease Δy and Δx and thereby increase maximum allowable velocities due to stability restrictions, the dispersion error terms

Table 3: MAGNITUDE OF DISPERSION COEFFICIENTS COMPARED TO THE THERMAL DIFFUSIVITY (λ_L) OF THE LIQUID.

$\lambda_L = 9.306 \times 10^{-4}$ cm^2/sec

u = 13.92 cm/sec; v = 5.22 cm/sec; x = y = 0.127cm

Δt (sec)	$\frac{1}{2}u^2\Delta t$ (cm^2/sec)	$\frac{1}{2}v^2\Delta t$ (cm^2/sec)	$uv\Delta t$ (cm^2/sec)
6.0	$0.625\lambda_L$	$0.088\lambda_L$	$\pm 0.468\lambda_L$
4.0	$0.416\lambda_L$	$0.059\lambda_L$	$\pm 0.312\lambda_L$
2.0	$0.208\lambda_L$	$0.029\lambda_L$	$\pm 0.156\lambda_L$
1.0	$0.104\lambda_L$	$0.015\lambda_L$	$\pm 0.078\lambda_L$
0.5	$0.052\lambda_L$	$0.007\lambda_L$	$\pm 0.039\lambda_L$

increase with increasing velocity or decreasing Δx and Δy. We ran digital-computer programs for the conduction-convection model at different values of Δt for the same $\Delta x = \Delta y = 0.127$ cm that was used for the conduction model. We found that the dispersion terms did not make any significant difference at $\Delta t = 1.0$ sec. At $\Delta t = 6.0$ sec, the numerical dispersion terms made a substantial difference in the accuracy of the theoretical results. The time required to complete a computer program to acquire the equivalent of two hours of experimental time was prohibitive for $\Delta t \leq 1.0$ sec. Perhaps, a faster computer would be very helpful. We conjecture that the numerical-dispersion coefficient $-uv\Delta t$ counteracts some of the effects of the coefficients $-\frac{1}{2}u^2\Delta t$ and $-\frac{1}{2}v^2\Delta t$, so that, when the last two-mentioned are of the order of 10 percent of λ_L, the net error effects are much smaller than that.

It happened also, that in our system, the maximum temperature gradients in the liquid phase occur along the y-coordinate direction; that is, in the direction such that $|vT_y| \gg |uT_x|$. Thus, v had a lot more influence on the magnitude of the temperature profiles than u did. But a glance at Table 3 reveals that the error terms due to v alone in the dispersion terms are much smaller than those introduced by u. Thus, the numerical-dispersion terms did not have as much influence on the theoretical results as as they would if the maximum temperature gradients had been in a direction to cause $|uT_x| \gg |vT_y|$.

EXPERIMENTAL EQUIPMENT AND PROCEDURE

Equipment

The principal elements of the equipment were a test cell, a 24-channel multipoint temperature recorder, and a refrigerator. The auxiliary elements were copper-constantan thermocouples, a power-driven liquid pump, methanol, some pipes and tubings, and a test-cell stand that could be swivelled to various inclined positions from the horizontal plane. The test material, n-hexadecane, was liquid at the ambient temperatures for the experiments.

Test Cell: The test cell (Fig. 1 and 5) had a constant cross-section of external dimensions 12.70 cm, and an overall height of 9.20 cm. It was composed of a copper cooling chamber soldered to one face of a 0.32-cm-thick copper plate (henceforth referred to as the cold plate or the bottom plate) which was in turn bolted and glued to one end of a plexiglas frame. The frame was glued and bolted to a 1.27-cm-thick plexiglas plate on the other end. Thus, the plexiglas frame, together with the plexiglas plate on one end and the copper plate on the other end formed a 10.16-cm-square, 3.81-cm-high cavity with 1.27-cm-thick walls for containing the test material, normal hexadecane. The cooling chamber was constructed from 0.64-cm copper plates soldered together.

FIGURE 5. THERMOCOUPLE LOCATIONS IN TEST CELL
Integers refer to thermocouples identified in Table 4.Other numbers are distances (cm).

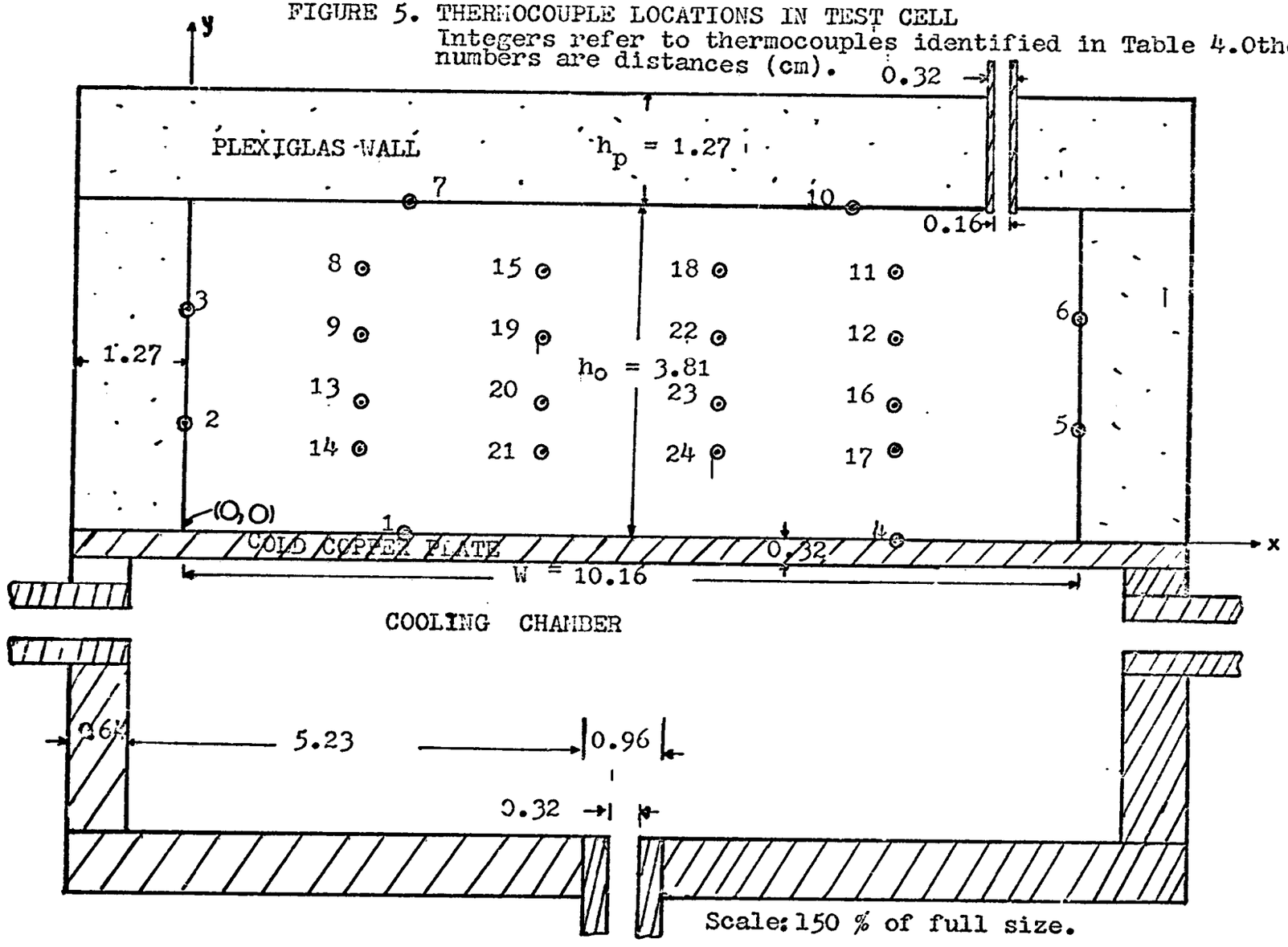

The test cell carried twenty-four copper-constantan thermocouples located at certain measured locations. Table (4) details the thermocouple locations. The coordinates given in the table were located and fixed as shown in Figure (1) and Figure (5). The positions could be off by ± 0.16 cm because of the limitations in the measuring accuracy.

Table 4: THERMOCOUPLE LOCATIONS IN TEST CELL

x = horizontal distance (parallel to the cold bottom plate), starting from left corner of test-cell cavity.

y = vertical distance from cold bottom plate

Each distance could be off by ± 0.16 cm

No. = the number assigned to a thermocouple

No.	x (cm)	y (cm)	No.	x (cm)	y (cm)	No.	x (cm)	y (cm)
1	2.54	0.00	13	2.03	1.52	3	0.00	2.54
4	8.13	0.00	20	4.06	1.52	6	10.16	2.54
14	2.03	1.02	23	6.10	1.52	8	2.03	3.05
21	4.06	1.02	16	8.13	1.52	15	4.06	3.05
24	6.10	1.02	9	2.03	2.29	18	6.10	3.05
17	8.13	1.02	19	4.06	2.29	11	8.13	3.05
2	0.00	1.27	22	6.10	2.29	7	2.54	3.81
5	10.16	1.27	12	8.13	2.29	10	7.62	3.81

Temperature Recorder: The recorder was a 24-channel, multipoint recorder sold by ACCO Bristol[34], model 66A-24 PGC 570, that operated on 120 volts of 60-cycle alternating current. It recorded temperatures in degrees Fahren-

heit in the range -100 °F to +200 °F (199.83 °K - 366.49 °K). It had a chart drive speed of 2.54 cm per minute and print speed of 2 seconds per point. The chart could be read with an accuracy of ±0.27 °K (0.5 °F).

Pump: The pump used to circulate the coolant (methanol) from the refrigerator to the test cell was a Chemical Rubber Company(35) "No-Seal" centrifugal pump, Model ABIP005N#. It operated on 115-volts, 60-cycle alternating current only. It could attain 50 revolutions per second and pump from 441.6 cc per second at a head of 30.5 cm to 262.8 cc per second at a head of 274.3 cm under normal atmospheric conditions.

Refrigerator: The refrigerator for the coolant was a Bar Ray of Brooklyn, New York, Model 557T refrigerator that operated on a 60-cycle, 115-volt alternating current. It had a regulator that could be used to adjust the steady-state temperature to which the refrigerant was cooled.

A schematic diagram of the assembled equipment is shown in Figure (6). A two-way tap-control valve permitted the circulation of the coolant in an auxiliary circuit until temperature equilibration was achieved in the coolant.

Experimental Procedure

The test material, n-hexadecane, (liquid at normal room temperature) was introduced into the test-cell cavity through a filler-port. An excess of the material was allowed to

FIGURE 6. BLOCK DIAGRAM OF ASSEMBLY OF MAIN EXPERIMENTAL EQUIPMENT.

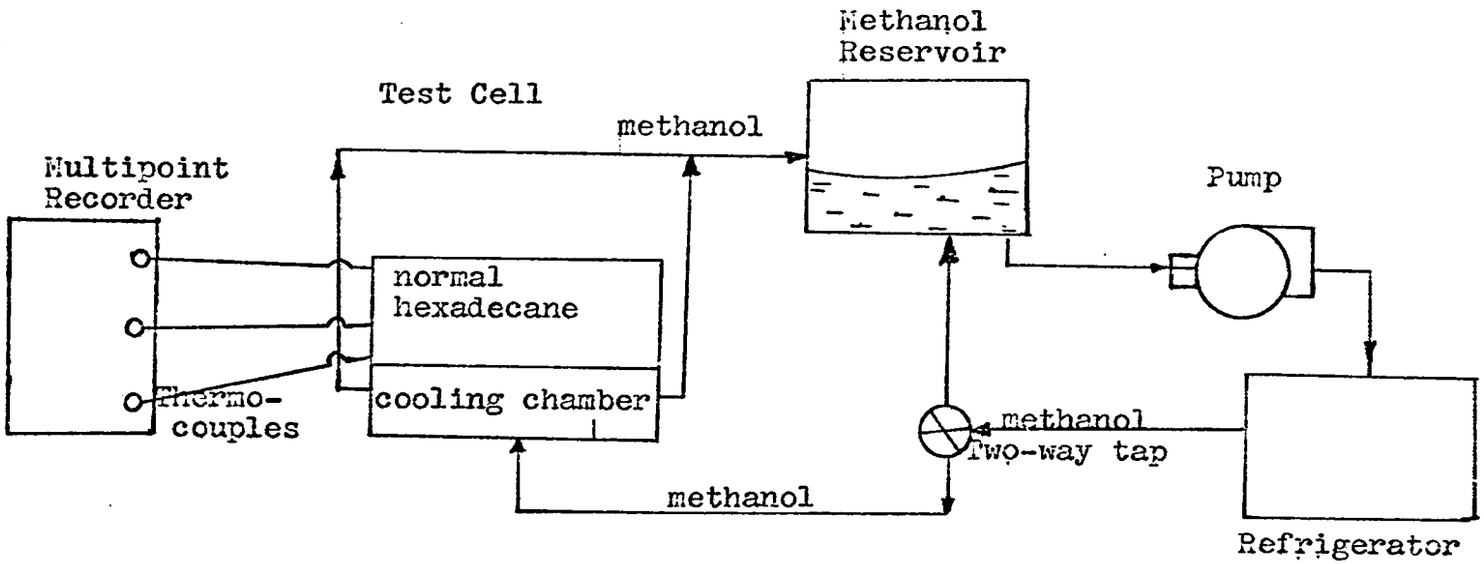

collect in an expansion chamber connected to a reservoir of the test material. In this way, air pockets in the test cell were kept to a minimum as the solidification progressed, by the introduction of new test material to assume the vacated volume.

The temperature recorder was turned on at the same time as the pump was turned on to circulate cold methanol to cool the bottom plate of the test cell. By use of the auxiliary circuit, a step change in the temperature of the test cell could be achieved. The experiments were performed with the cell inclined at the following angles from the horizontal plane: 0°, 15°, 30°, 45° and 60°. Studious attempt was made to approximate the same starting conditions for all runs-- the same cooling rate, the same low temperature for the coolant and the same ambient temperature. The ambient temperature was approximately controlled by setting the room thermostat at a constant level for about 24 hours before an experimental run. Before each run the thermocouples were calibrated on the recorder by testing against room temperature as recorded by a mercury thermometer. When all 24 thermocouples recorded the same temperature within $\pm 0.27\ ^{\circ}K$, the experiment was begun. Room temperature was watched continually during the course of an experiment via a mercury thermometer. The temperature at the start of an experiment, as recorded by the 24 thermocouples, usually

did not deviate from that recorded by the mercury thermometer by more than 1.1 °K. Flow of coolant was kept approximately constant from run to run by opening all the valves to their fullest extent. The pump had only one speed setting. The low temperature of the coolant was regulated by the "cut in" temperature of the refrigerator which was set constant at about 272 °K. Methanol was used as the coolant because it stayed liquid at this low temperature whereas water became ice. With such a setting, the coolant could be brought to a low temperature of about 270 °K.

The experiments were usually terminated after about 2 hours when more than half of the test material had solidified. The temperatures, read from the charts, were then plotted against time. The bottom-plate temperatures were fitted into a polynomial function of time, comprising a ramp decay followed by a constant temperature. For a given set of starting conditions, the experiments were repeated to test for reproducibility.

The test material was practical n-hexadecane ($n\text{-}C_{16}H_{34}$) distributed by the Eastman Kodak Company[36] for chemical purposes. It had small impurities that influenced its solidification temperature. The solidification range was given by the manufacturer as 291.0 °K - 289.2 °K. However, we found that our sample froze at 290.6 °K (17.5 °C).

COMPARISON OF EXPERIMENTAL AND THEORETICAL RESULTS

Test for the Reproducibility of Experimental Data

Two experimental runs under similar conditions of angle of inclination of test cell, cut-in temperature of refrigerator, flow rate of coolant, chart speed and ambient temperatures as close as possible to each other were tested for the reproducibility of the data. It was estimated that experimental errors due to thermocouples, chart reading, and ambient temperature would cause as much as $\pm 0.83\ ^{o}K$ error in the experimental data. Thus, the mean of the differences of the temperatures recorded by the same thermocouple in both experimental runs were estimated with a 99% level of confidence.

First of all the temperatures were plotted on the same temperature-versus-time graph. Then, 17 points were selected on the time axis and the temperatures of the two runs were read off. The difference of the temperatures was obtained for each of the seventeen points. Thus, a sample mean of the differences and a sample standard deviation were calculated. A confidence interval was calculated at the 99% level of confidence. If the confidence interval fell within $\pm 0.83\ ^{o}K$, the data were accepted as reproducible. These calculations were performed for each of the 24 thermo-

couples for a given pair of experimental runs under test. Fig. 7 gives sample graphs for testing reproducibility of data for experimental Runs 9 and 10.

Let e_i be the difference between temperatures recorded by the same thermocouple between a pair of experimental runs under identical conditions at a point i in time and let $\bar{e}$ be the mean of a sample of size n of such differences. Then the true mean m_e of the differences, at 99% level of confidence, lies in the interval

$$\bar{e} - ts/\sqrt{n} < m_e < \bar{e} + ts/\sqrt{n} \quad \text{inclusive} \tag{44}$$

where s is the standard deviation of the sample of size n, and t is calculated from the Student t-distribution at the upper 0.5% tail.

For our system, $t_{0.005,\ 17} = 2.921$, and $n = 17$,

$$s = \frac{n \sum_{i=1}^{n} e_i^2 - \left(\sum_{1=1}^{n} e_i\right)^2}{n(n-1)} . \tag{45}$$

Thus, the confidence interval is

$$\bar{e} - 2.921s/\sqrt{17} < m_e < \bar{e} + 2.921s/\sqrt{17}. \tag{46}$$

This interval must lie within the limits of experimental error before a pair of runs may be accepted as being reproducible. The test for reproducibility of data was performed

FIGURE 7. GRAPHICAL TEST FOR REPRODUCIBILITY OF EXPERIMENTAL DATA.

⊙ Run 9: T_a=301.22°K ; α=30°

⊡ Run 10: T_a=301.49°K ; α=30°

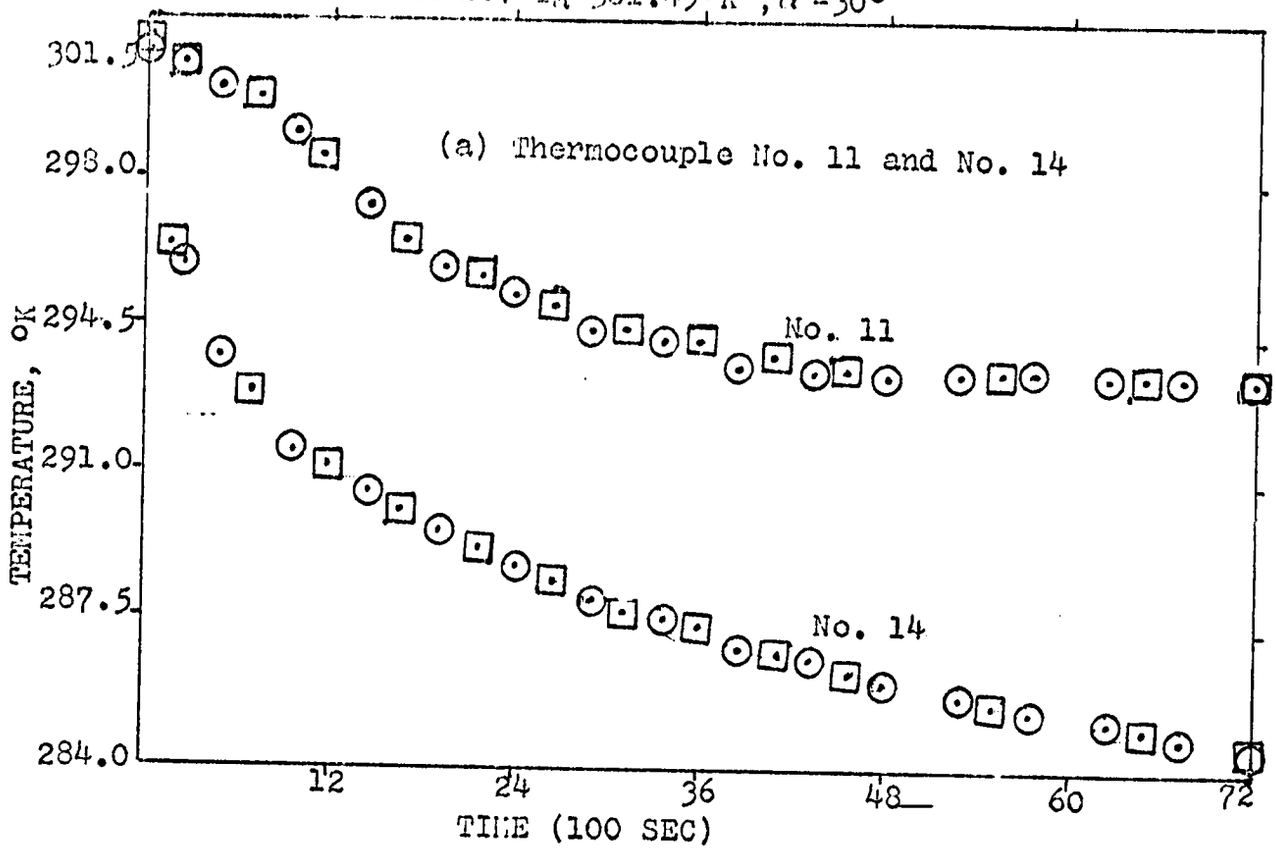

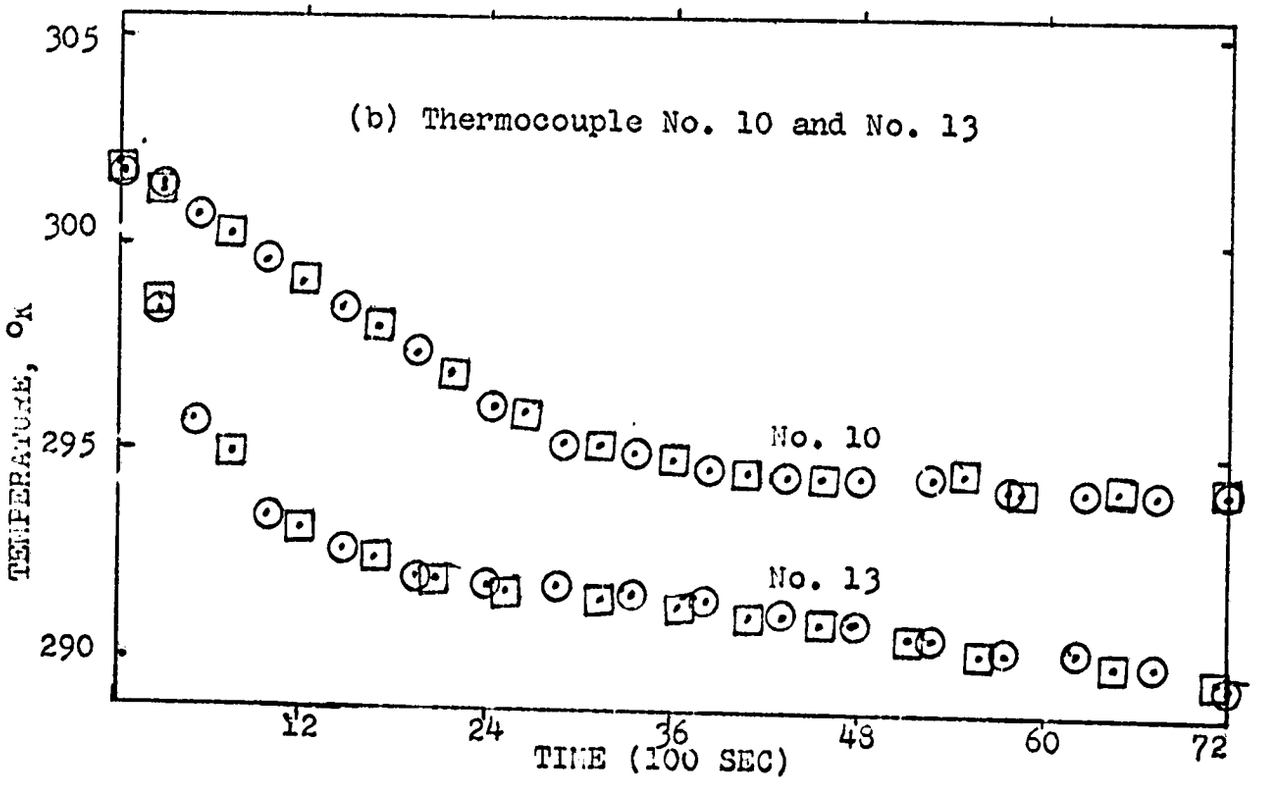

for all 8 pairs of runs and for each thermocouple. Table 5 shows a sample test result for experimental Runs 9 and 10.

Table 5: REPRODUCIBILITY TEST BETWEEN RUN 9 AND RUN 10

The decision "accept" means that results are reproducible. The confidence interval must lie within ± 0.83 °K for the results to be accepted as reproducible. Level of confidence = 99%.

Thermocouple Number	$\bar{e}$ °K	s °K	Confidence Interval °K	Decision
1	0.033	0.092	-0.033, 0.098	accept
2	0.065	0.251	-0.112, 0.243	accept
3	0.278	0.278	0.081, 0.474	accept
4	0.033	0.092	-0.033, 0.098	accept
5	0.040	0.407	-0.247, 0.328	accept
6	0.251	0.334	0.014, 0.488	accept
7	0.069	0.209	-0.079, 0.217	accept
8	0.053	0.458	-0.271, 0.377	accept
9	0.125	0.131	0.033, 0.217	accept
10	0.152	0.316	-0.072, 0.376	accept
11	0.180	0.239	0.001, 0.349	accept
12	0.243	0.250	0.066, 0.420	accept
13	0.176	0.154	0.067, 0.285	accept
14	0.229	0.202	0.086, 0.372	accept
15	0.114	0.167	-0.004, 0.232	accept
16	0.051	0.117	-0.032, 0.134	accept
17	0.090	0.343	-0.153, 0.333	accept
18	0.238	0.244	0.065, 0.411	accept
19	0.066	0.288	-0.139, 0.270	accept
20	0.040	0.173	-0.083, 0.163	accept
21	0.033	0.280	0.082, 0.231	accept
22	0.131	0.210	-0.018, 0.279	accept
23	0.049	0.293	0.158, 0.256	accept
24	0.107	0.185	0.024, 0.238	accept

Table 6 lists all 16 experimental runs in pairs according to reproducible pairs.

Table 6: EXPERIMENTAL RUNS LISTED IN REPRODUCIBLE PAIRS

First values of temperature correspond to experimental runs shown first in the first column.

Runs	α^o	T_a, ^oK	Cold plate steady temperature, ^oK
1; 2	0°	300.7; 300.7	270.4; 270.4
3; 4	0°	300.1; 300.4	269.8; 269.8
5; 6	15°	298.7; 298.7	270.4; 270.4
7; 8	60°	298.7; 298.7	270.4; 270.4
9; 10	30°	301.2; 301.5	269.8; 269.8
11; 12	45°	300.1; 300.1	269.8; 269.8
13; 14	45°	301.5; 301.5	269.8; 269.8
15; 16	60°	301.5; 301.5	270.4; 270.4

Presentation of Experimental and Theoretical Data

The experimental data for all the 16 experimental runs are presented in Appendix A. Figures (8) to (18) show comparisons of experimental and theoretical data. The experimental runs were performed under conditions listed in Table 6. Figures (8) and (9) were obtained for experimental runs with the cell sitting on a horizontal plane. Remarkably good agreement was obtained between the experimental data and theoretical conduction data, thus indicating that when the cell was sitting on a horizontal plane, heat transfer was by conduction with negligible convection. Obviously, a convection model could not predict the results of Figures (8) and (9). The data have been presented according to distance y from the cooled bottom plate. The data from the experimental runs at angle 0° (horizontal) indicated that temperatures were functions of time and distance,

y, from the cooled plate, but not of horizontal distance x, as would be expected from a conduction model with our given boundary conditions.

Figures (10) to (18) present results obtained with the test cell inclined at different angles from the horizontal, starting with a 15° angle. A study of the experimental points on these graphs reveals the presence and importance of convective heat transfer. Now, the temperature profiles become functions of horizontal distance x. Here, again, as in Figures (8) and (9), the temperature graphs have been arranged according to vertical distance y from the cold plate. At a given vertical distance y, the maximum and minimum temperatures along a horizontal direction, x, have been plotted on the same graph. Other thermocouples with in-between temperatures have been plotted singly. Thus, the separation of temperatures caused by convection along a horizontal direction was revealed in each case.

The general effect of convective heat transfer would appear to be increased heat-transfer rate, resulting in lower temperatures throughout the cell and faster freezing rate than would be obtained with conduction heat transfer only. Also, convection changed the shape of the interface from being flat to a curved shape (Fig. 13). More freezing occurred near the pivot x = 0 of angle of inclination than near x = W.

The effect of increasing angle was to increase the

cooling-down of that part of the cell to the right of the plane x = W/2. The greater the angle of inclination, the more the cell is cooled down below pure conduction temperature profile. It would seem that after certain temperature gradients were achieved, the cooling rate was greatly reduced. The magnitude of maximum deviation of temperature along a horizontal direction at a given height, y, from the cold plate was observed experimentally to depend more on the temperature difference between initial temperature T_a and solidification temperature, T_f. Rough estimates of this difference were found to be approximately $\frac{1}{2}(T_a - T_f)$ irrespective of the angle of inclination. However, the rate of attainment of such maximum differences differed with angles and could not be estimated.

Figures (10) to (18) show trends in temperature profiles as solidification with convection progressed. The theoretical curves could not be brought to match closer with the experimental curves, because stability limitations from the finite difference approximations of the temperature equations would not allow us to use the maximum possible velocities from the velocity profiles.

If velocities could be increased without violating the stability criteria of the finite difference solutions, then it is felt that it would be possible to reach the proper maximum velocity when the theoretical and experimental curves

would be very close to each other. At such a time one could calculate empirically the maximum velocities for the system as functions of angle α. With the true maximum velocities known, one could then find the proper value of $(T - \bar{T})$ involved in the gravity approximations in the velocity profiles.

Rough estimates of fractions of maximum velocities that we actually used were obtained as follows. At the start of convection, a critical Rayleigh number was assumed based on values available in the literature. From the critical Rayleigh number, ΔT_o at the start of convection was computed and used in Equation (28) to calculate the maximum velocity component u^*_{max} ($u_{max} > v_{max}$). Then, ratios of the actual u_{max} used and this computed u^*_{max} were obtained for different angles. The ratios were then the fractions of initial maximum velocity (or in other words, gravity levels) that we could attain at the very start of convection. Equation (47) gives the relationship for the velocity ratios or gravity level Q:

$$Q = 0.95\ (2\lambda_L/\Delta x)/B_{cr} = 45.6h_o/R_{a_{cr}}\Delta x \sin\alpha \qquad -(47)$$

where $R_{a_{cr}}$ = critical Rayleigh number

$$= -\beta g h_o^3 \Delta T_{o_{cr}} / (\lambda_L \nu \bar{\sigma}_L)$$

and h_o = height of liquid in test cell at the start of convection.

A half of the height of the liquid phase at the start of convection was used because the temperature gradient was still confined to $y < h/2$. The factor 0.95 appeared in Equation (47) because we used 95% of the maximum velocity allowed by stability requirements of the finite difference solution.

Table 7 shows gravity levels (fractions of maximum velocity obtained) against magnitudes of angle of inclination α. It shows that, as the angle of inclination increased, our stability- allowable maximum velocity became a smaller fraction of the maximum velocity predicted by Equation (28) at the start of convection. As solidification progressed, the velocity in the system could approach the actual maximum velocity that we used and could also become smaller than that. It must be emphasized that the gravity levels in Table 7 correspond to the start of convection only.

Table 7: GRAVITY LEVELS AT START OF CONVECTION, (Q)

$\Delta x = 0.127$ cm. $\qquad R_{a_{cr}} = 3{,}500$

u_{max} actually used $= 1.9\lambda_L / \Delta x = 13.92 \times 10^{-3}$ cm/sec

$\lambda_L = 9.306 \times 10^{-4}$ cm^2/sec

α^o	Gravity Level, Q
15^o	0.68
30^o	0.39
45^o	0.28
60^o	0.23

FIGURE 8. EXPERIMENTAL AND THEORETICAL DATA FOR RUN 2:
$\alpha = 0^{\circ}$; $T_a = 300.66^{\circ}K$

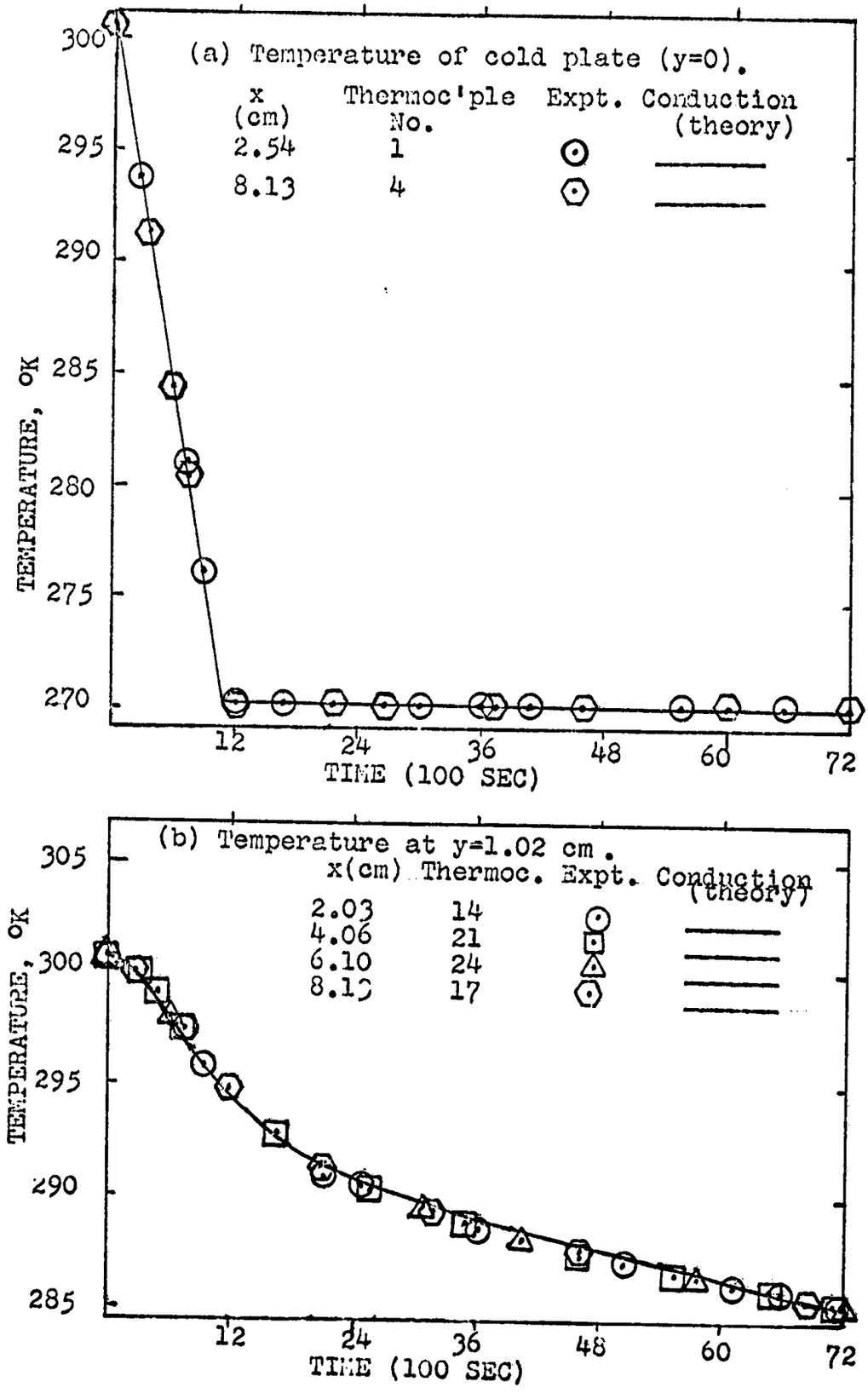

FIGURE 8 (contd). RUN 2: $\alpha = 0^{\circ}$; $T_a = 300.66^{\circ}K$

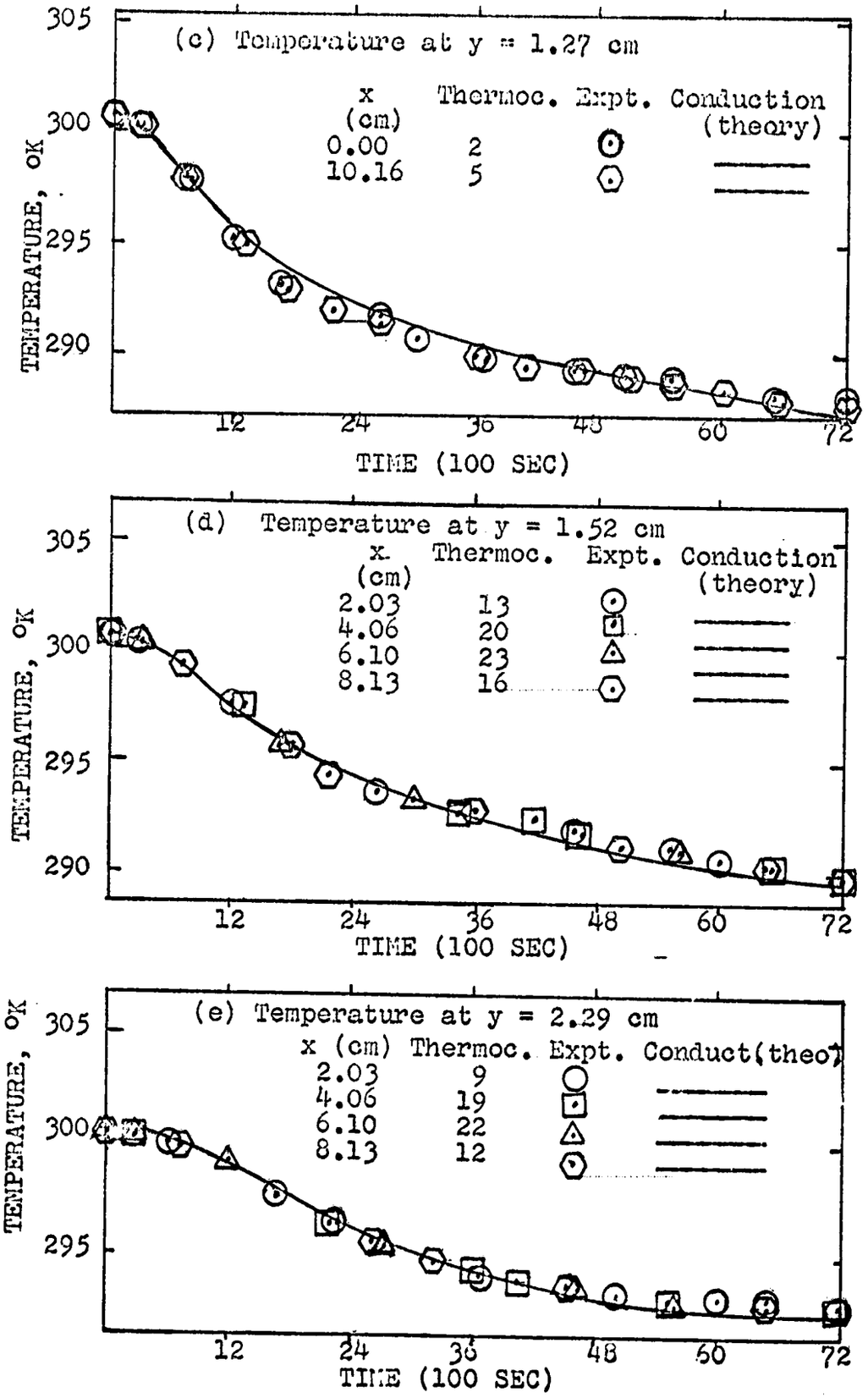

FIGURE 8 (contd). RUN 2 : $\alpha = 0^{o}$; $T_a = 300.66\ ^{o}K$

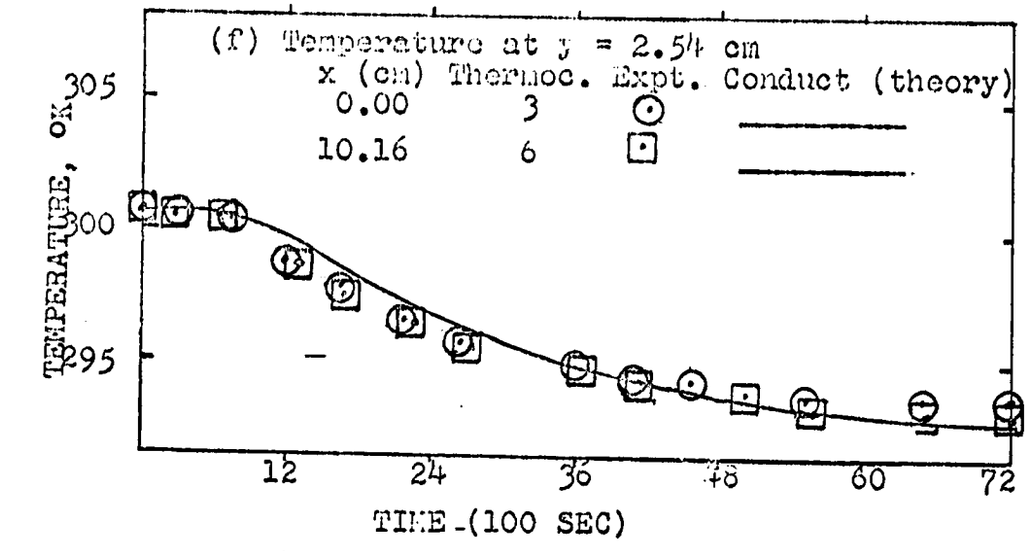

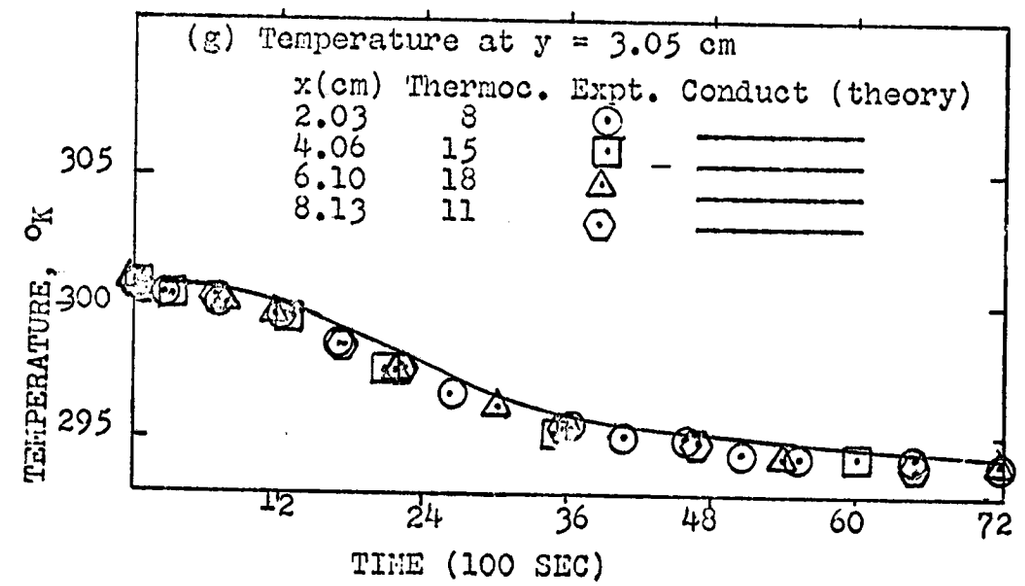

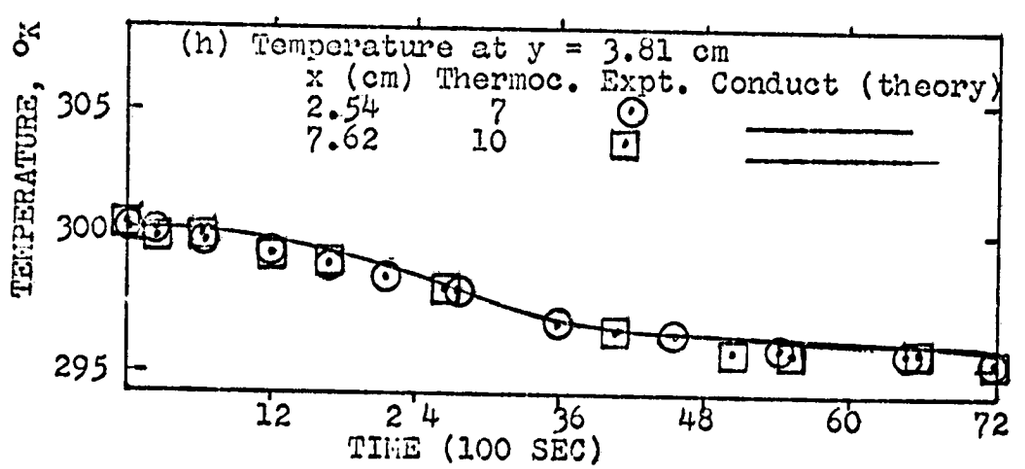

FIGURE 9. EXPERIMENTAL AND THEORETICAL DATA FOR RUN 3: $\alpha = 0^{\circ}$; $T_a = 300.11\ ^{\circ}K$

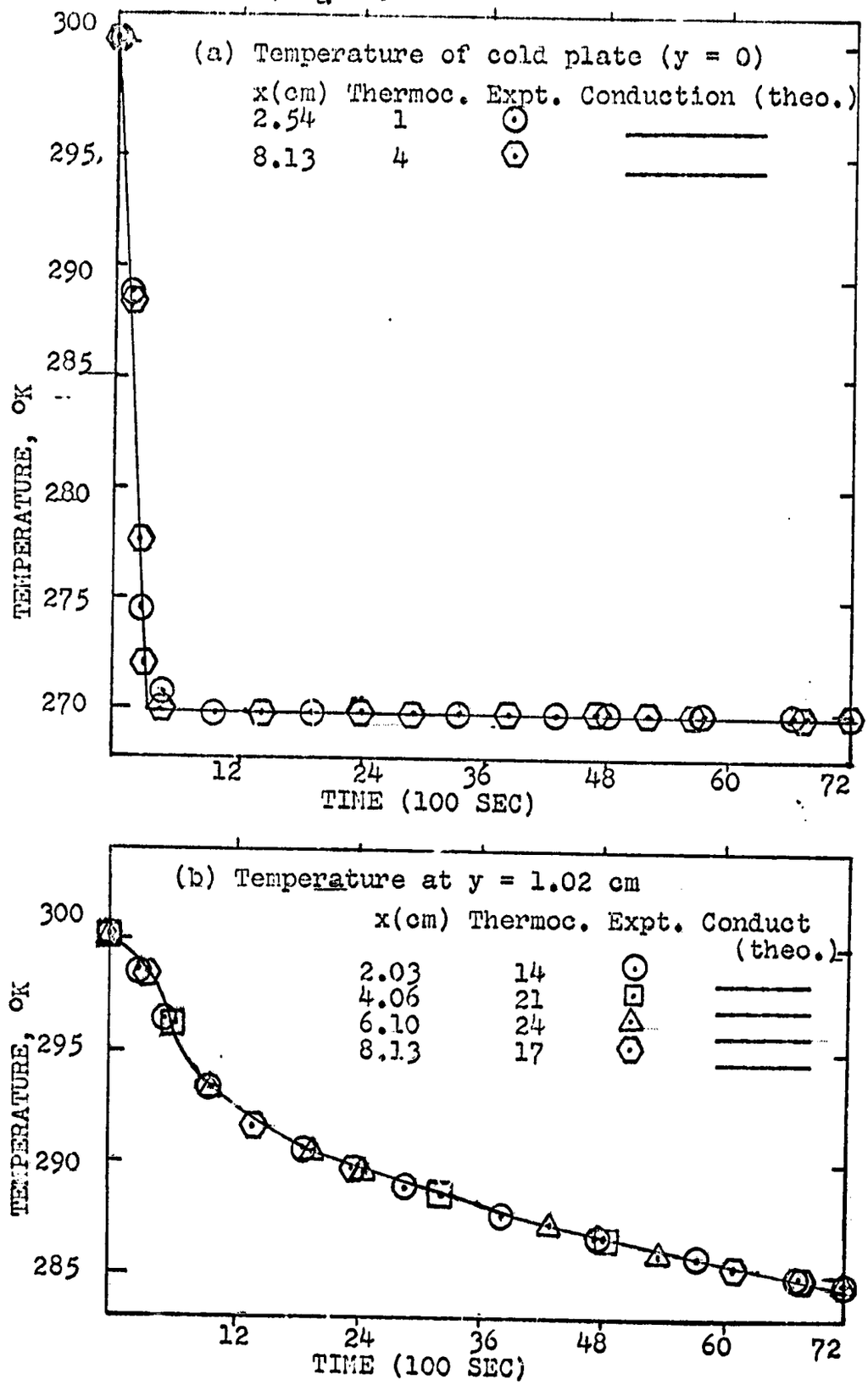

FIGURE 9 (contd). RUN 3; α = 0° ; Ta = 300.11 °K

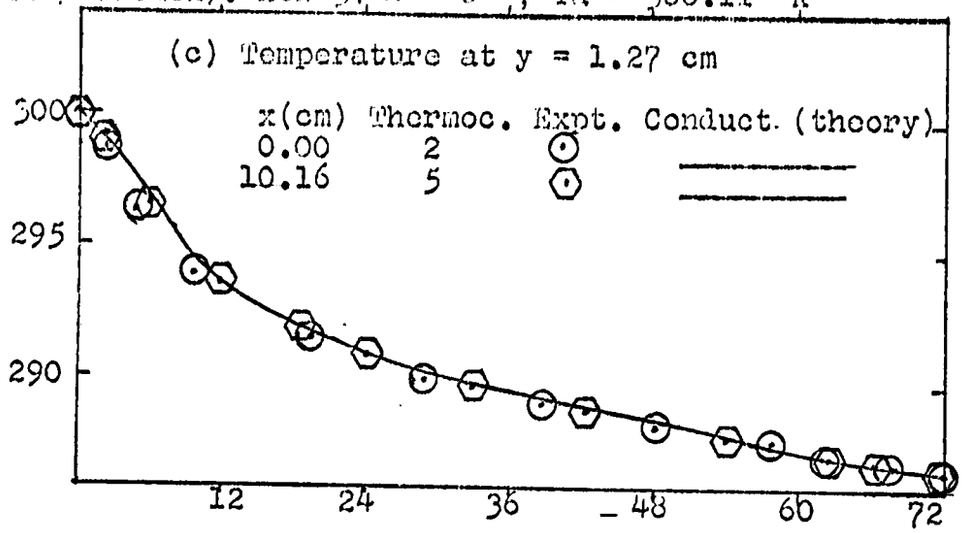

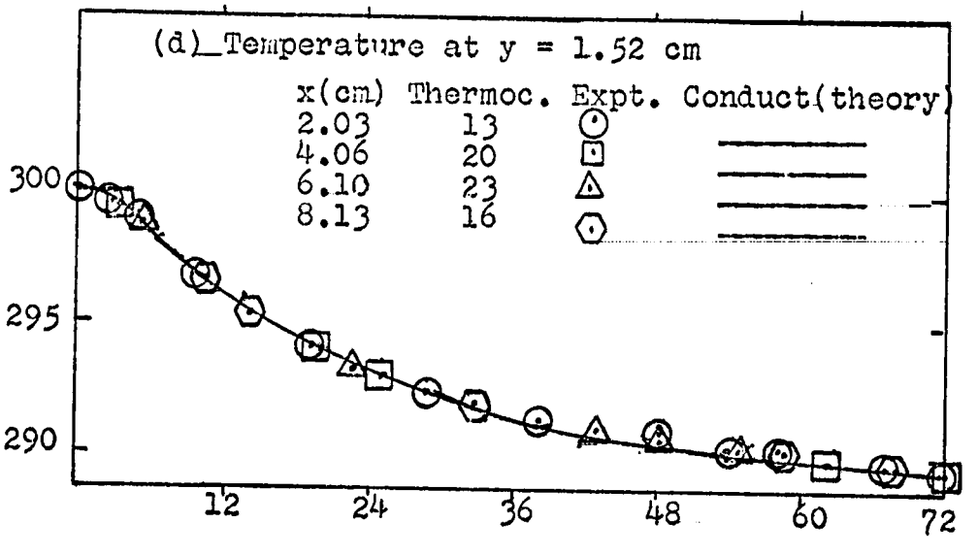

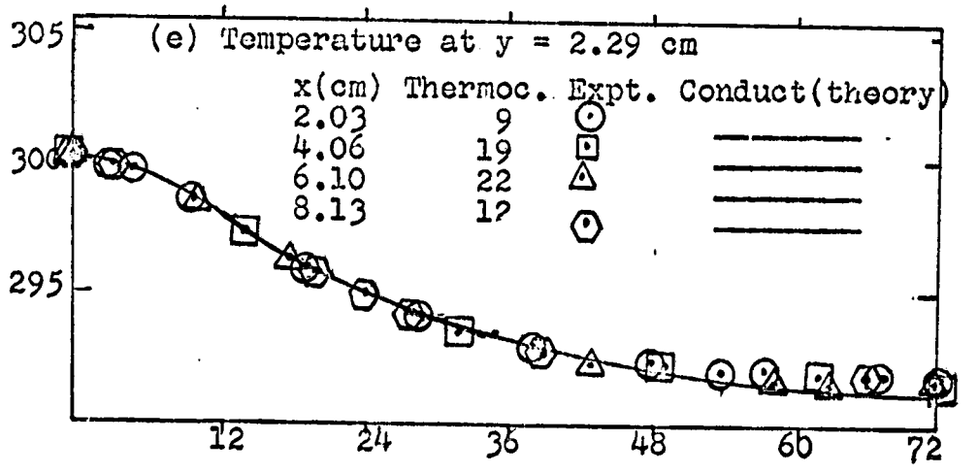

FIGURE 9 (contd). RUN 3: $\alpha = 0^{\circ}$; $T_a = 300.11\ ^{\circ}K$

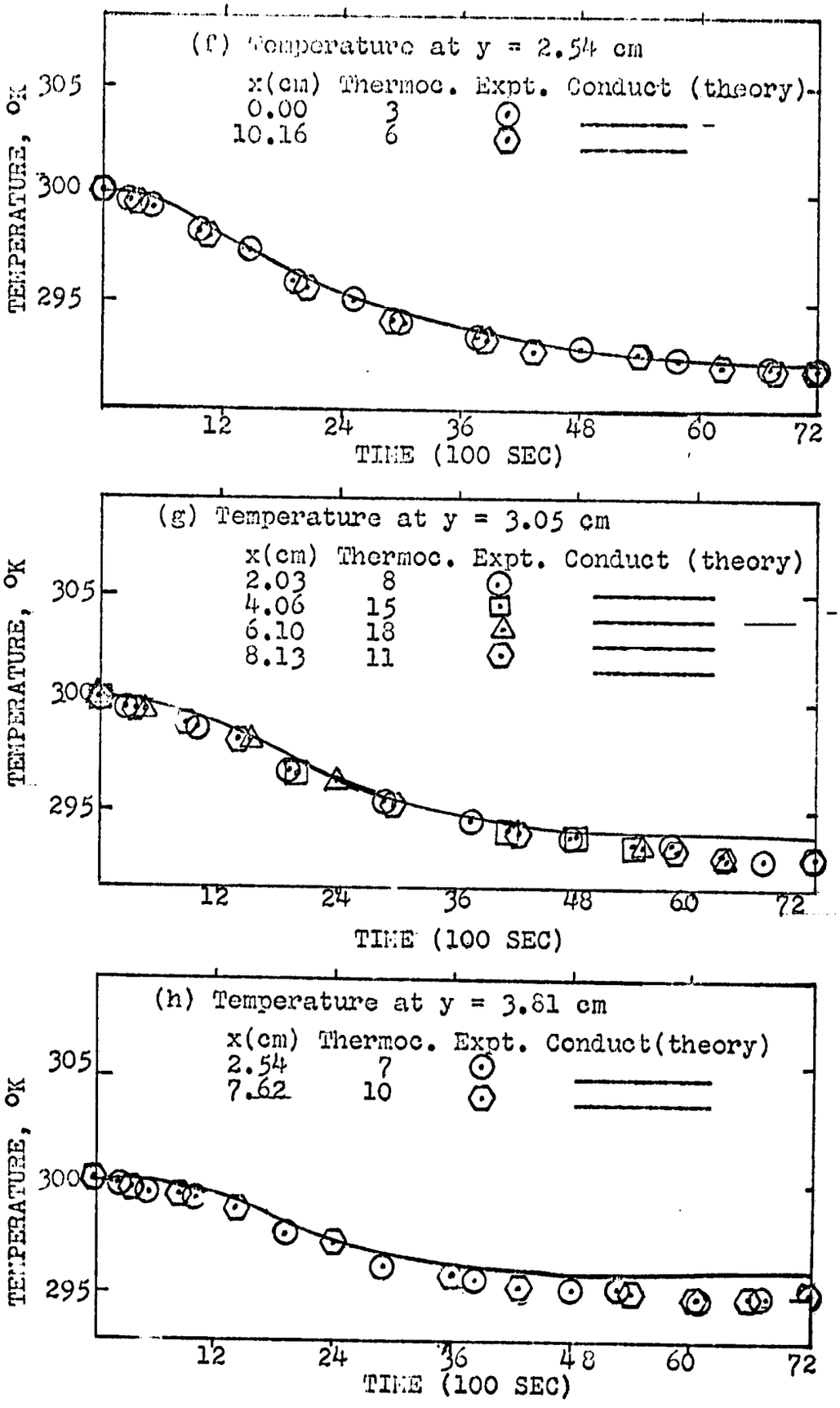

FIGURE 10. EXPERIMENTAL AND THEORETICAL DATA FOR RUN 6:
$\alpha = 15^{o}$; $T_a = 298.72\ ^{o}K$

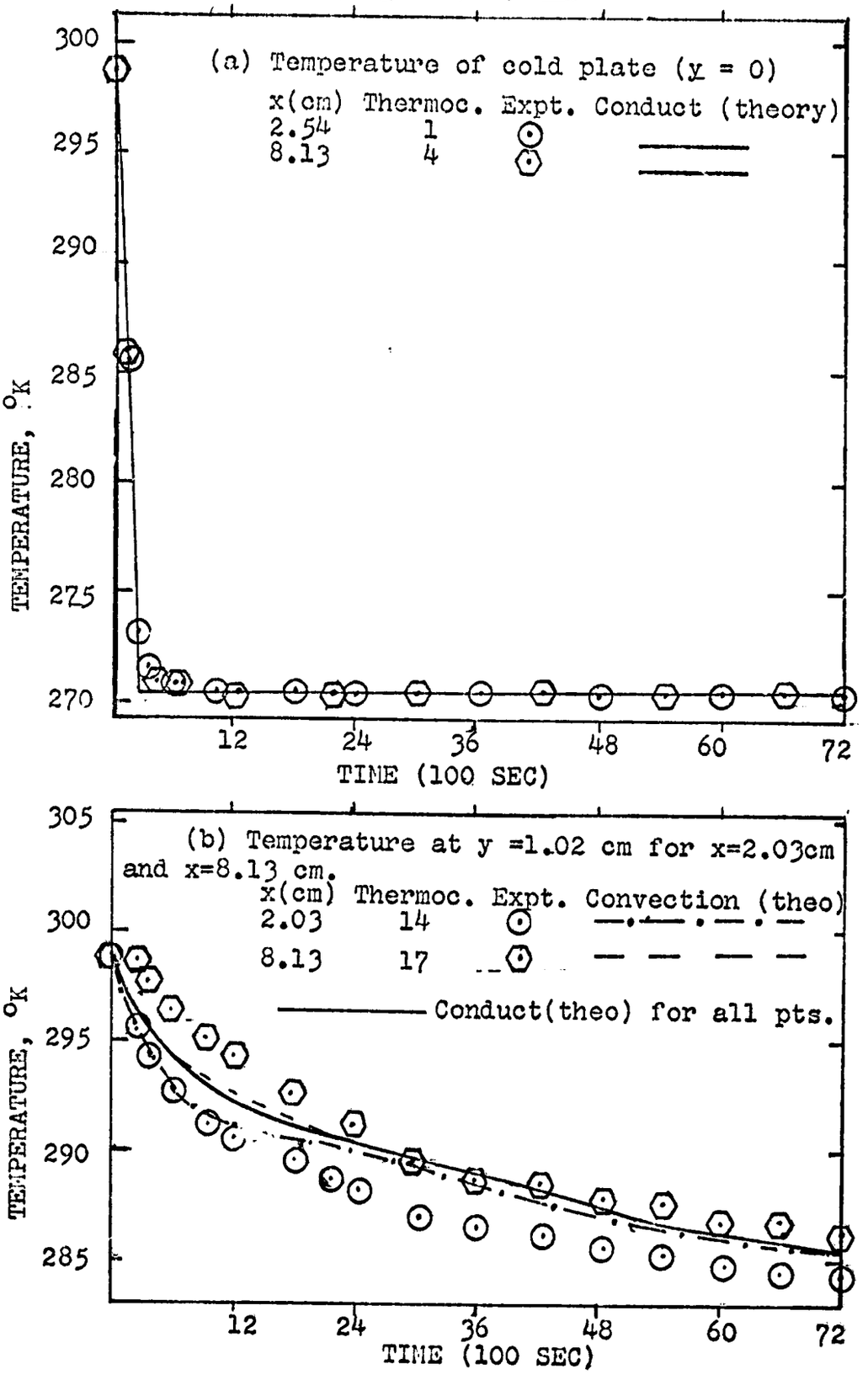

FIGURE 10 (contd). RUN 6: $\alpha = 15^{o}$; Ta = 298.72 ^{o}K

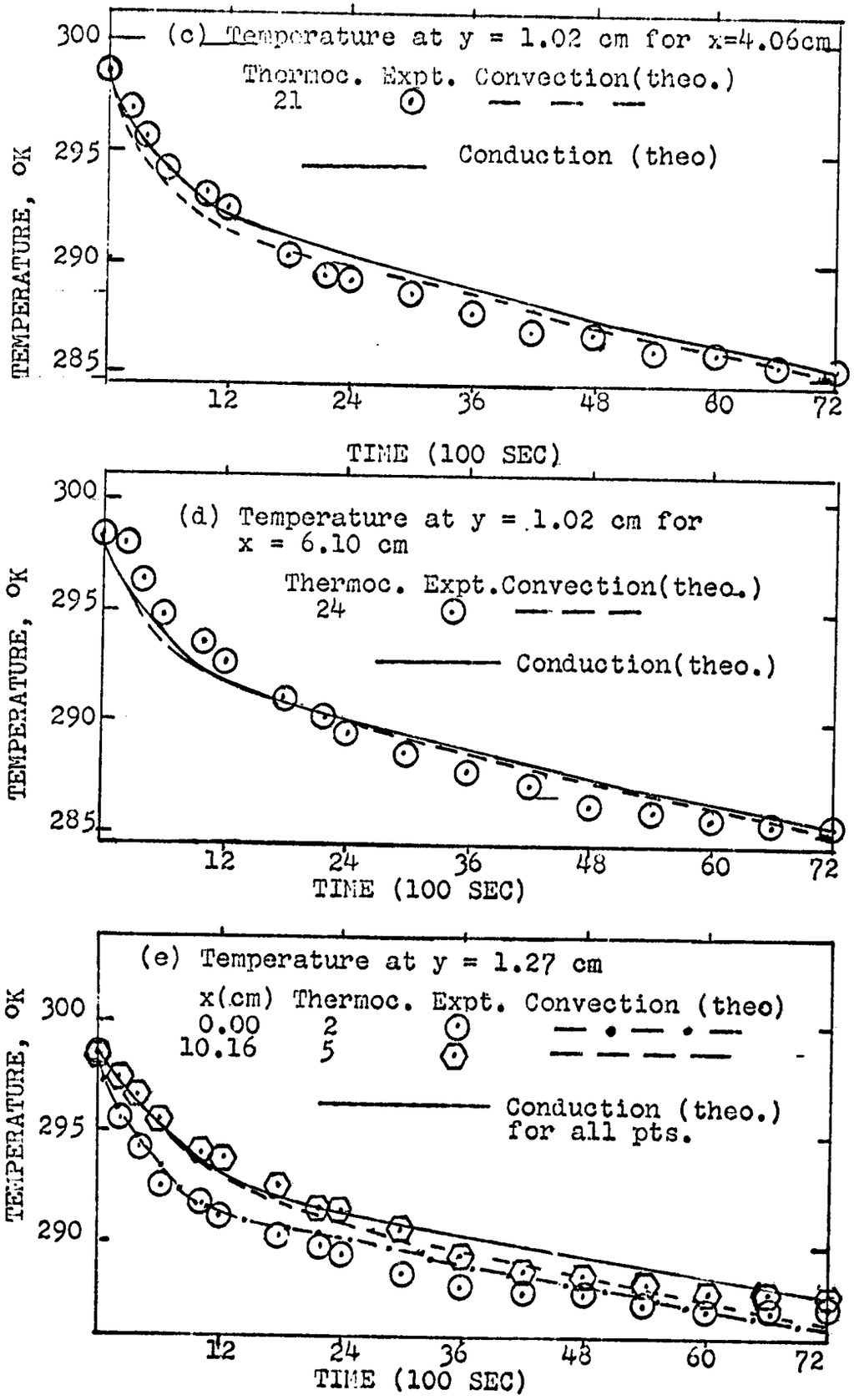

FIGURE 10 (contd). RUN 6: $\alpha = 15^{o}$; $T_a = 298.72\ ^{o}K$

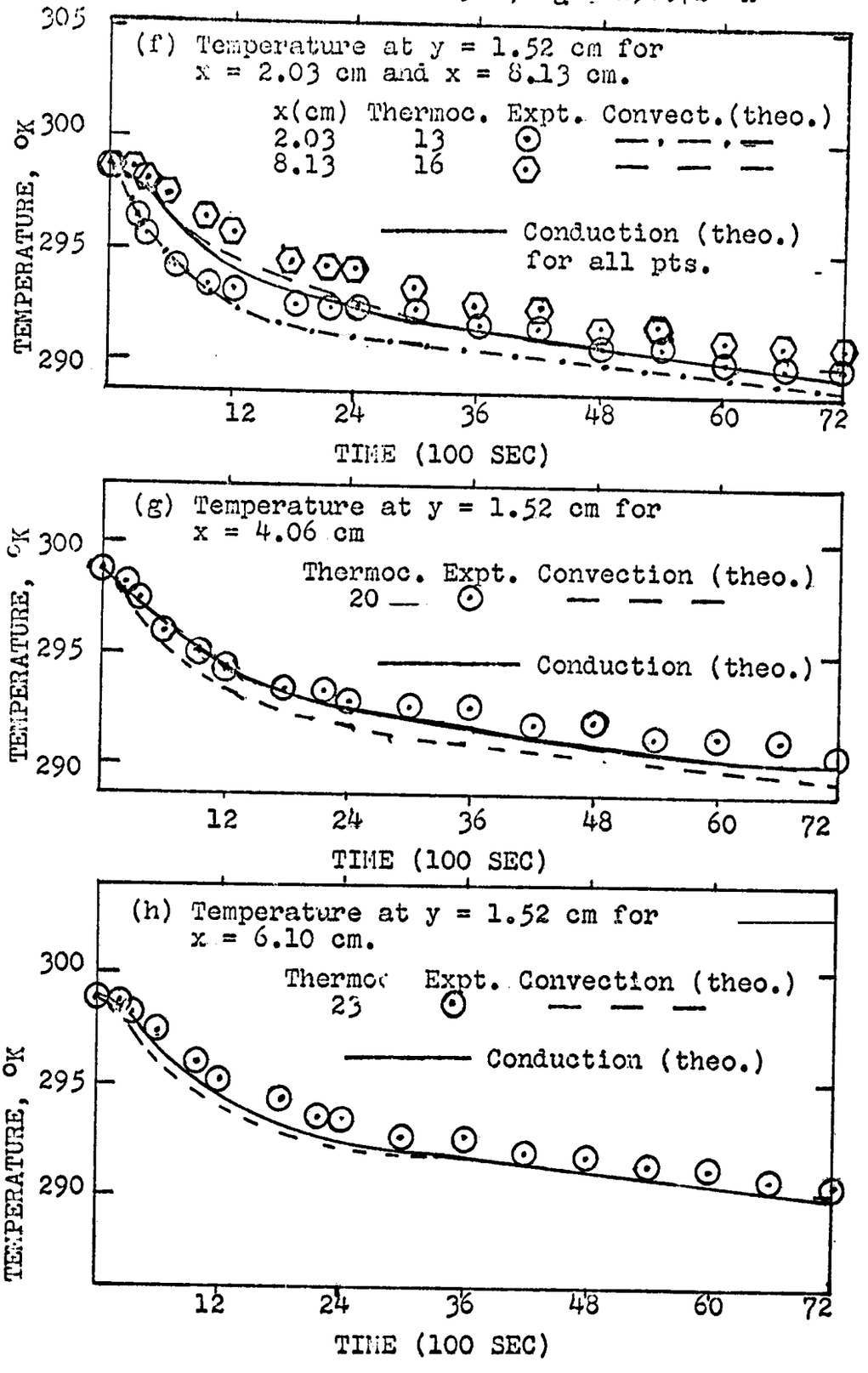

FIGURE 10 (contd). RUN 6: $\alpha = 15^{o}$; $T_a = 298.72\ ^{o}K$

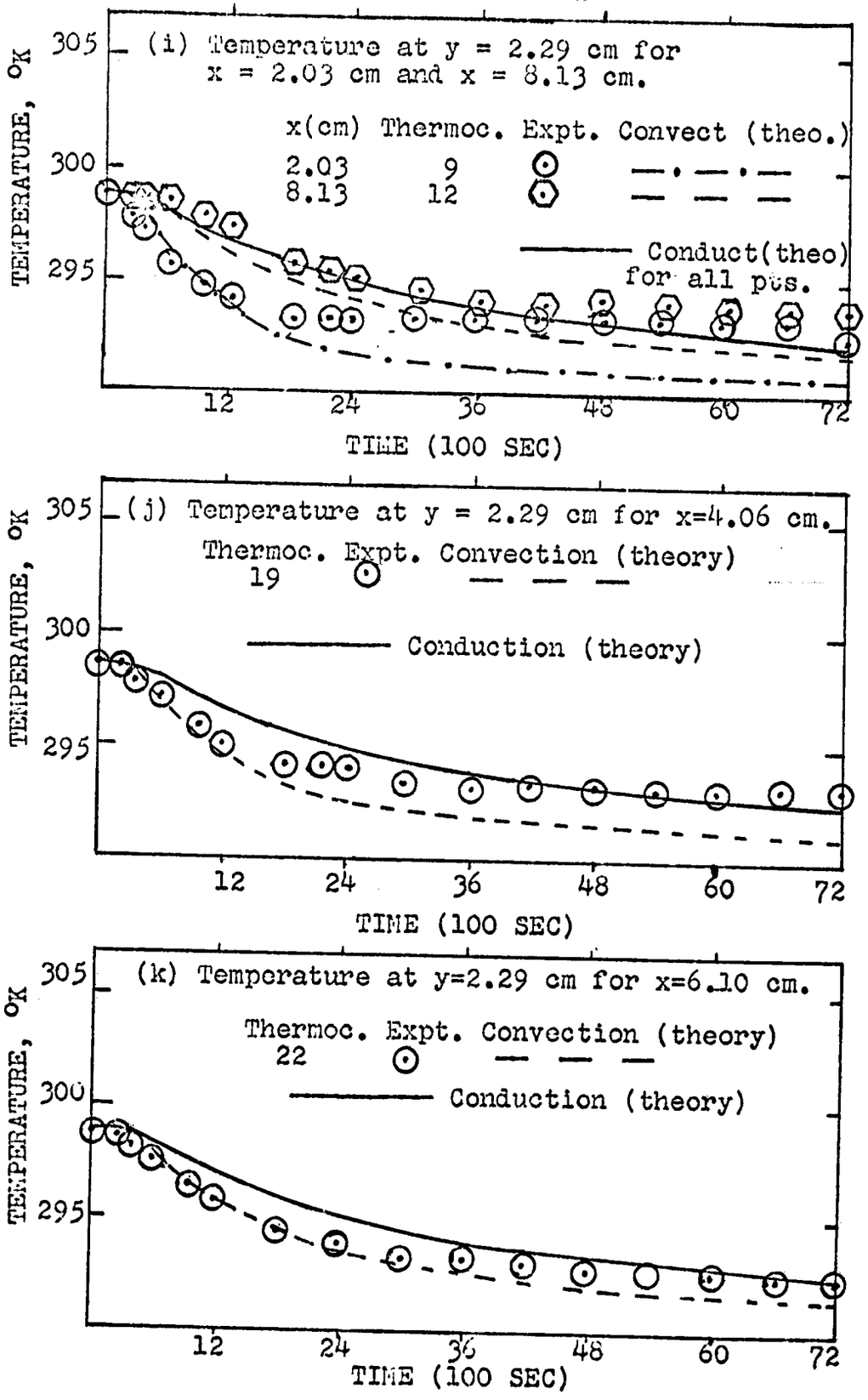

FIGURE 10 (contd). RUN 6: $\alpha = 15^{\circ}$; $T_a = 298.72\ ^{\circ}K$

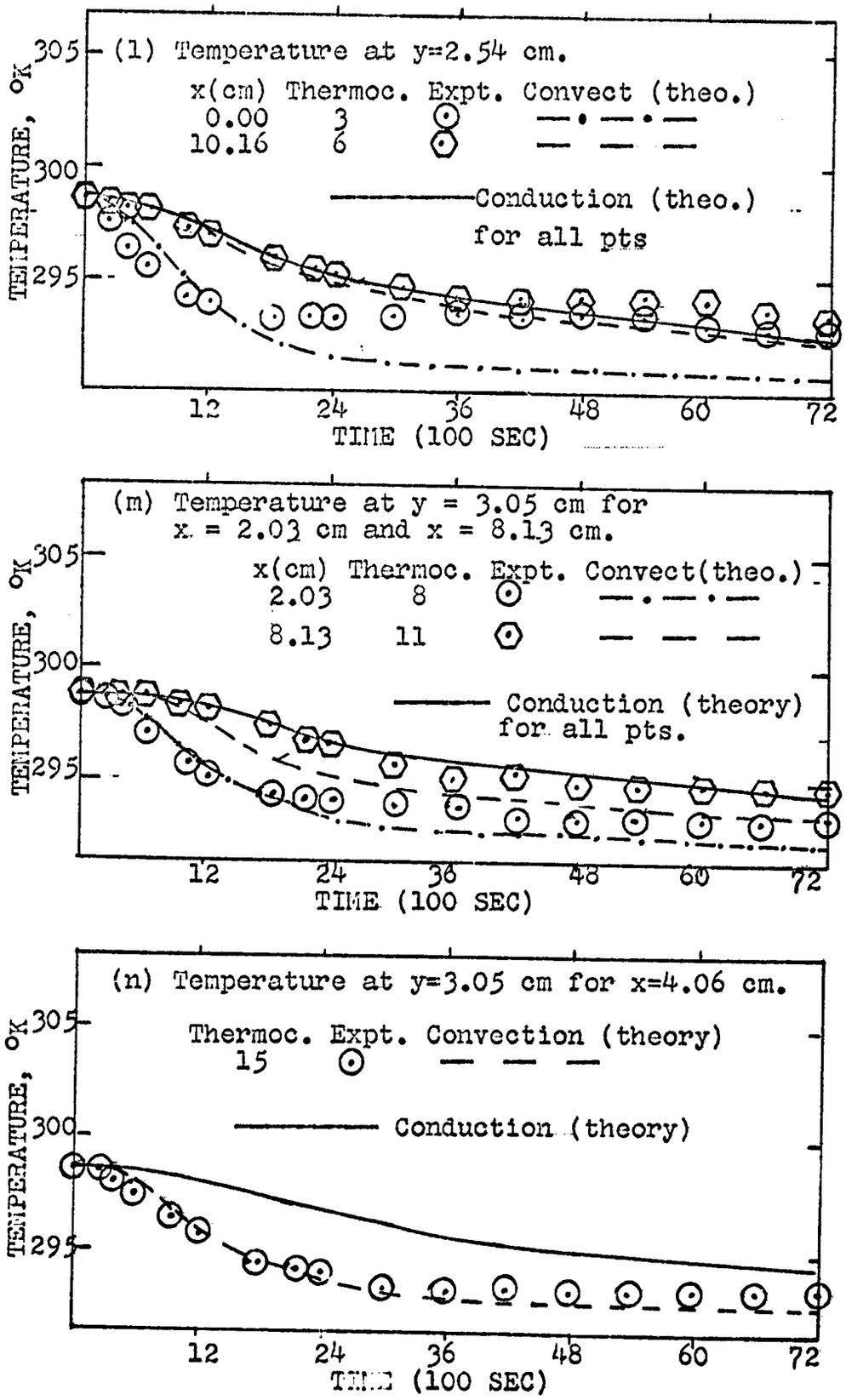

FIGURE 10 (contd). RUN 6: $\alpha = 15^{\circ}$; $T_a = 298.72\ ^{\circ}K$

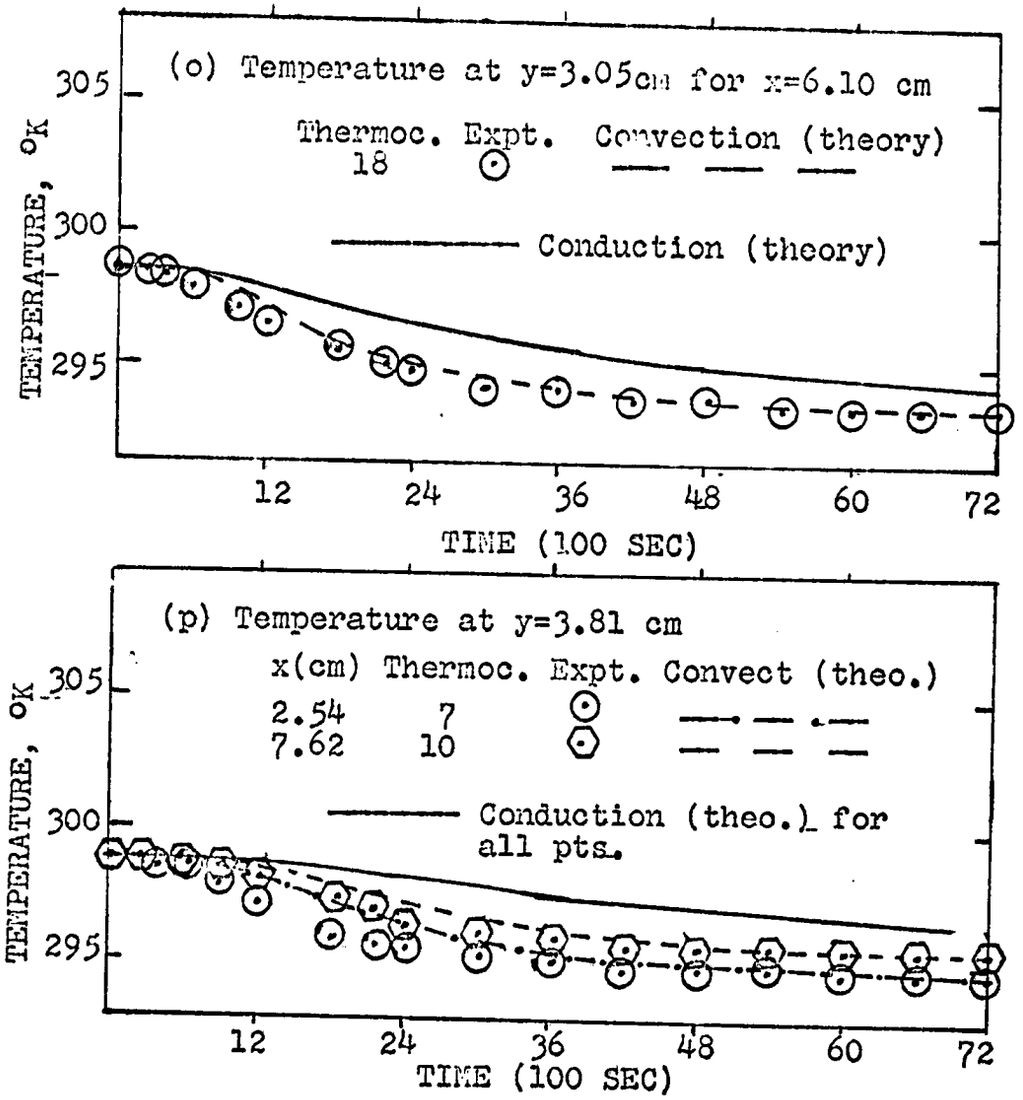

FIGURE 11. INITIAL STREAMLINES IN TEST CELL (THEORETICAL).

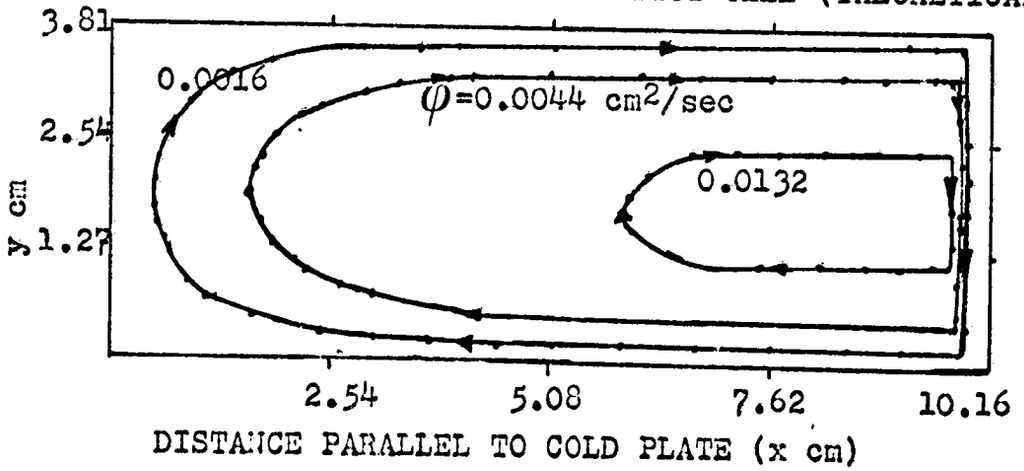

FIGURE 12. HEIGHT OF SOLID PHASE AT $\alpha = 15^{\circ}$

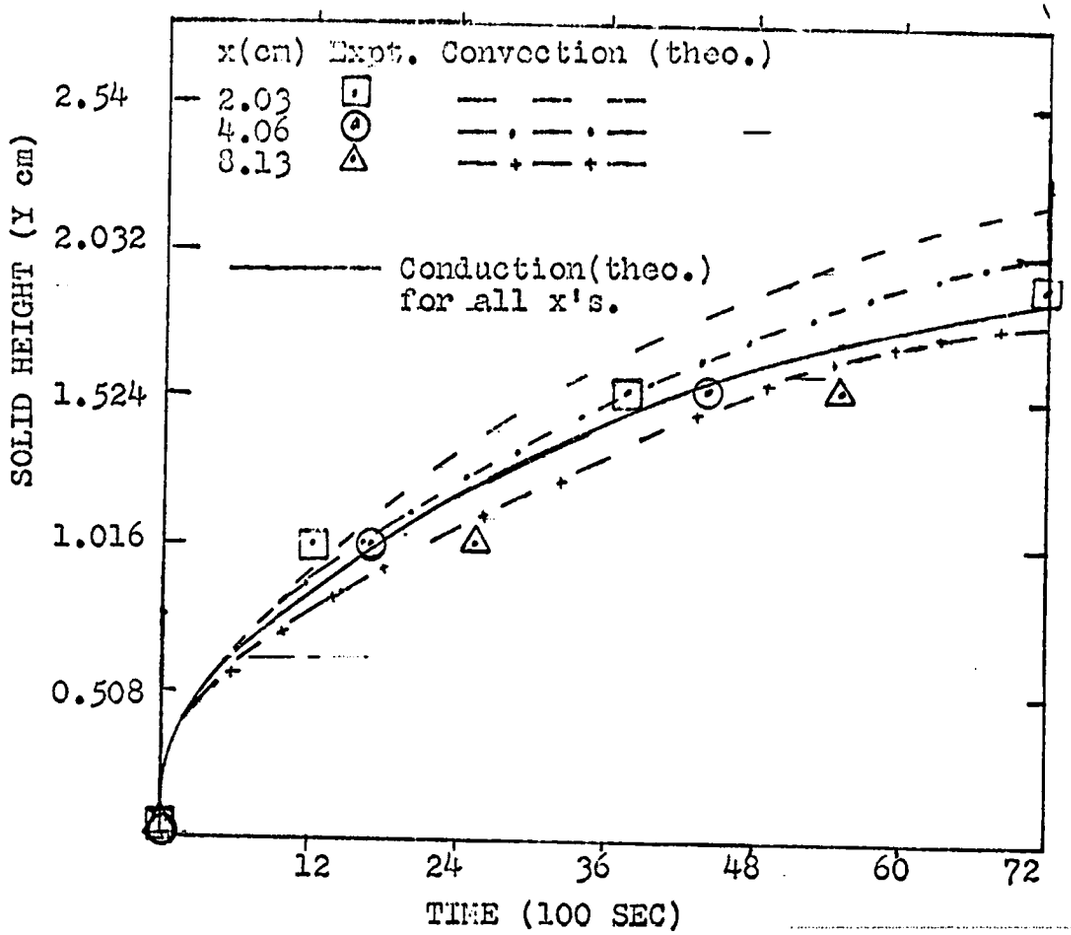

FIGURE 13. INTERFACE SHAPE AT t = 7200 SEC (THEORETICAL)

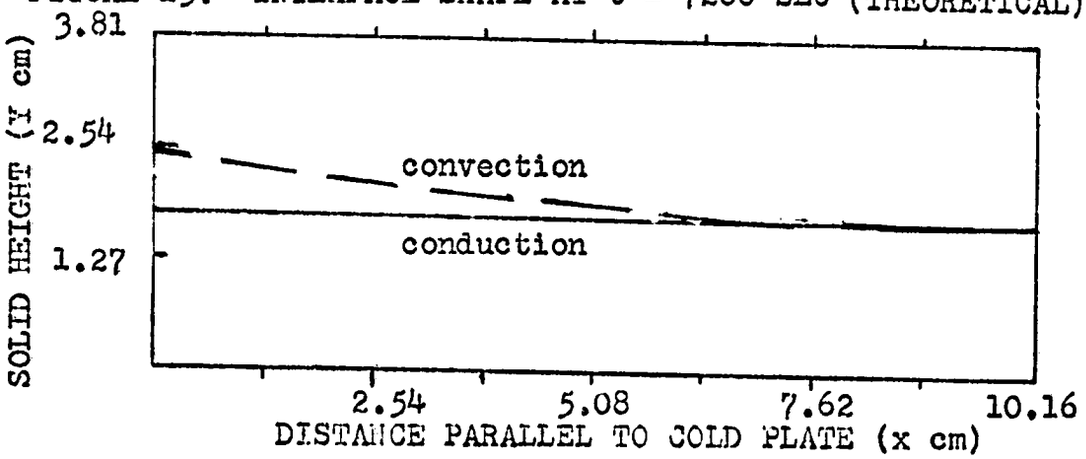

FIGURE 14. EXPERIMENTAL AND THEORETICAL DATA FOR RUN 7: $\alpha = 60^{\circ}$; $T_a = 298.72\ ^{\circ}K$

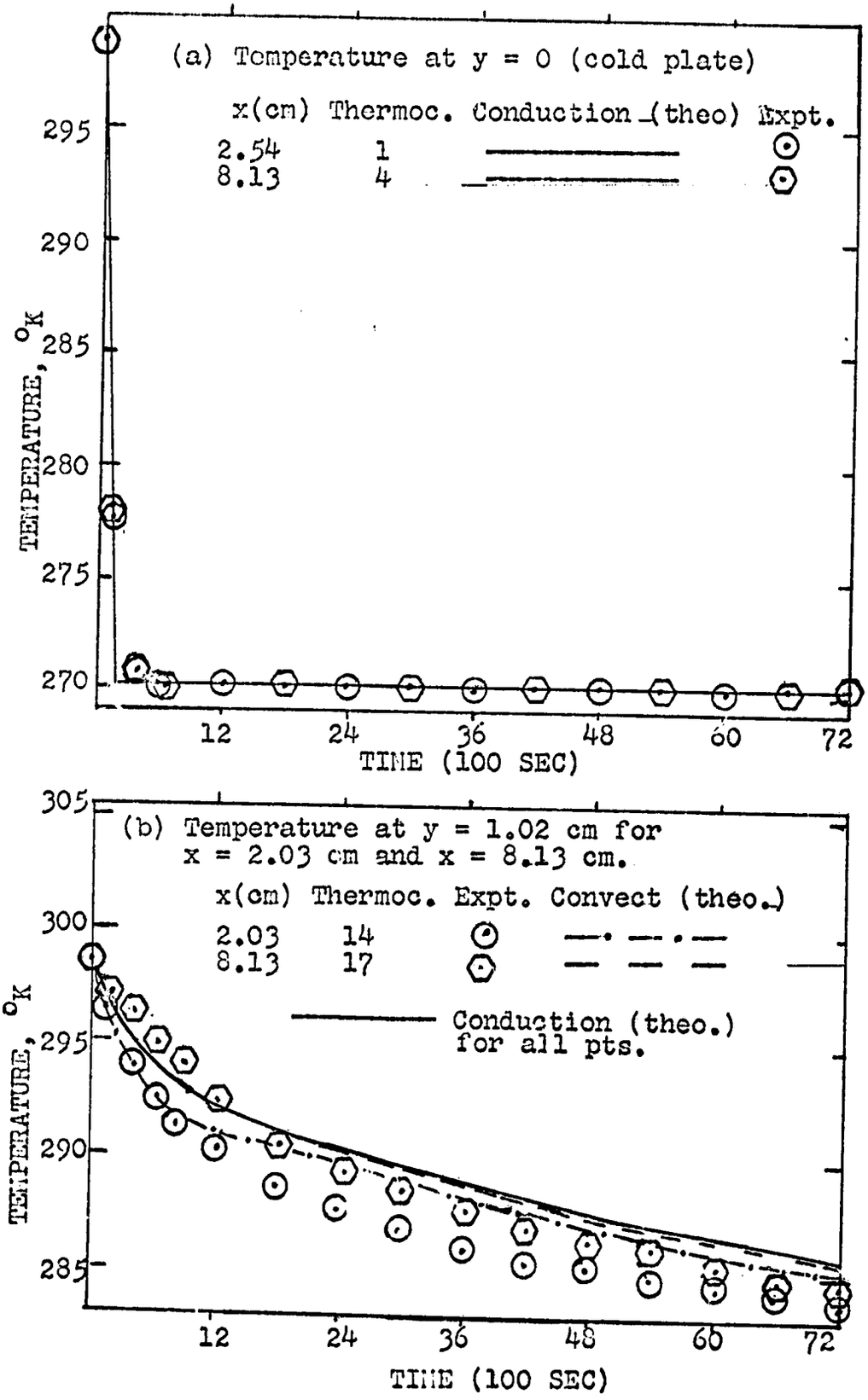

FIGURE 14 (contd). RUN 7: $\alpha = 60^{\circ}$; $T_a = 298.72\ ^{\circ}K$

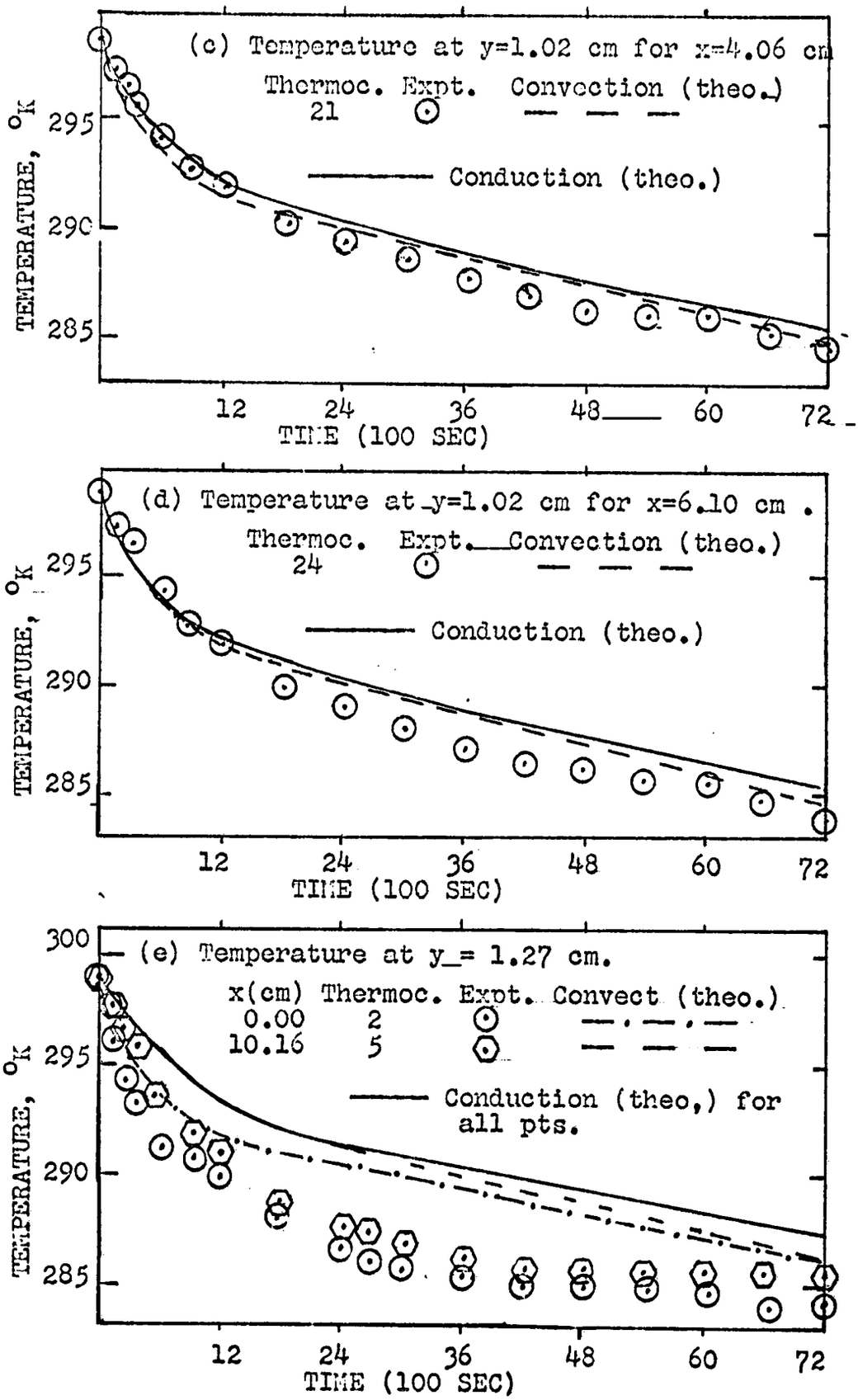

FIGURE 14 (contd). RUN 7: $\alpha = 60^{\circ}$; $T_a = 298.72\ ^{\circ}K$

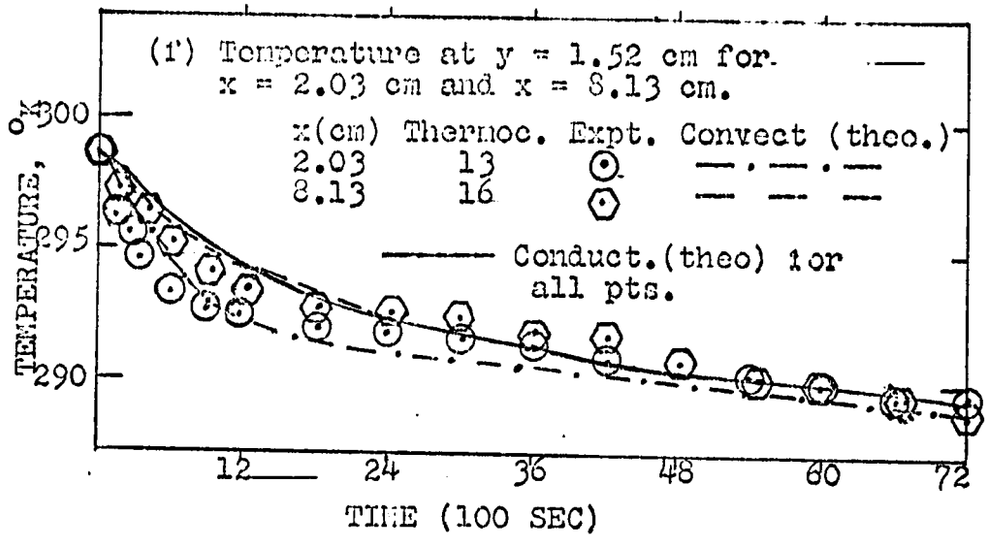

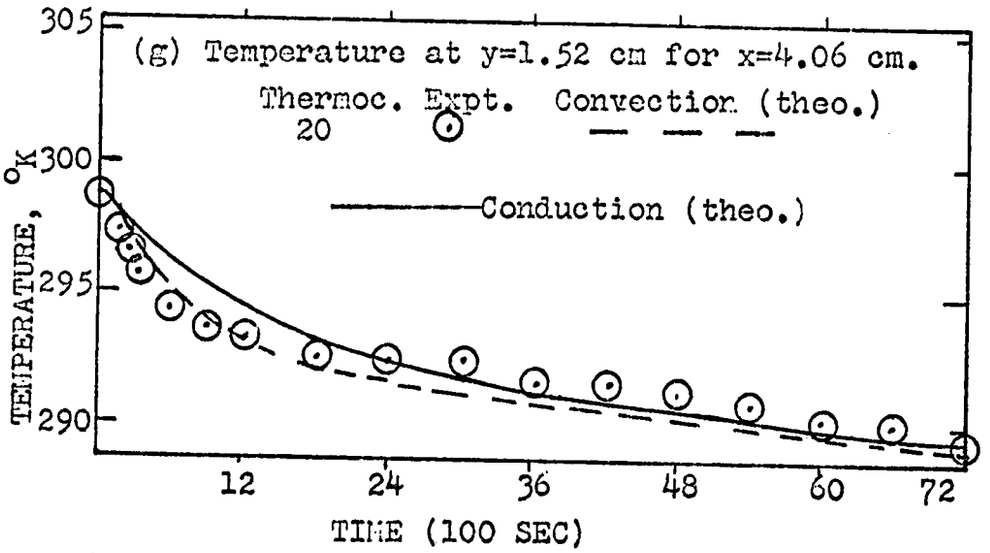

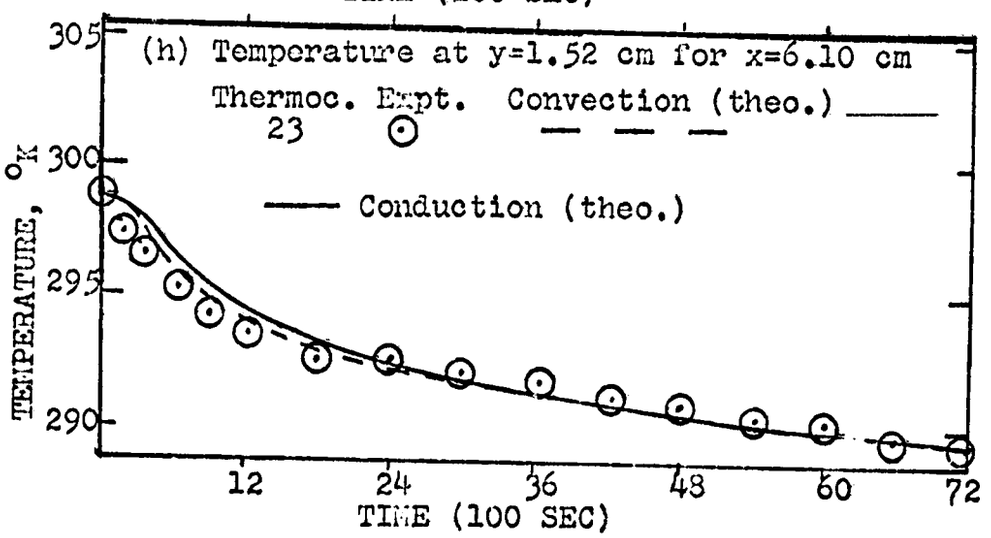

FIGURE 14 (contd). RUN 7: $\alpha = 60^{\circ}$; $T_a = 298.72\ ^{\circ}K$

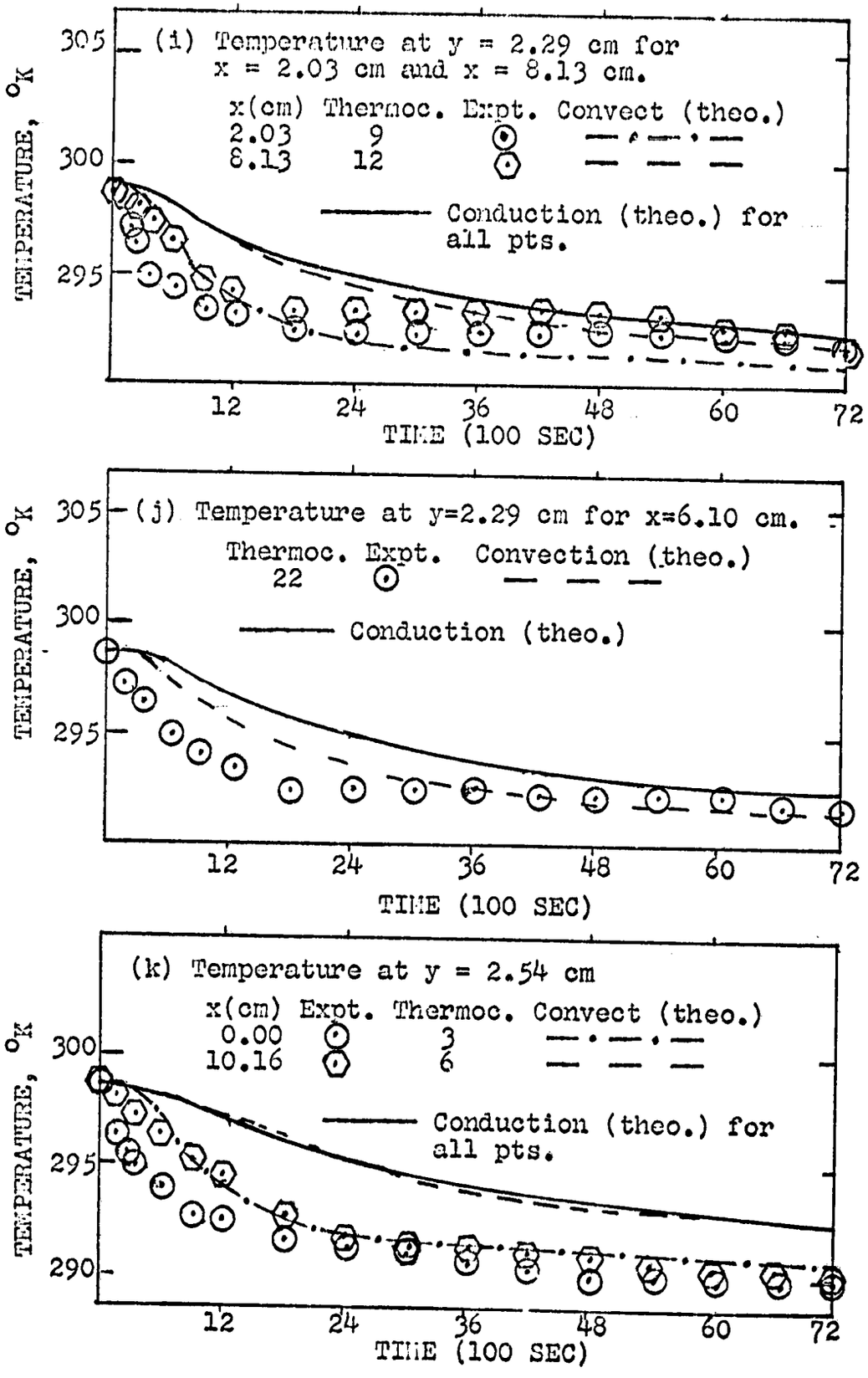

FIGURE 14 (contd). RUN 7: $\alpha = 60^{\circ}$; $T_a = 298.72\ ^{\circ}K$

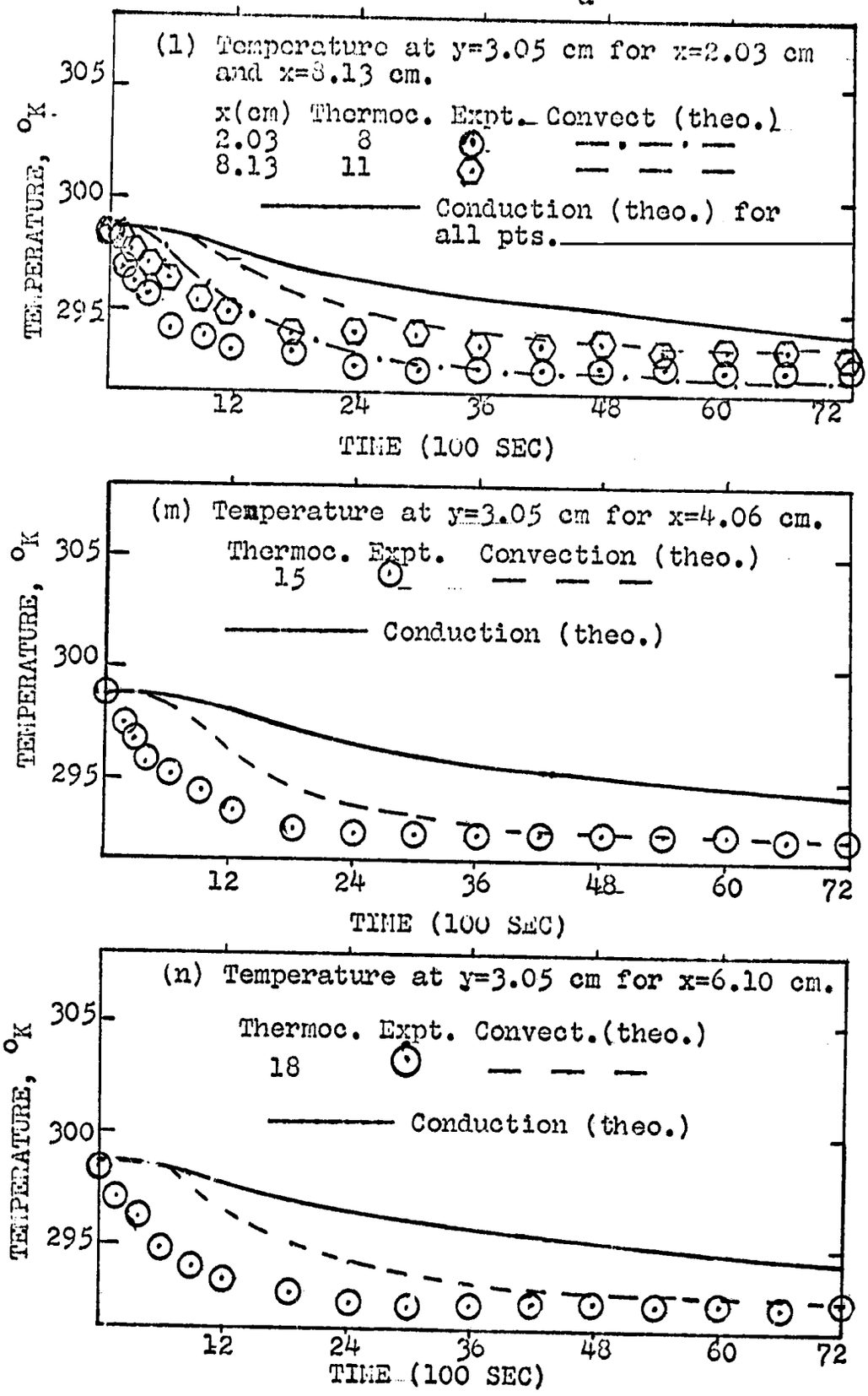

FIGURE 14 (contd). RUN 7: $\alpha = 60^{\circ}$; $T_a = 298.72\ ^{\circ}K$

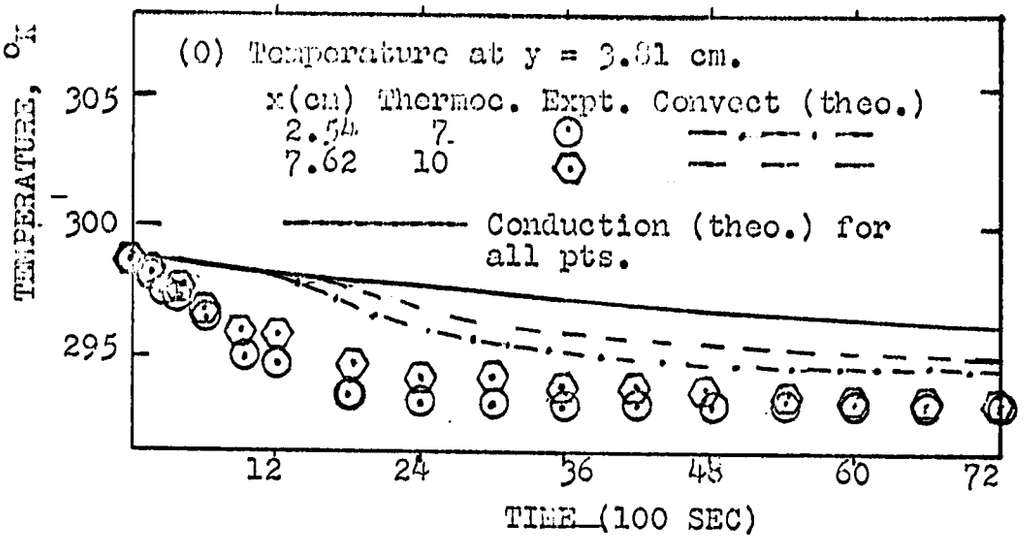

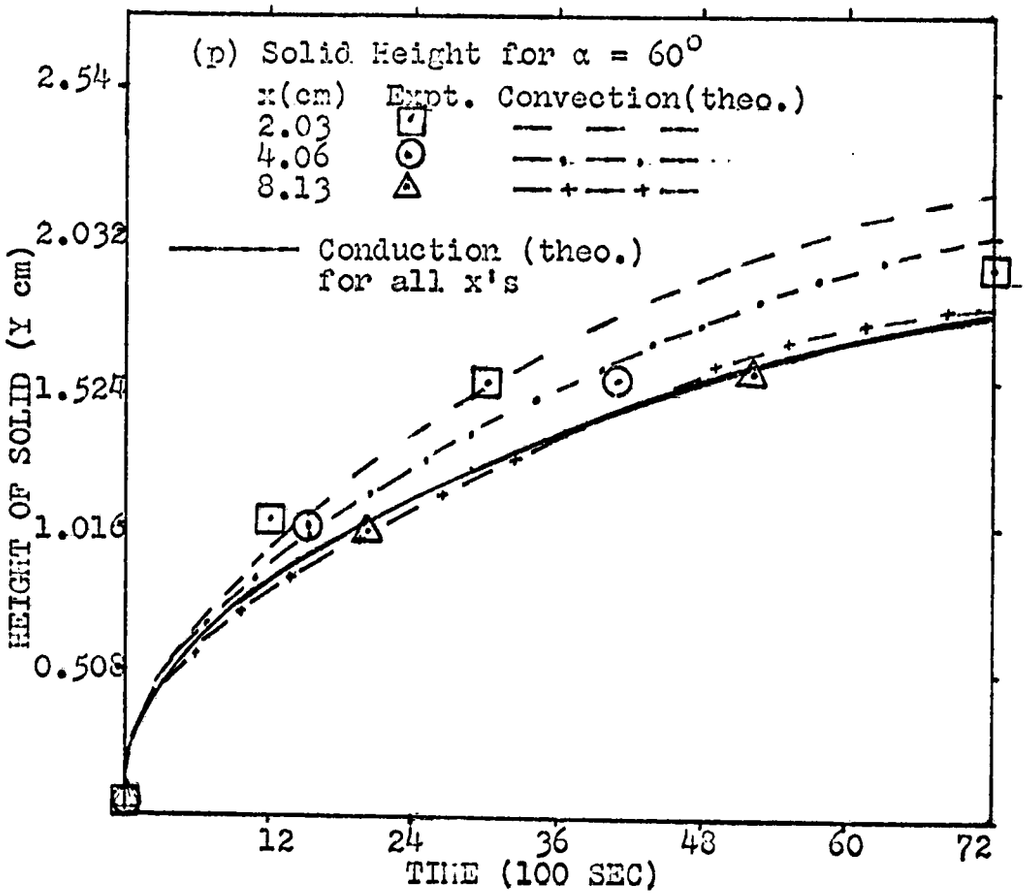

FIGURE 15. EXPERIMENTAL AND THEORETICAL DATA FOR RUN 9: $\alpha = 30^{\circ}$; $T_a = 301.22\ ^{\circ}K$

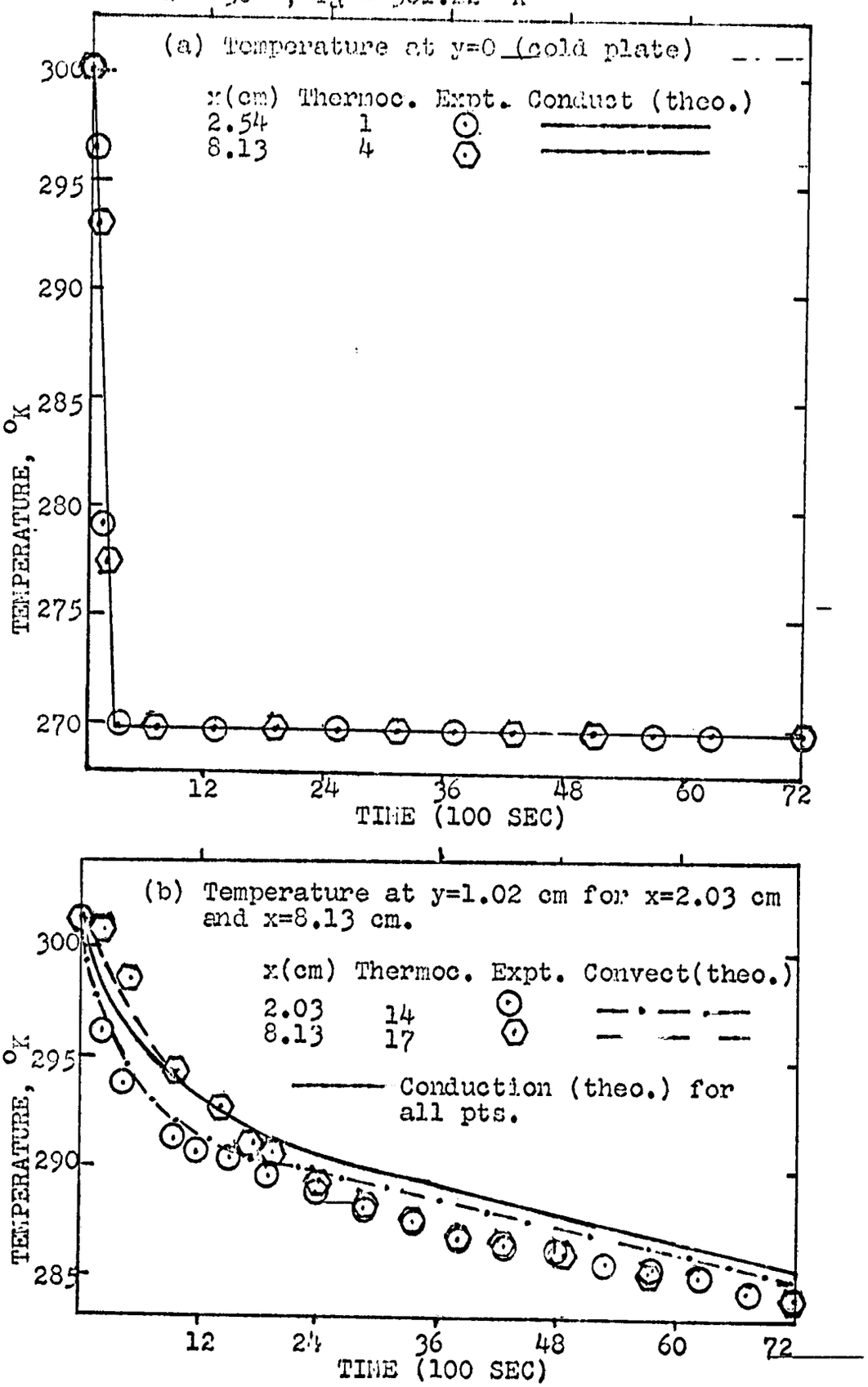

FIGURE 15 (contd). RUN 9: $\alpha = 30^{\circ}$; $T_a = 301.22\ ^{\circ}K$

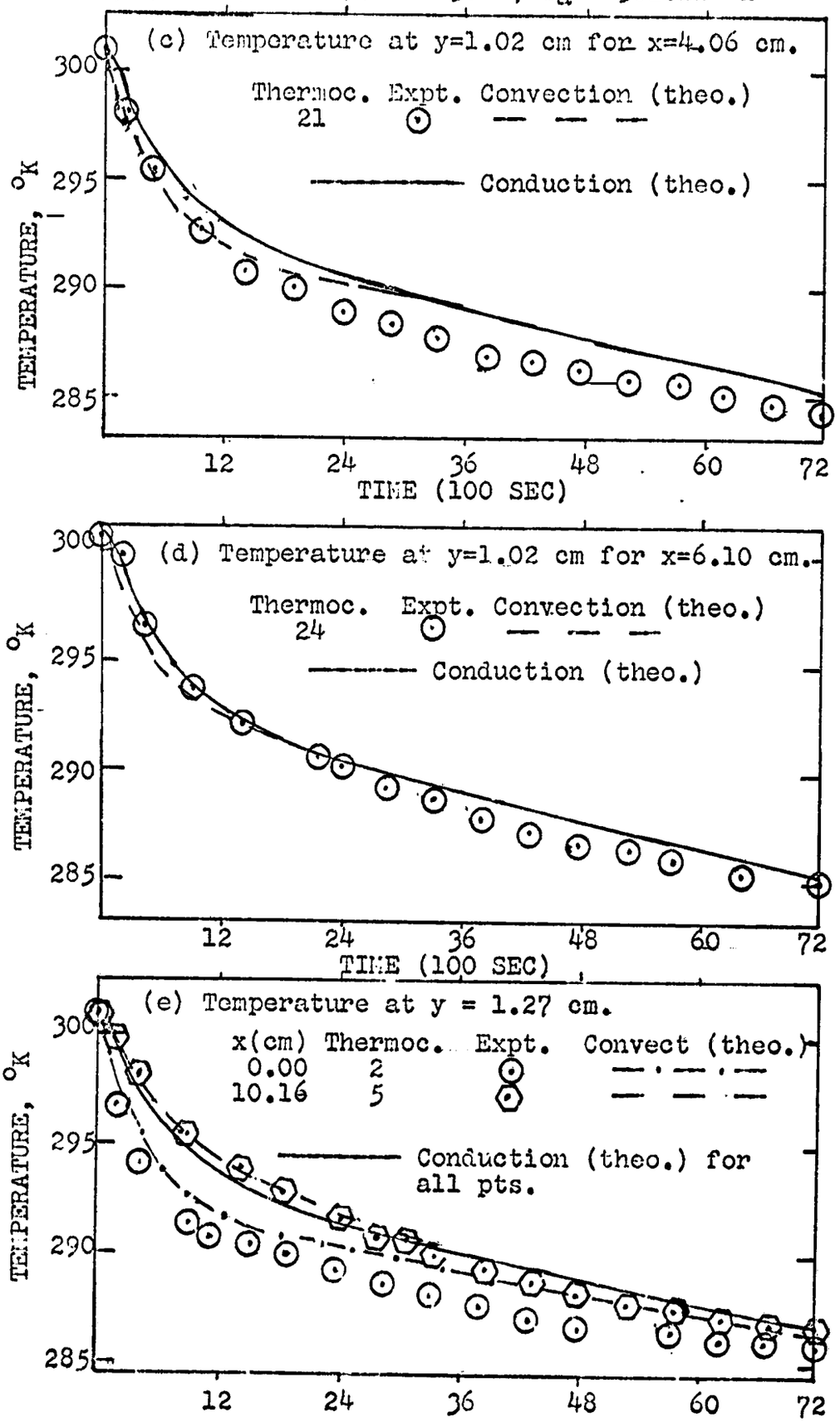

FIGURE 15 (contd). RUN 9: $\alpha = 30^{\circ}$; $T_a = 301.22\ ^{\circ}K$

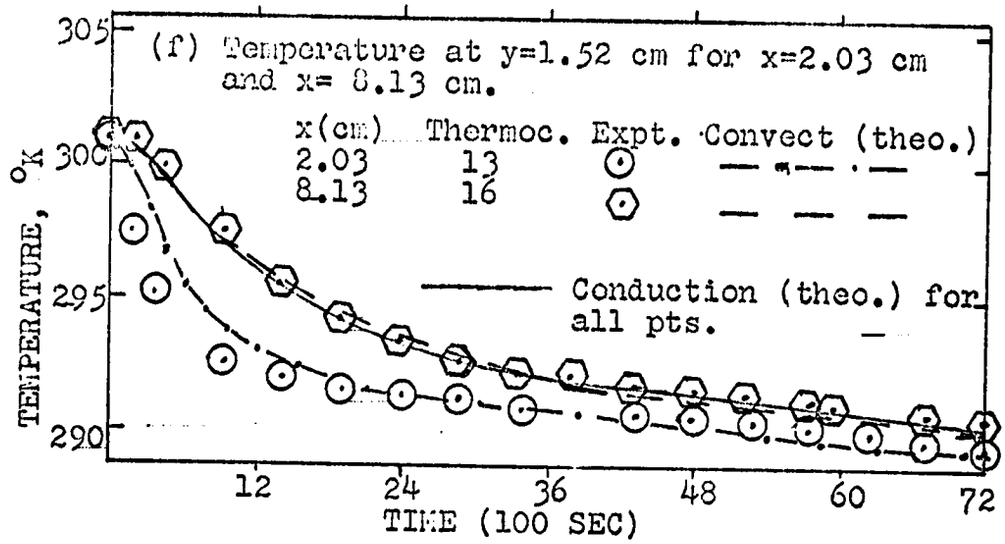

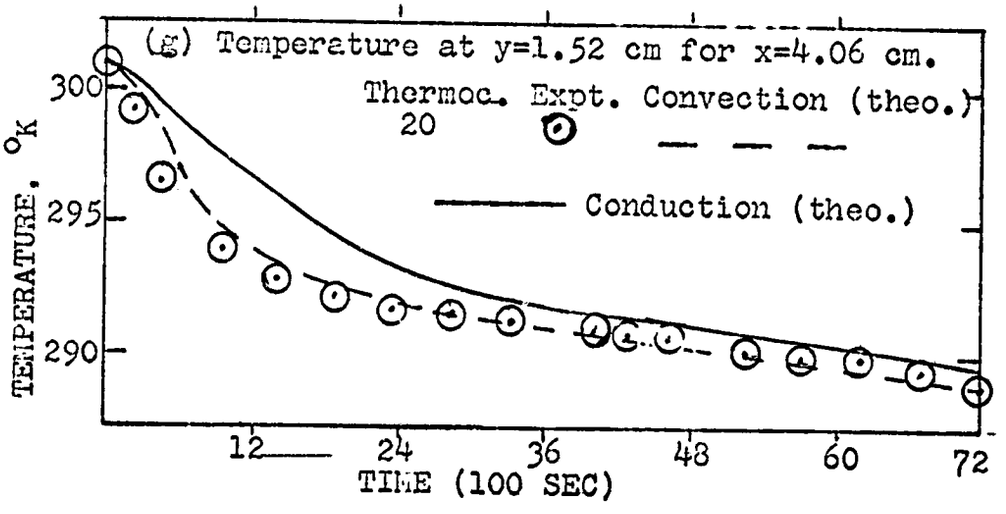

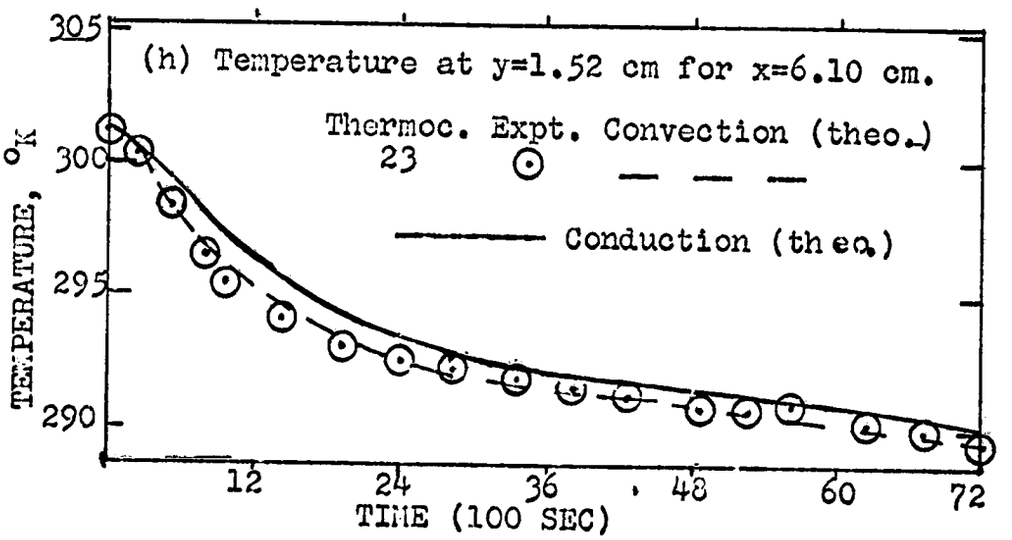

FIGURE 15 (contd). RUN 9: $\alpha = 30^{\circ}$; $T_a = 301.22\ ^{\circ}K$

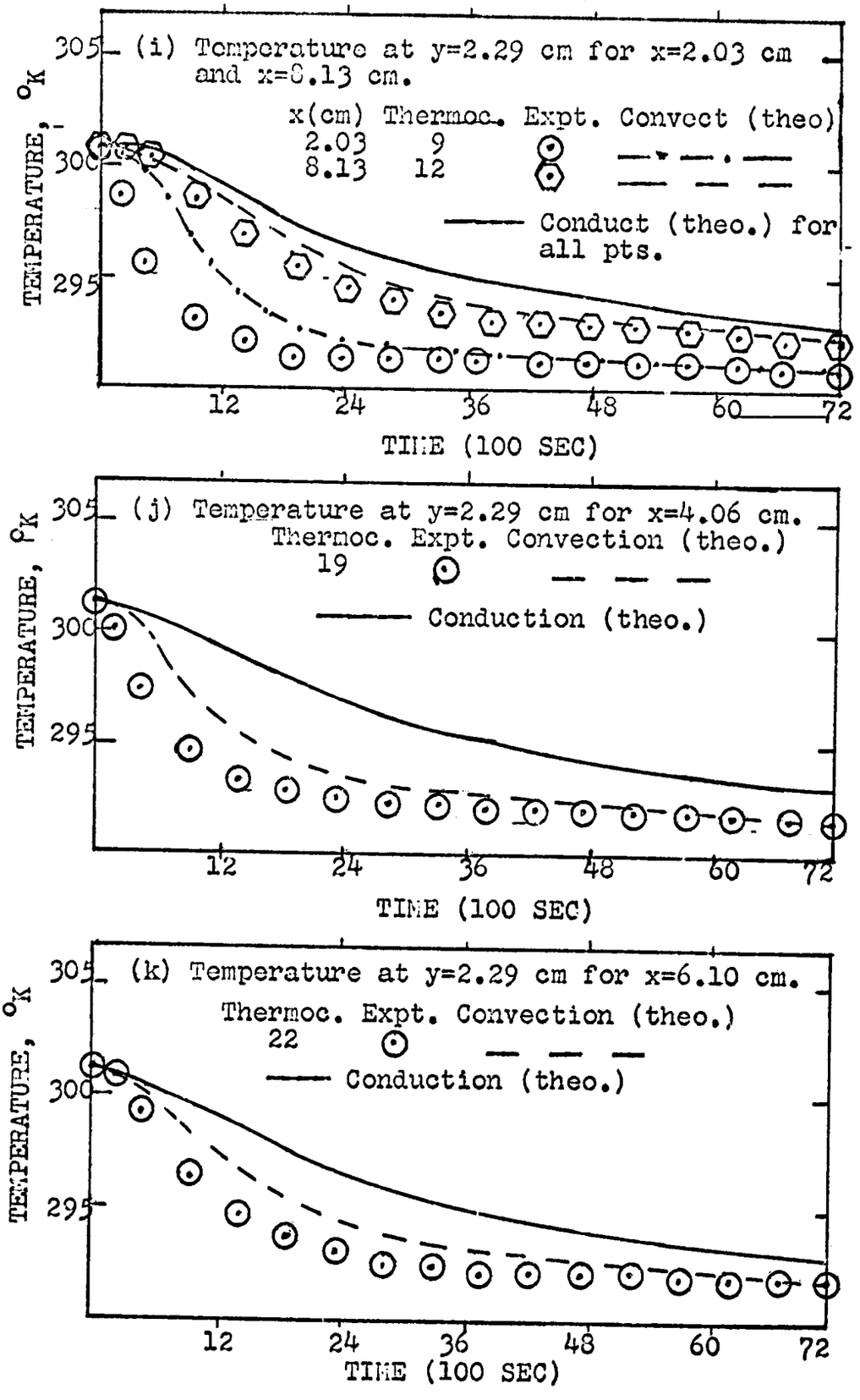

FIGURE 15 (contd). RUN 9: $\alpha = 30^{\circ}$; $T_a = 301.22\ ^{\circ}K$

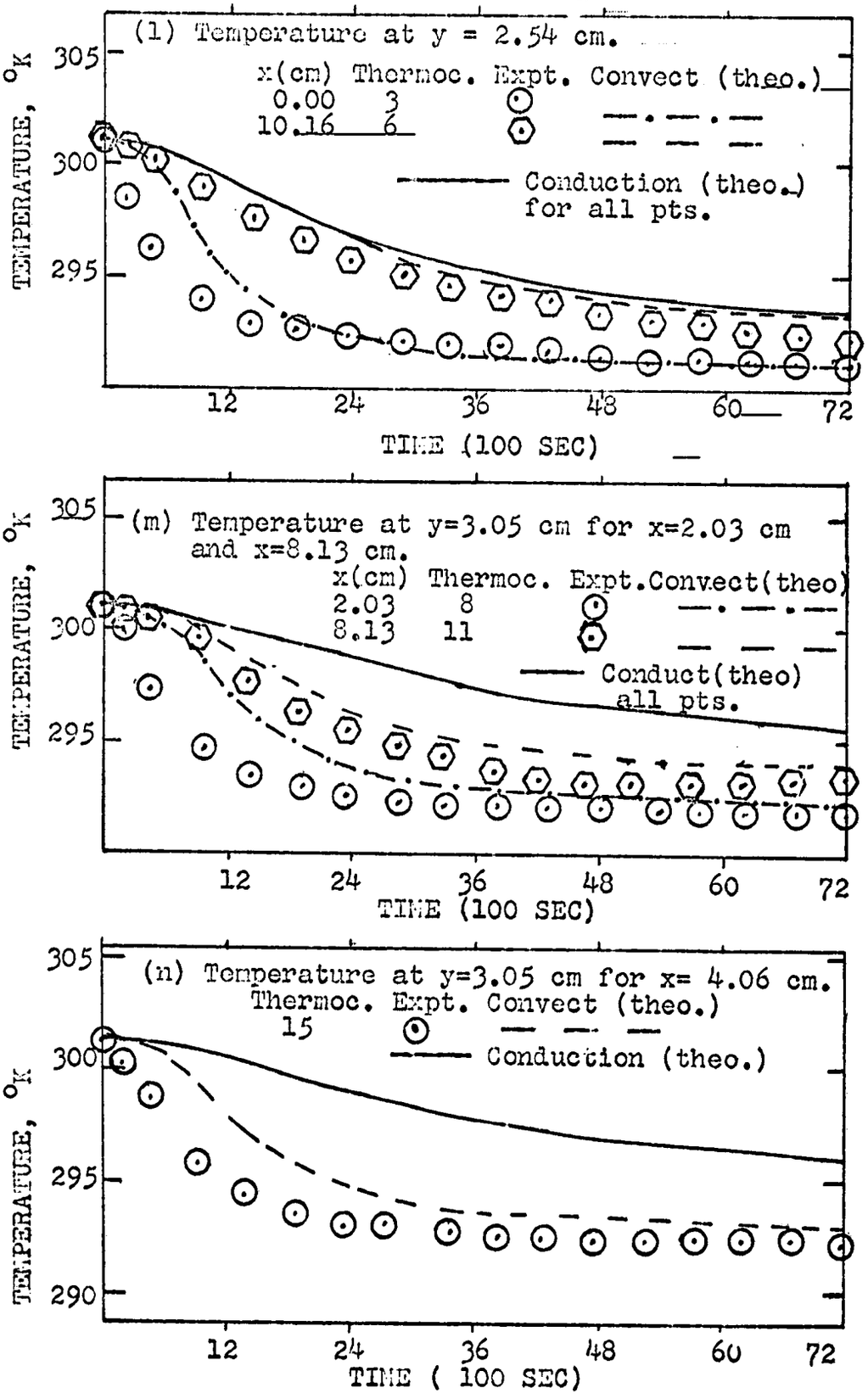

FIGURE 15 (contd). RUN 9: $\alpha = 30^{\circ}$; $T_a = 301.22\ ^{\circ}K$

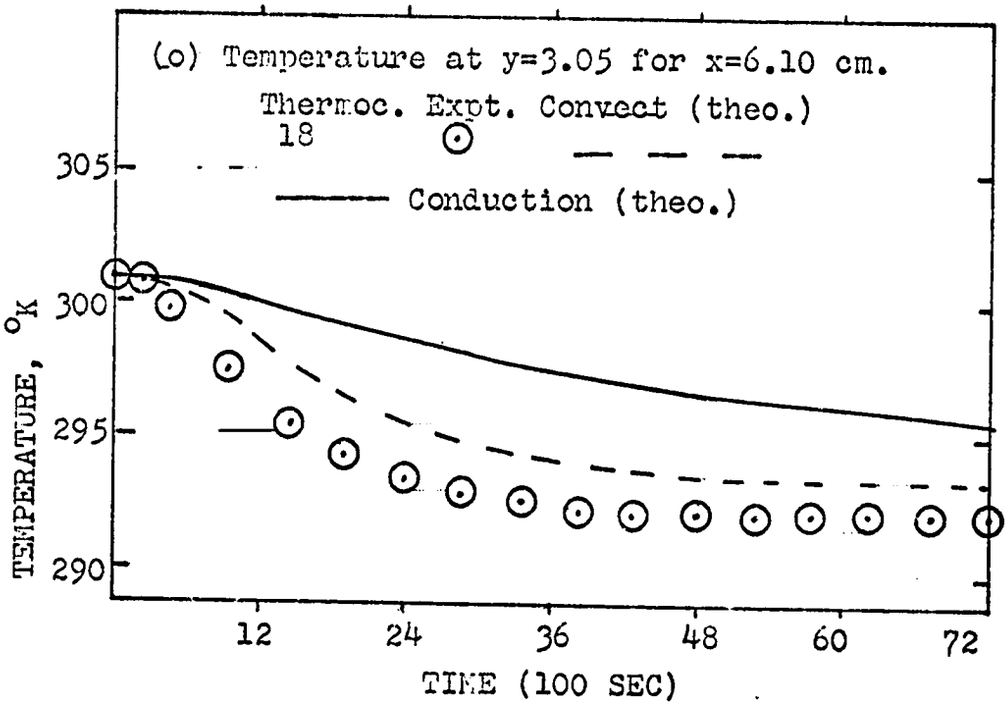

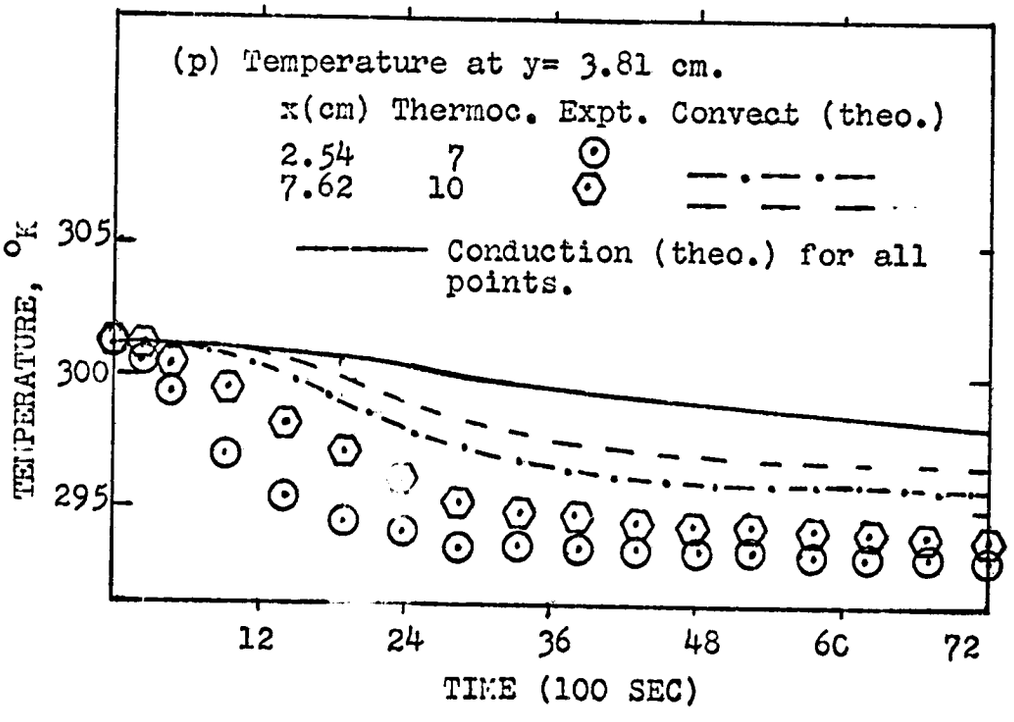

FIGURE 16. EXPERIMENTAL AND THEORETICAL DATA FOR RUN 11:
$\alpha = 45^{\circ}$; Ta = 300.11 °K

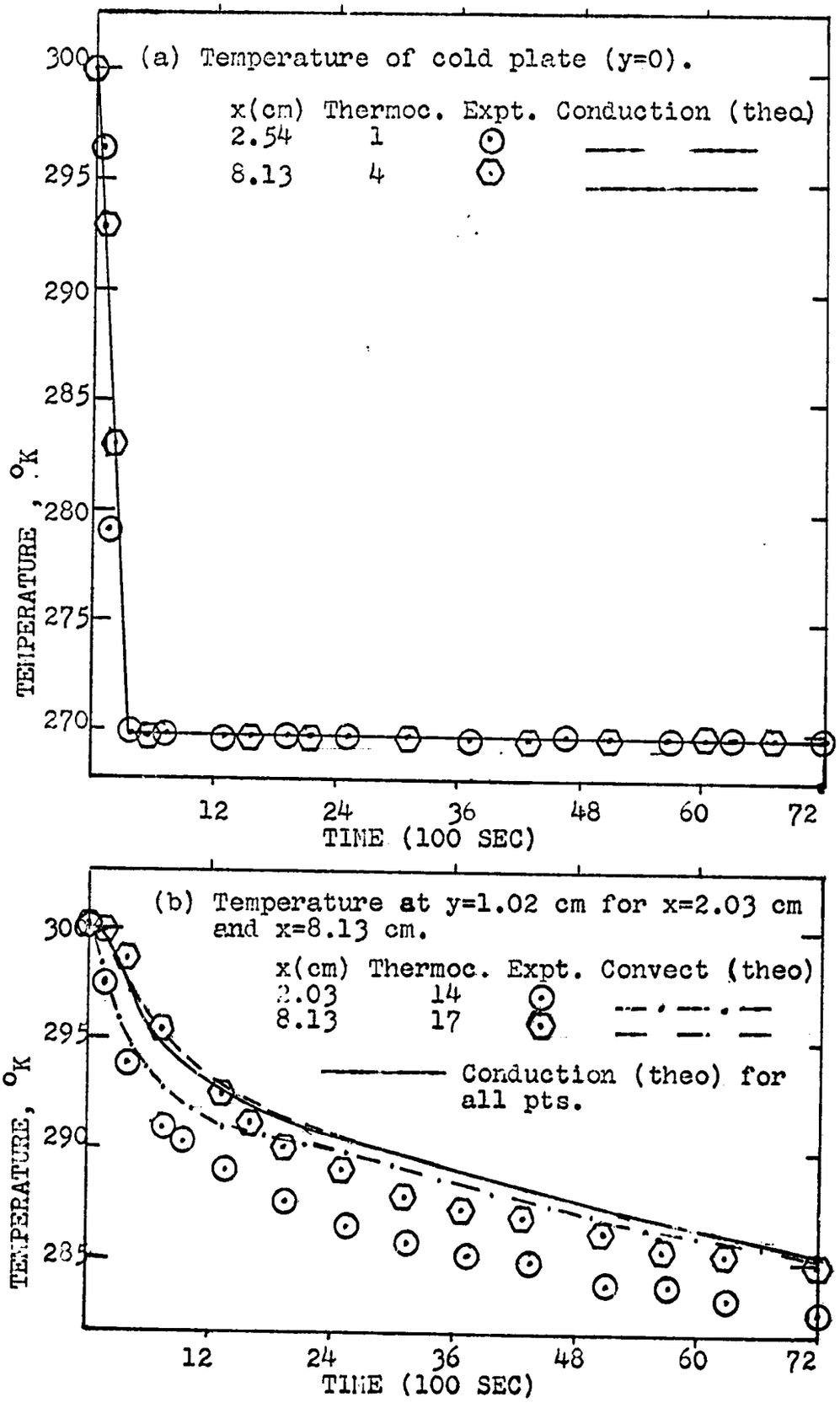

FIGURE 16 (contd)..RUN 11: $\alpha = 45^{\circ}$; $T_a = 300.11^{\circ}K$

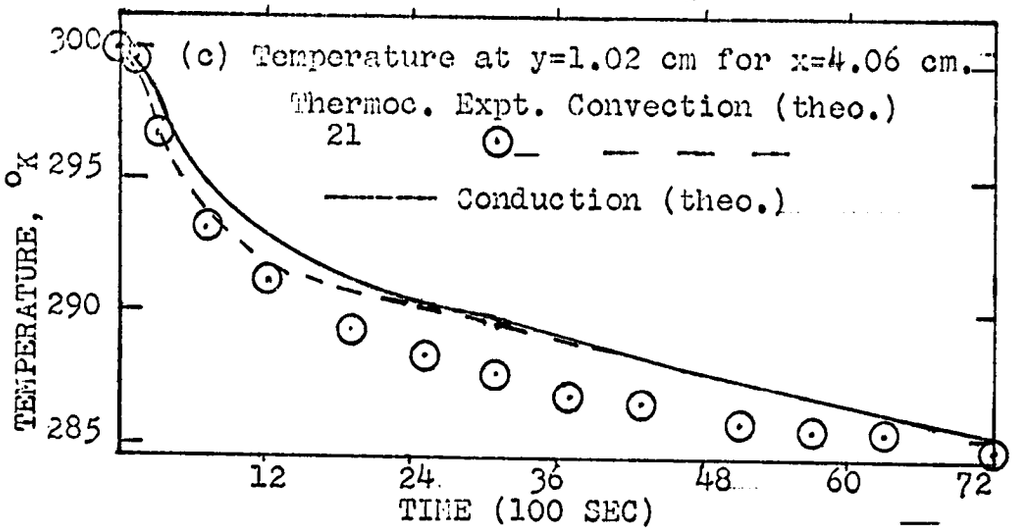

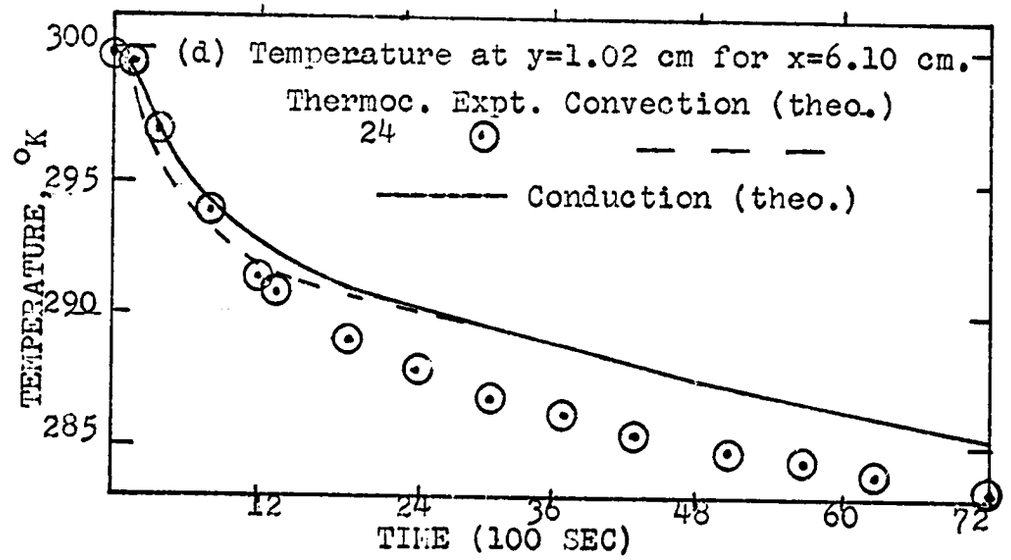

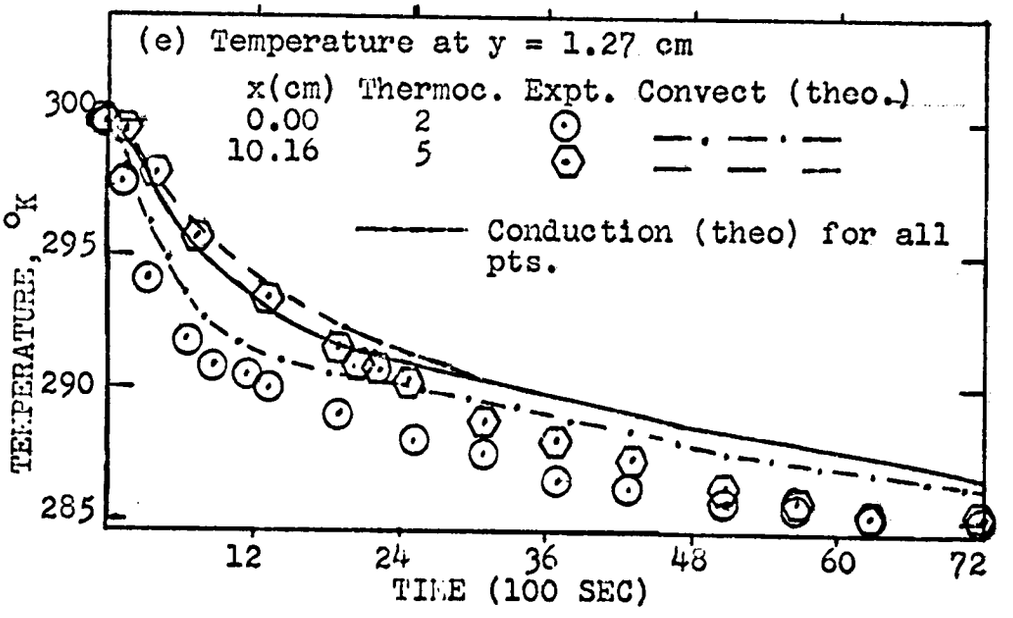

FIGURE 16 (contd). RUN 11: $\alpha = 45^{\circ}$; $T_a = 300.11\ ^{\circ}K$

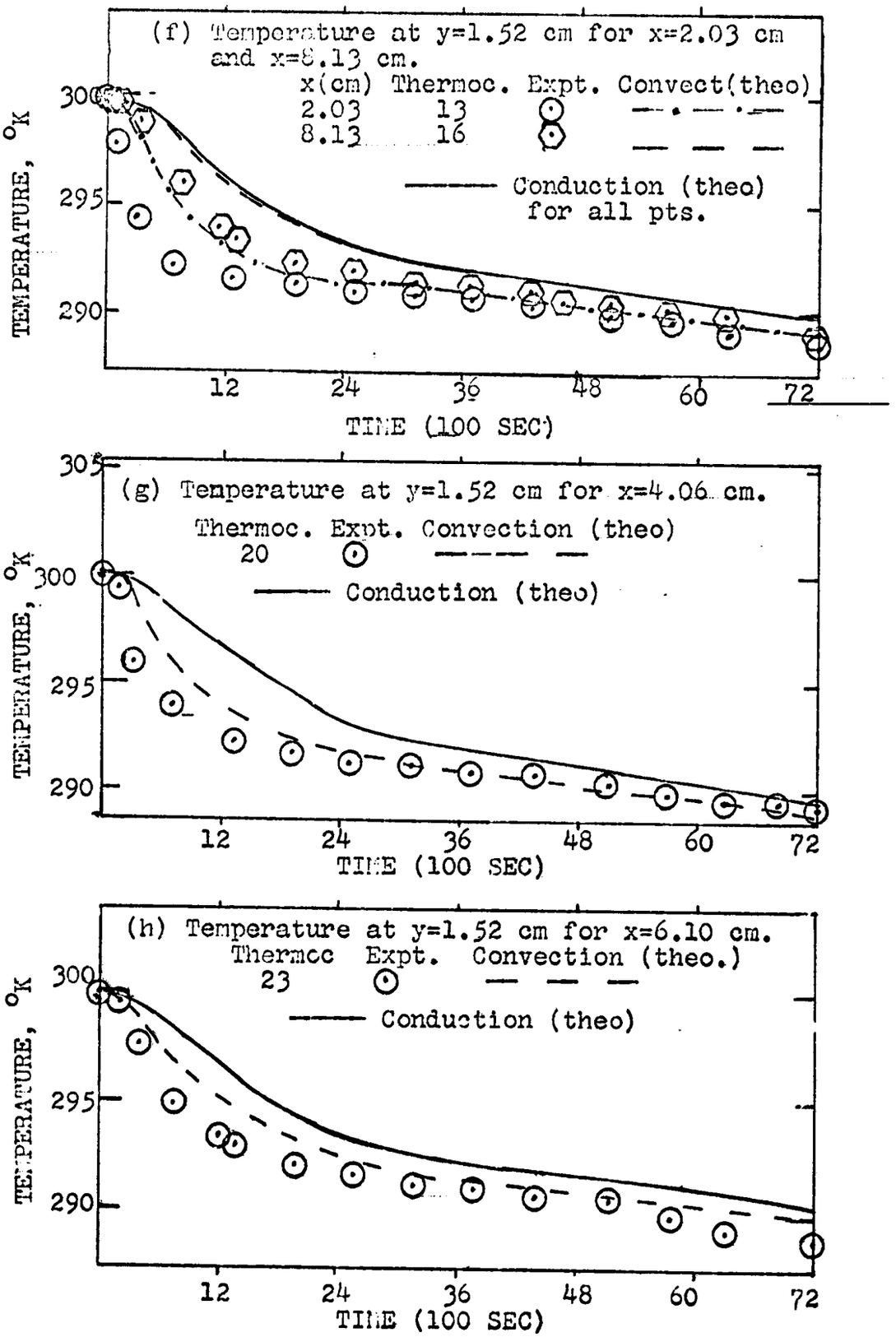

FIGURE 16 (contd). RUN 11: $\alpha = 45^{\circ}$; $T_a = 300.11\ ^{\circ}K$

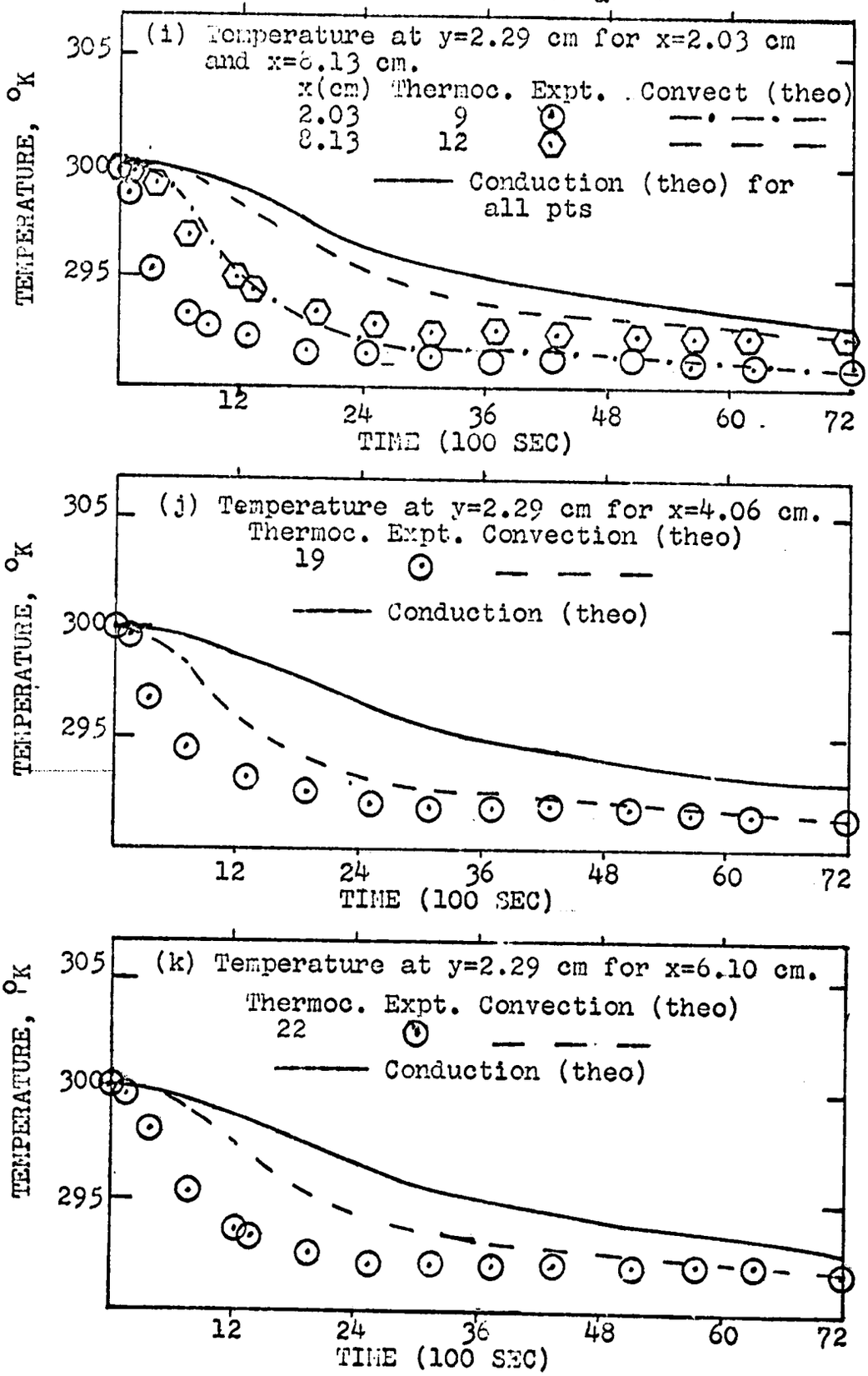

FIGURE 16 (contd).. RUN 11: $\alpha = 45^{\circ}$; $T_a = 300.11\ ^{\circ}K$

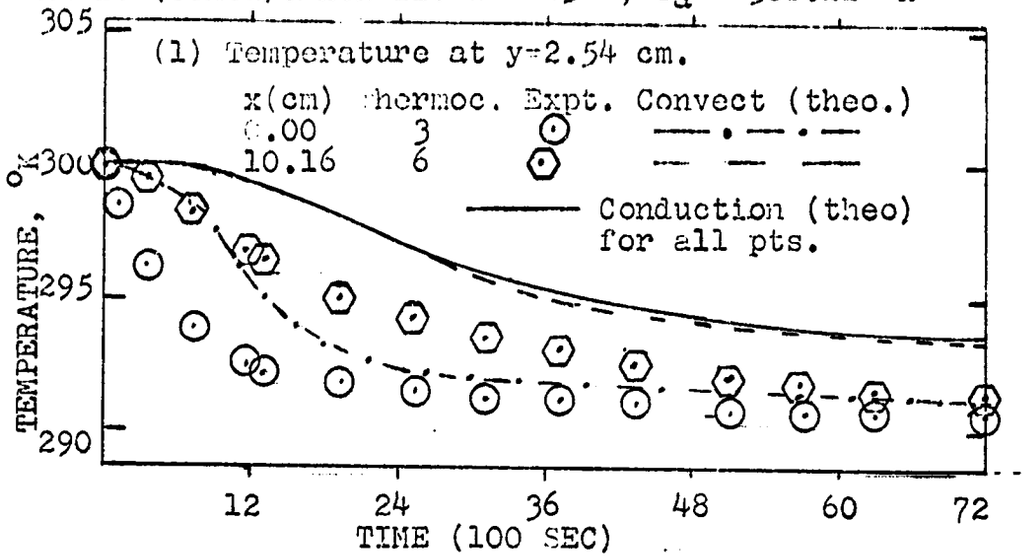

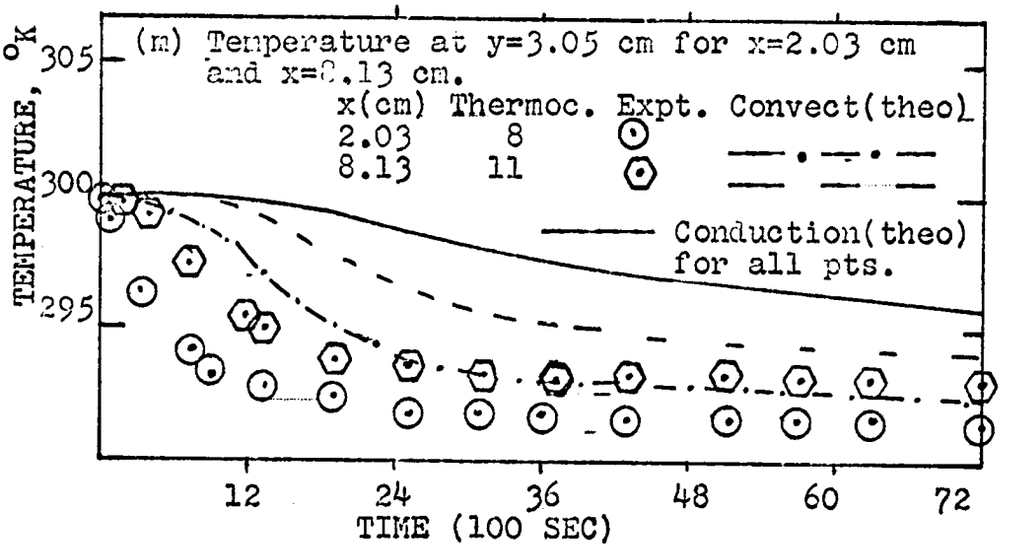

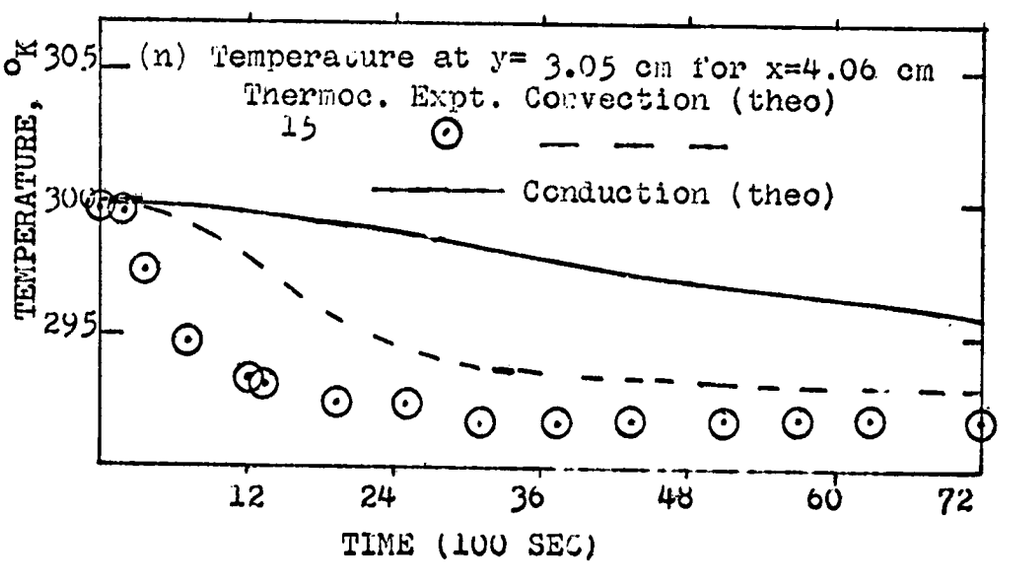

FIGURE 16 (contd). RUN 11: $\alpha = 45^{\circ}$; $T_a = 300.11\ ^{\circ}K$

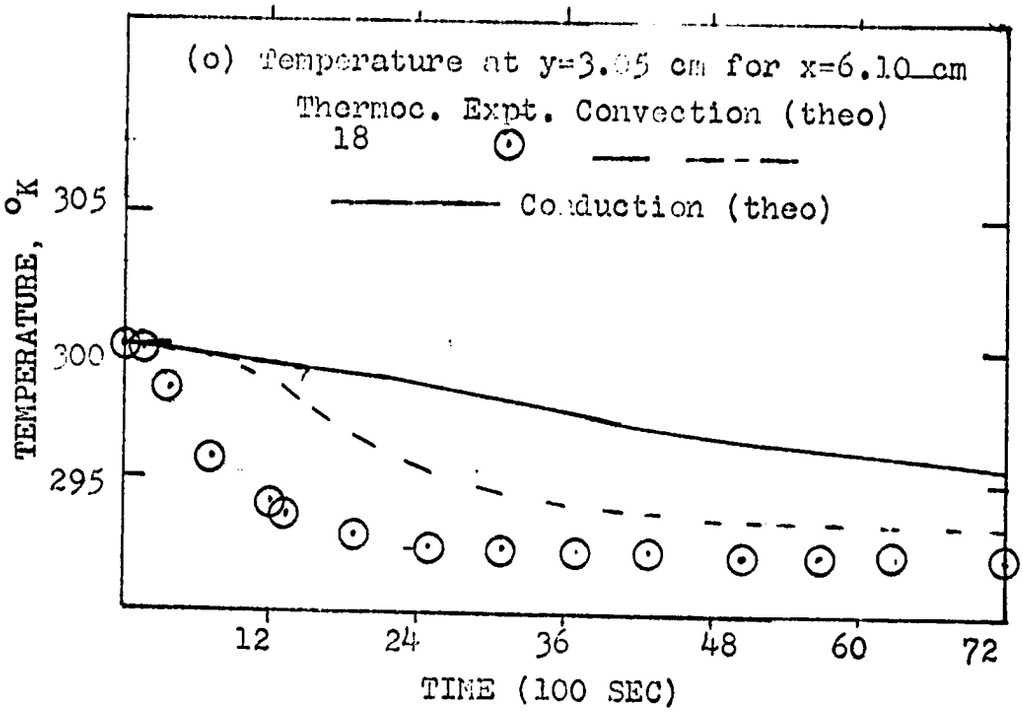

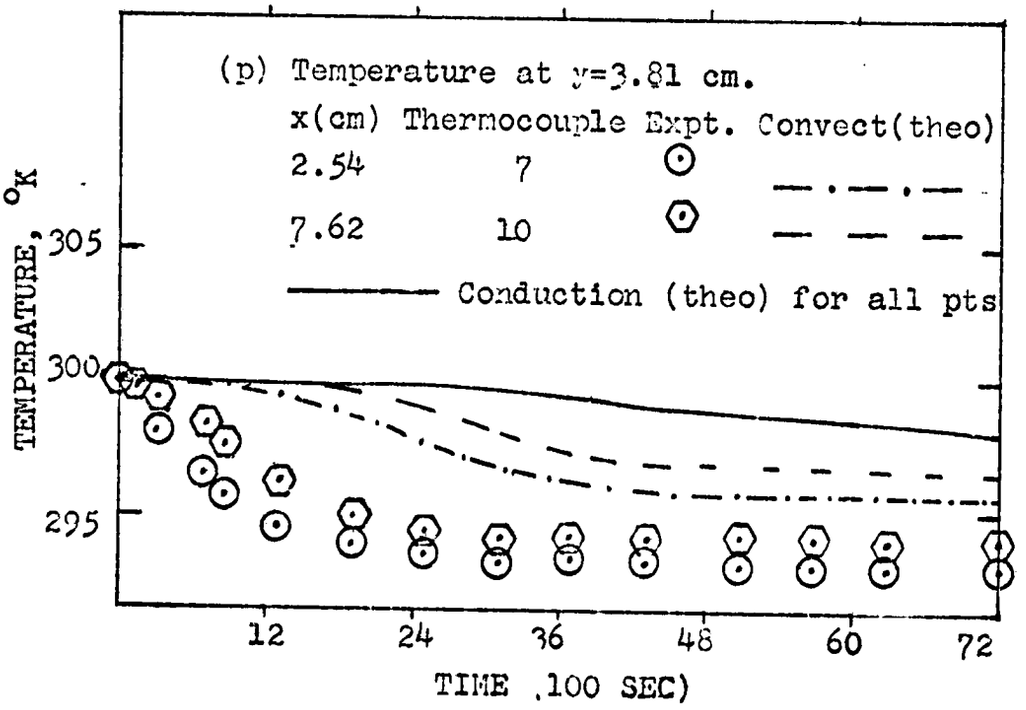

FIGURE 17. EXPERIMENTAL AND THEORETICAL DATA FOR RUN 14: $\alpha = 45^0$; $T_a = 301.49\ ^0K$

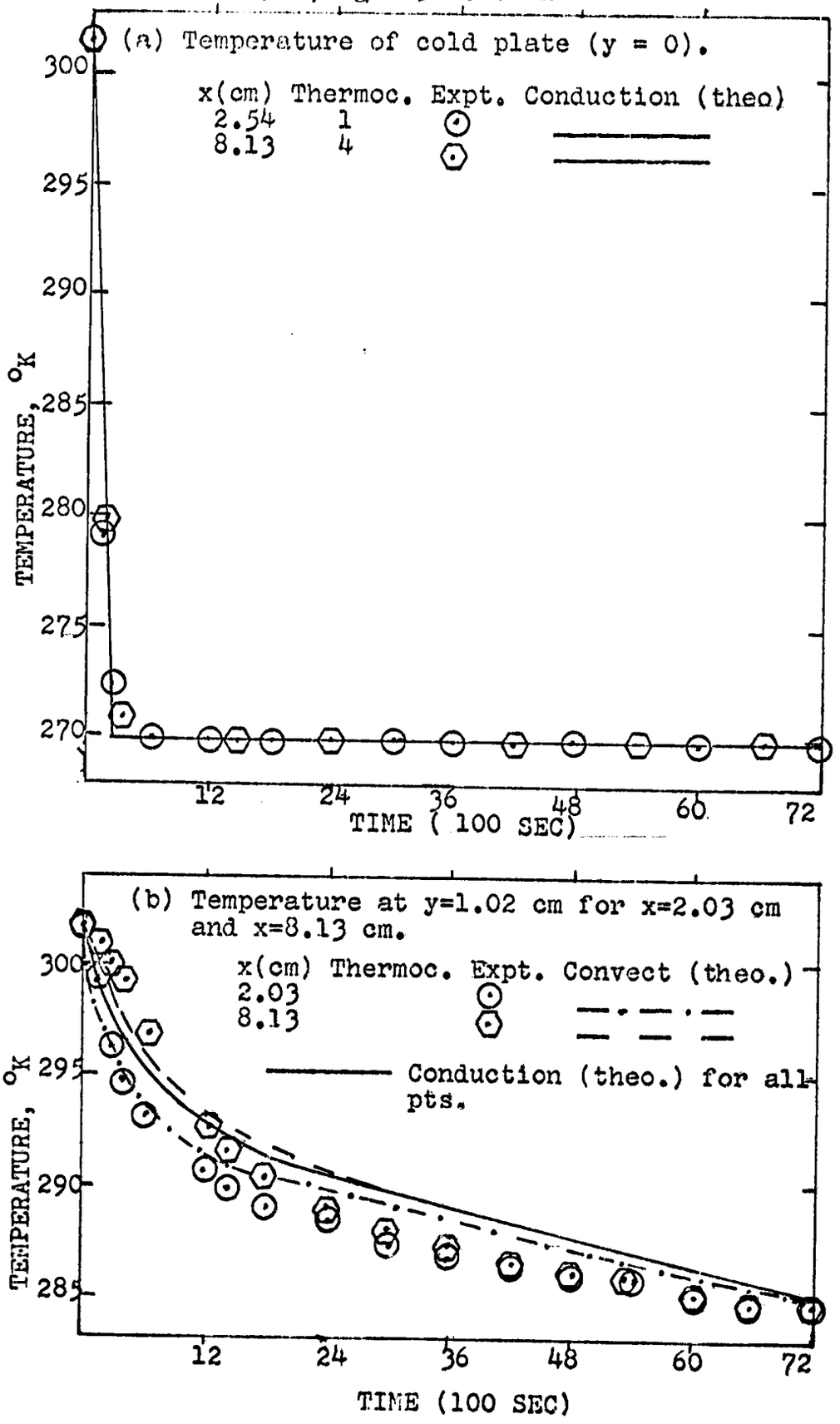

FIGURE 17 (contd). RUN 14: $\alpha = 45^{\circ}$; $T_a = 301.49\ ^{\circ}K$

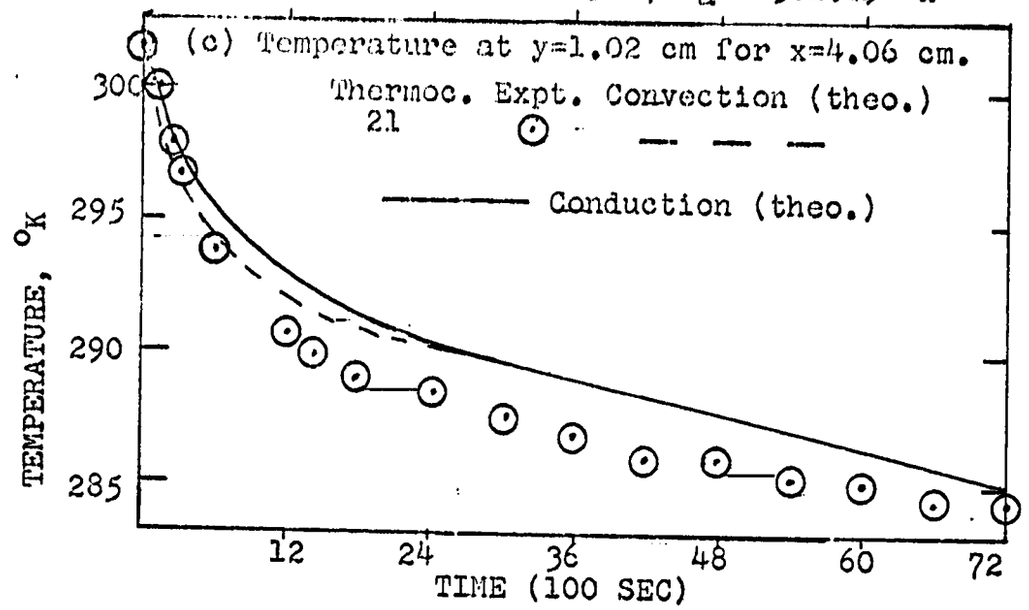

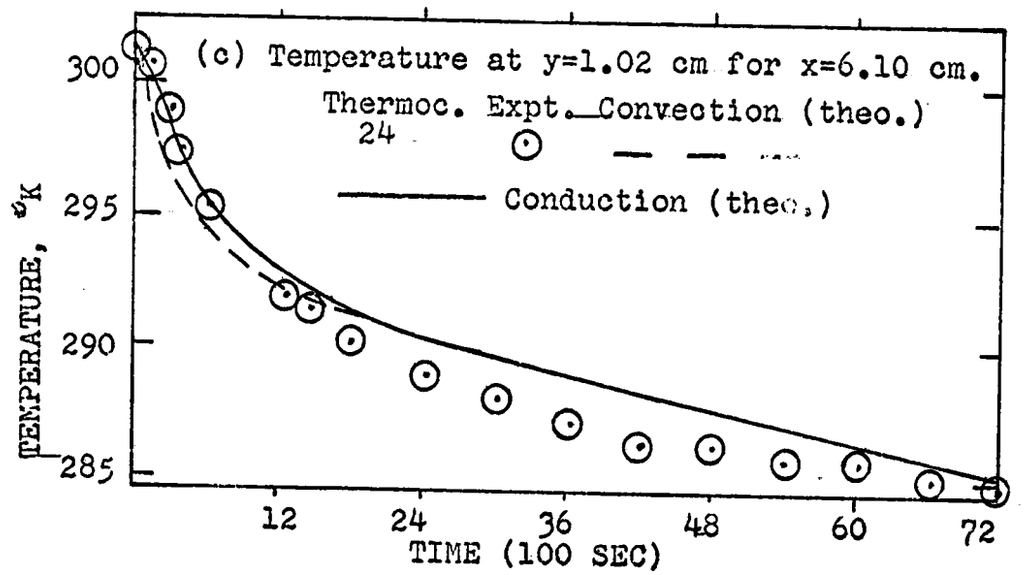

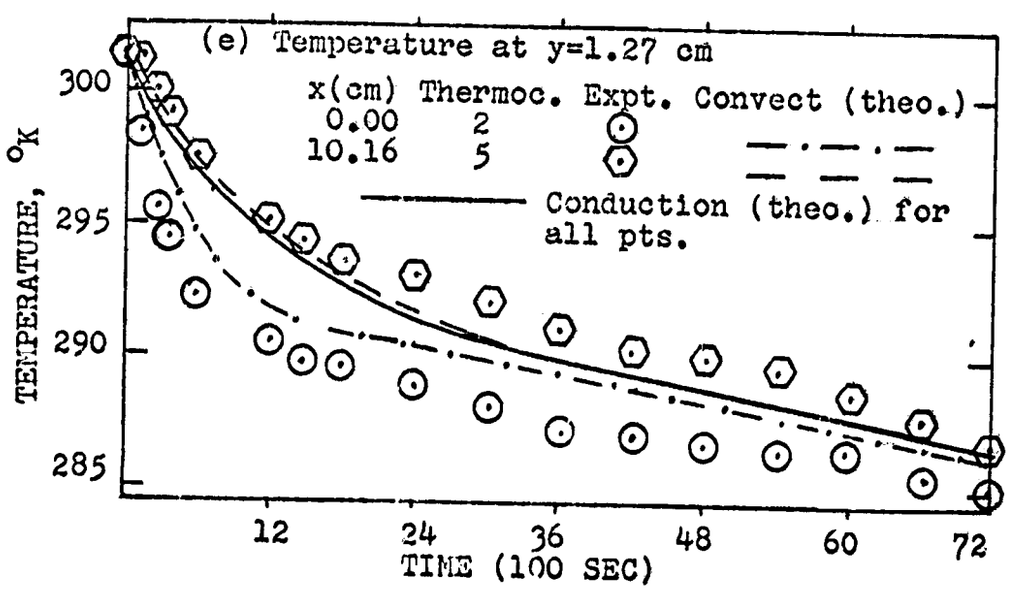

FIGURE 17 (contd). RUN 14: $\alpha = 45^{\circ}$; $T_a = 301.49\ ^{\circ}K$

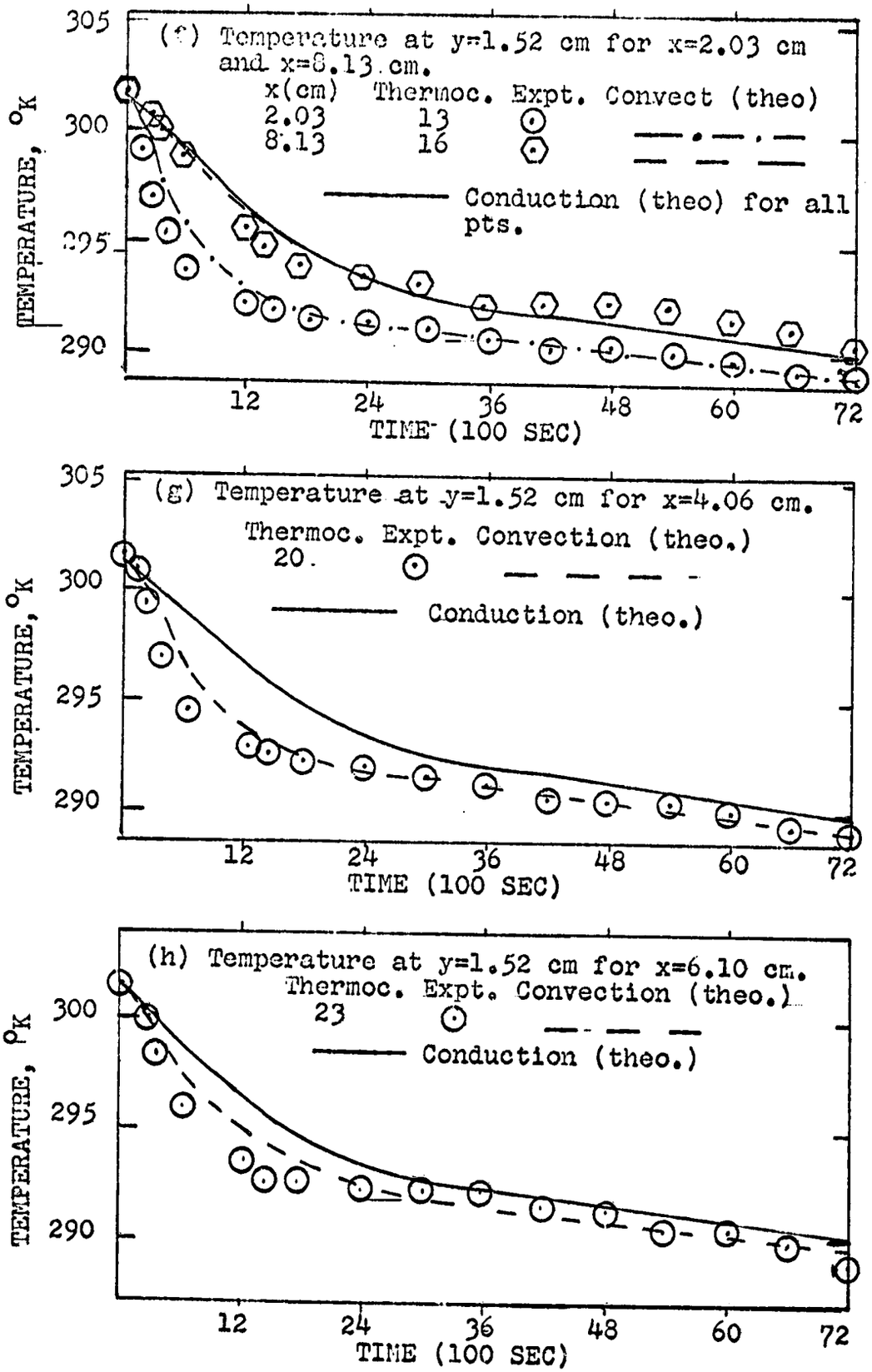

FIGURE 17 (contd). RUN 14: $\alpha = 45^{o}$; $T_a = 301.49\ ^{o}K$

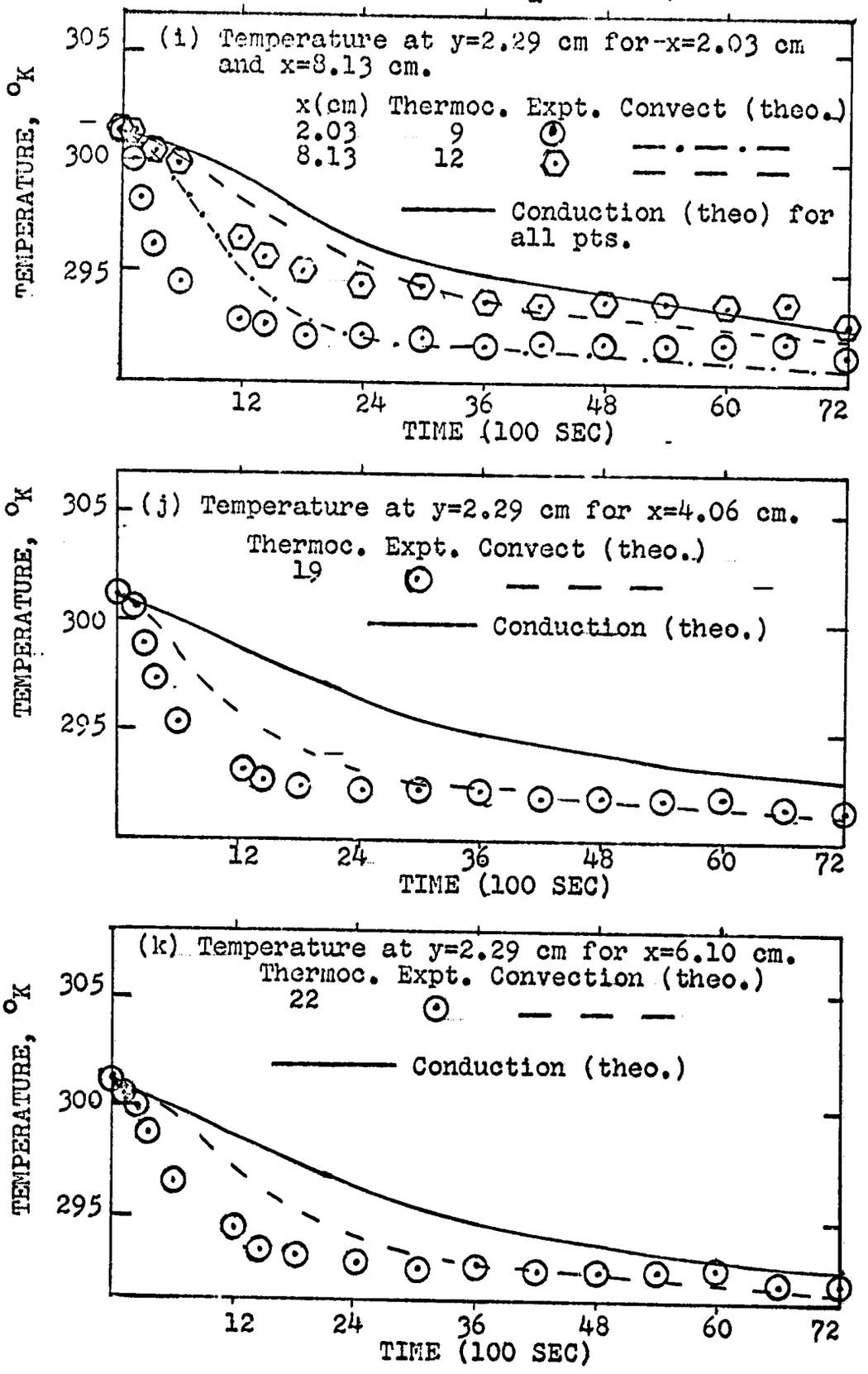

FIGURE 17 (contd). RUN 14: $\alpha = 45^{\circ}$; $T_a = 301.49\ ^{\circ}K$

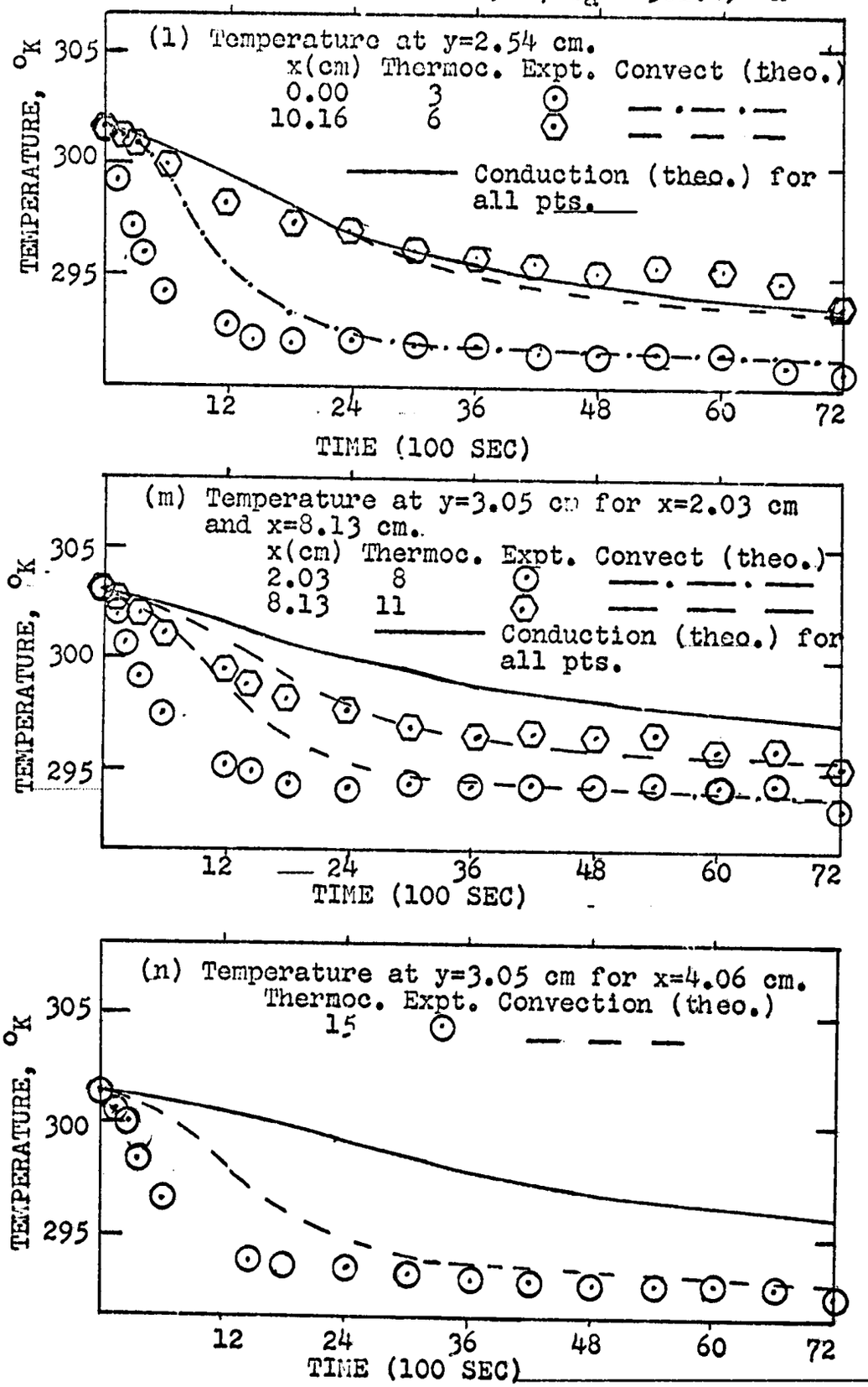

FIGURE 17 (contd). RUN 14: $\alpha=45^{\circ}$; T_a = 301.49 $^{\circ}K$

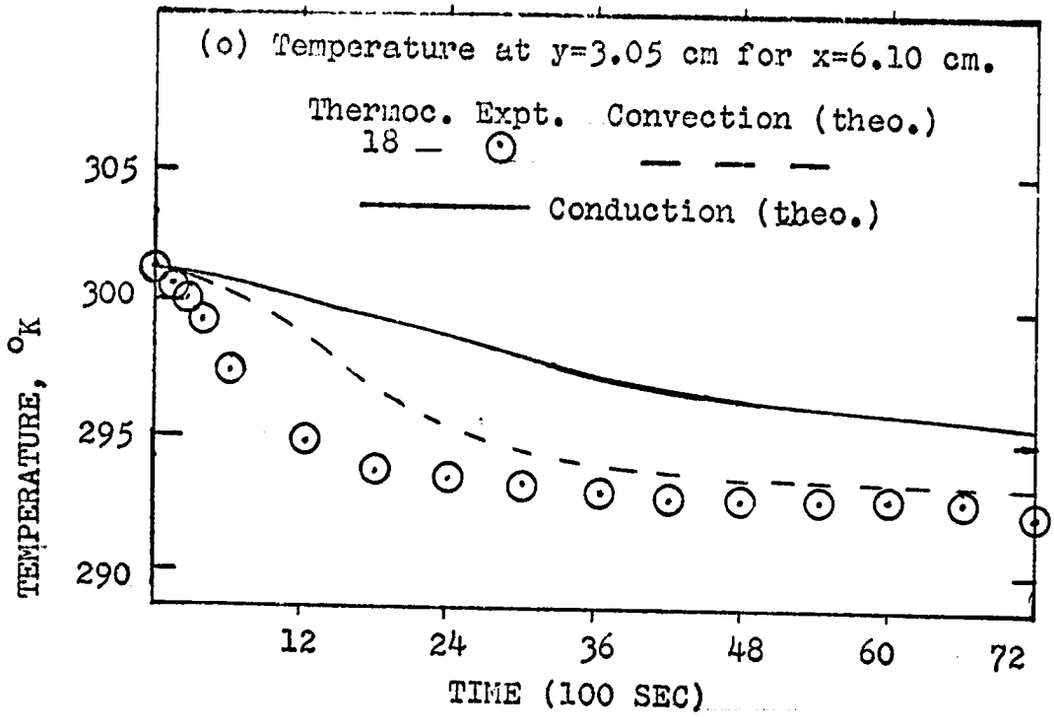

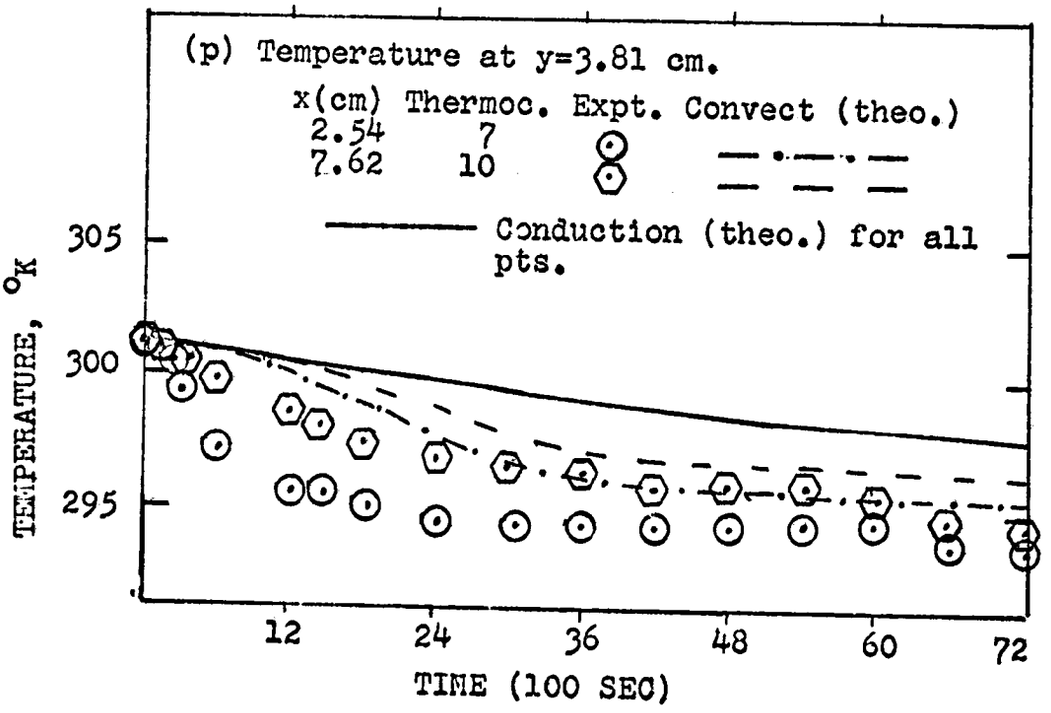

FIGURE 18. EXPERIMENTAL AND THEORETICAL DATA FOR RUN 15: $\alpha = 60^{o}$; $T_a = 301.49\ ^{o}K$

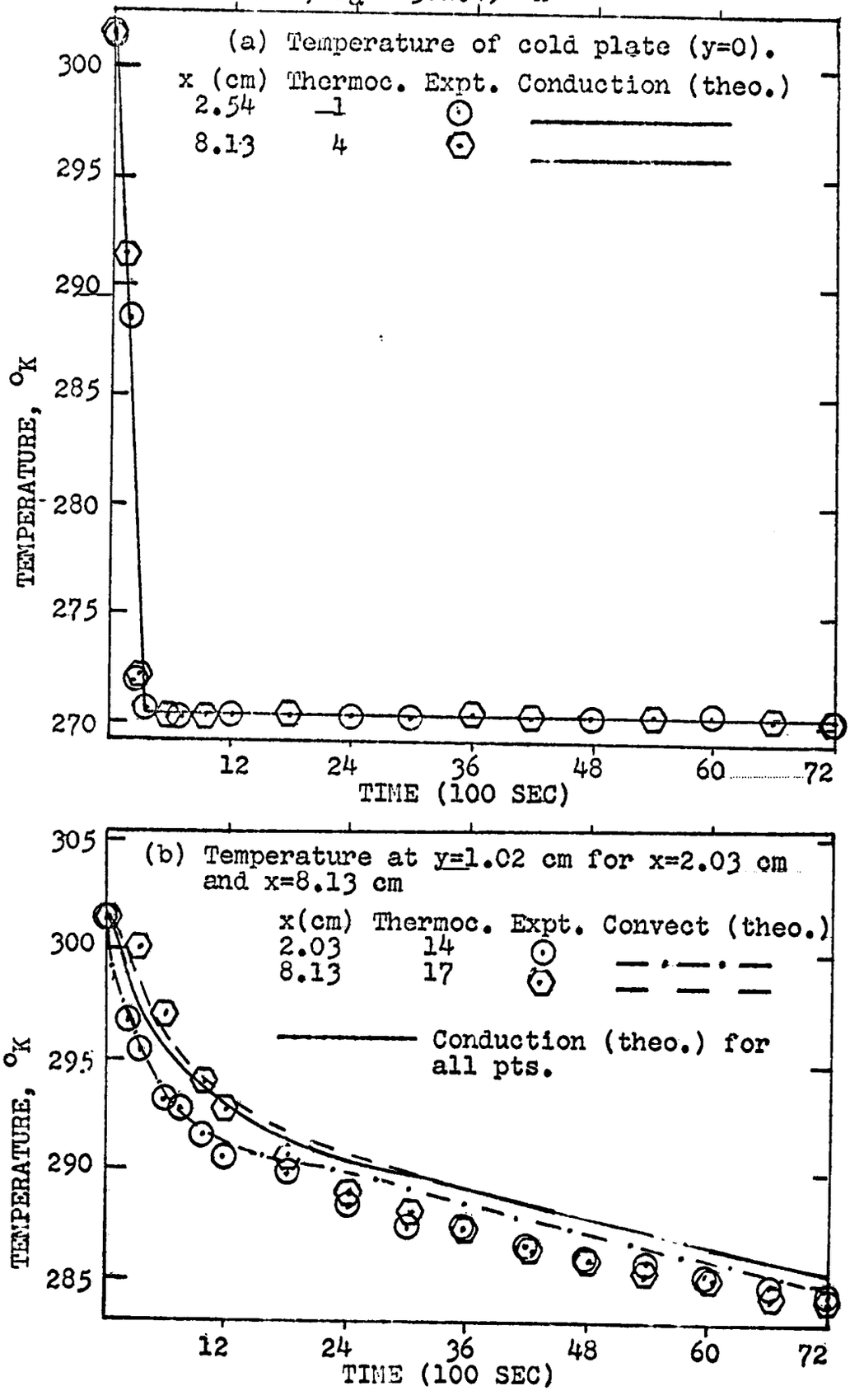

FIGURE 18 (contd). RUN 15: $\alpha=60^{\circ}$; T_a = 301.49 $^{\circ}$K

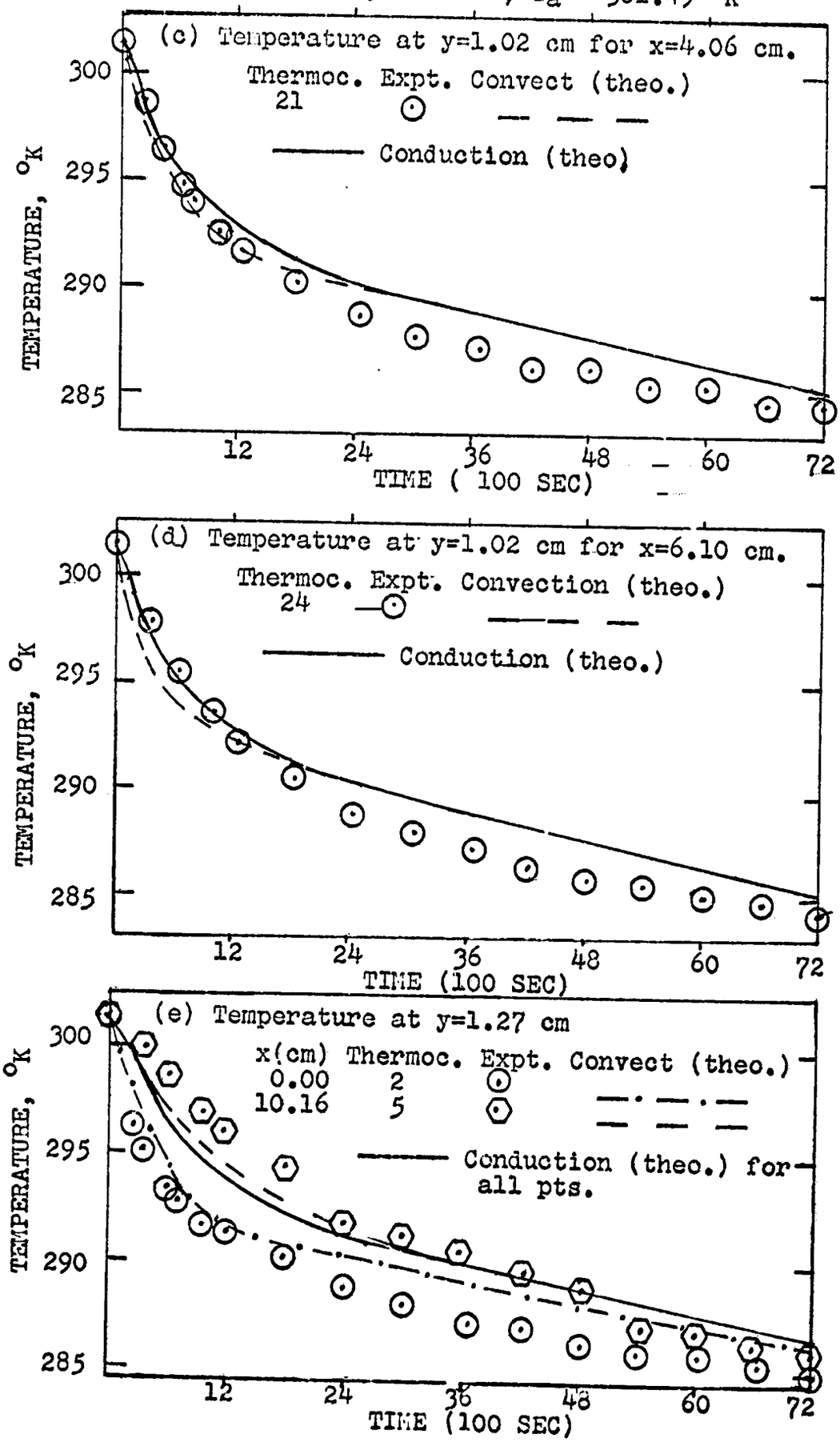

FIGURE 18 (contd). RUN 15: $\alpha = 60^{\circ}$; $T_a = 301.49\ ^{\circ}K$

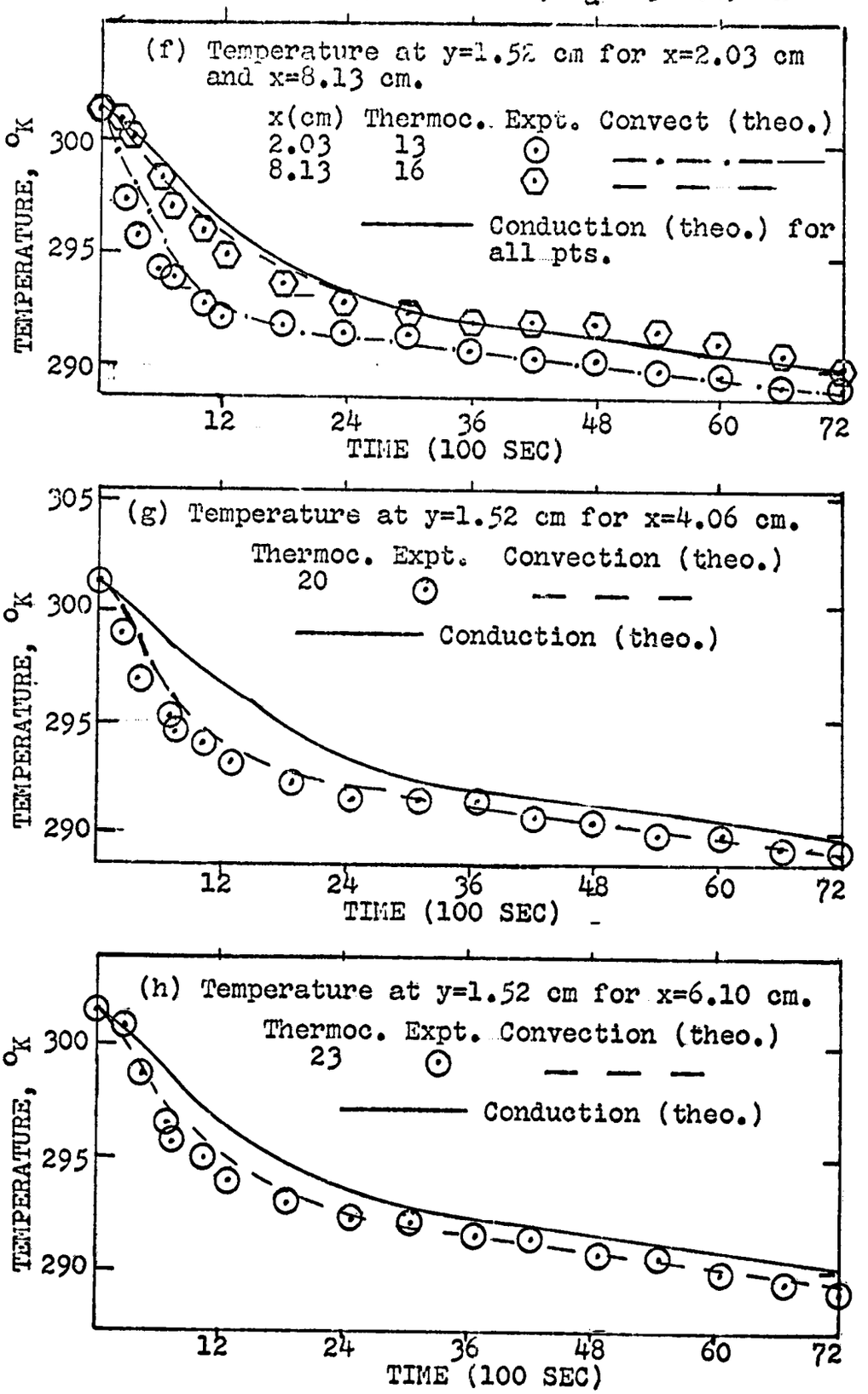

FIGURE 18 (contd). RUN 15: $\alpha = 60^{\circ}$; $T_a = 301.49\ ^{\circ}K$

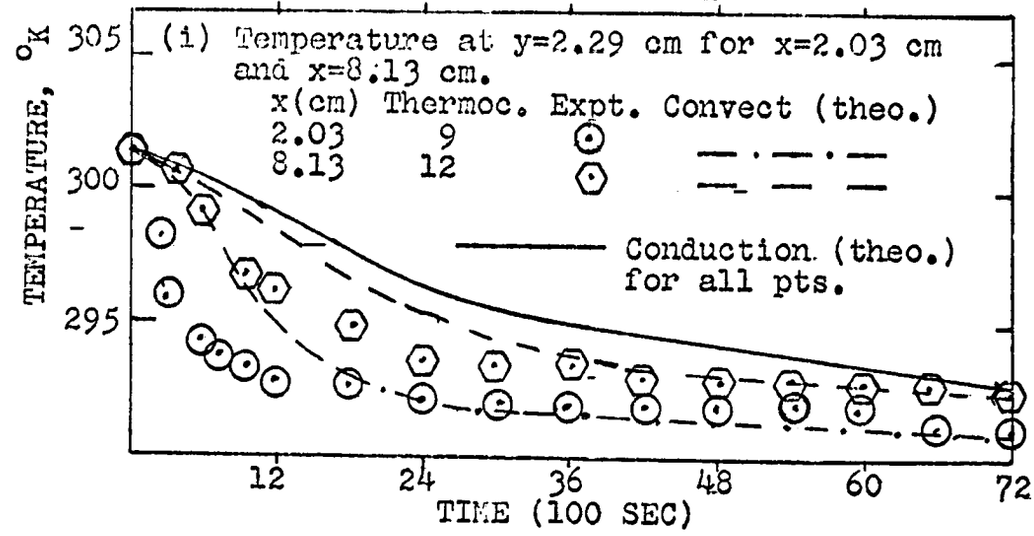

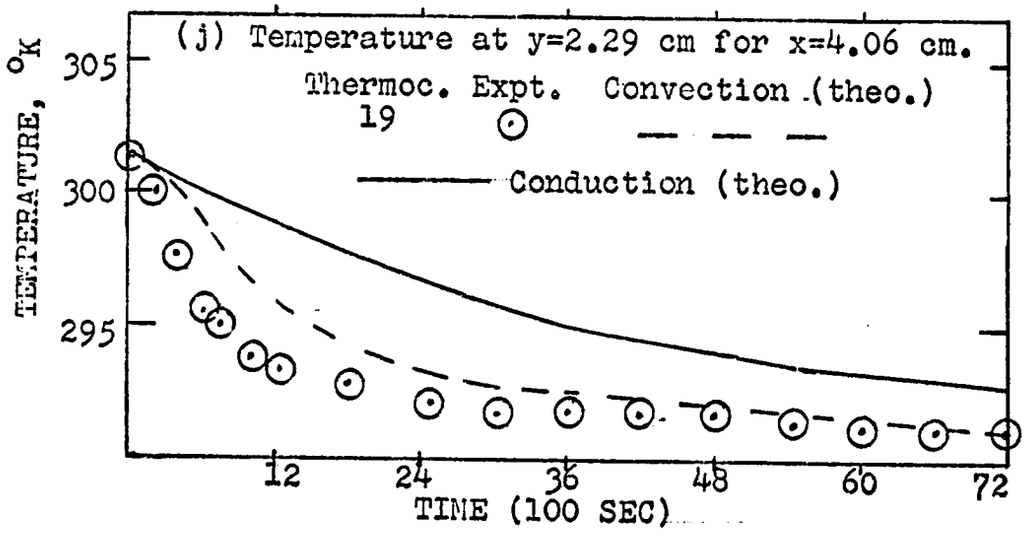

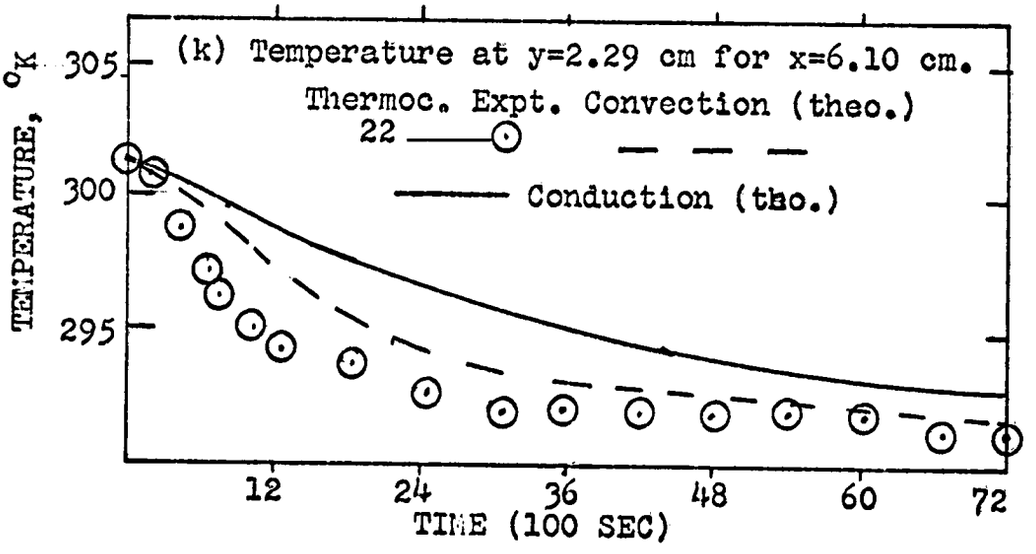

FIGURE 18 (contd). RUN 15: $\alpha = 60^{\circ}$; $T_a = 301.49\ ^{\circ}K$

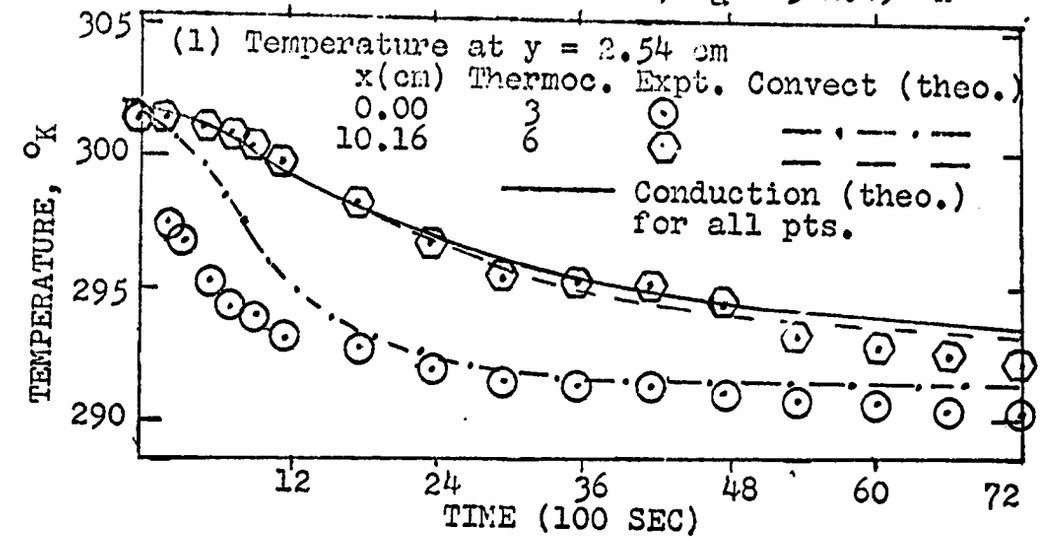

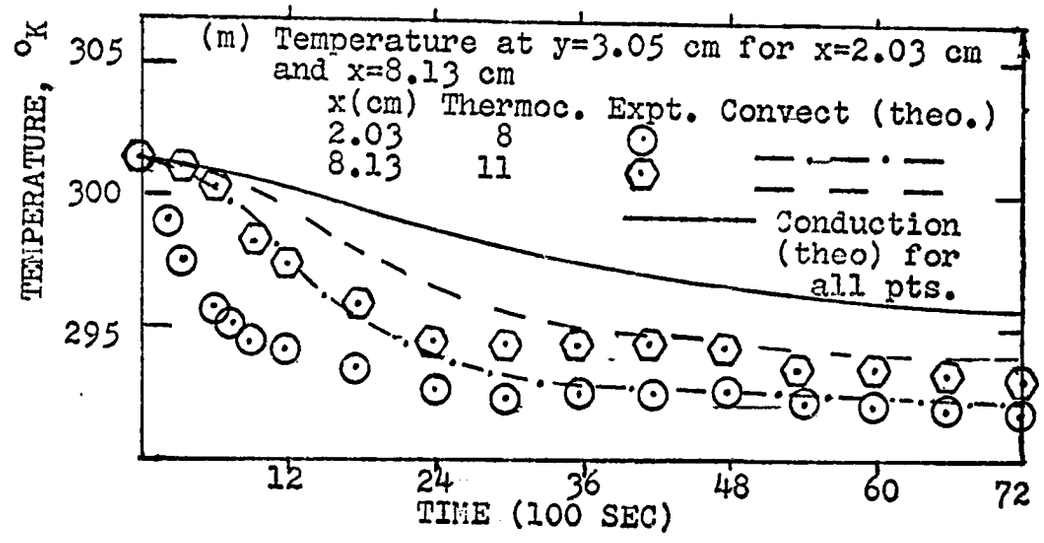

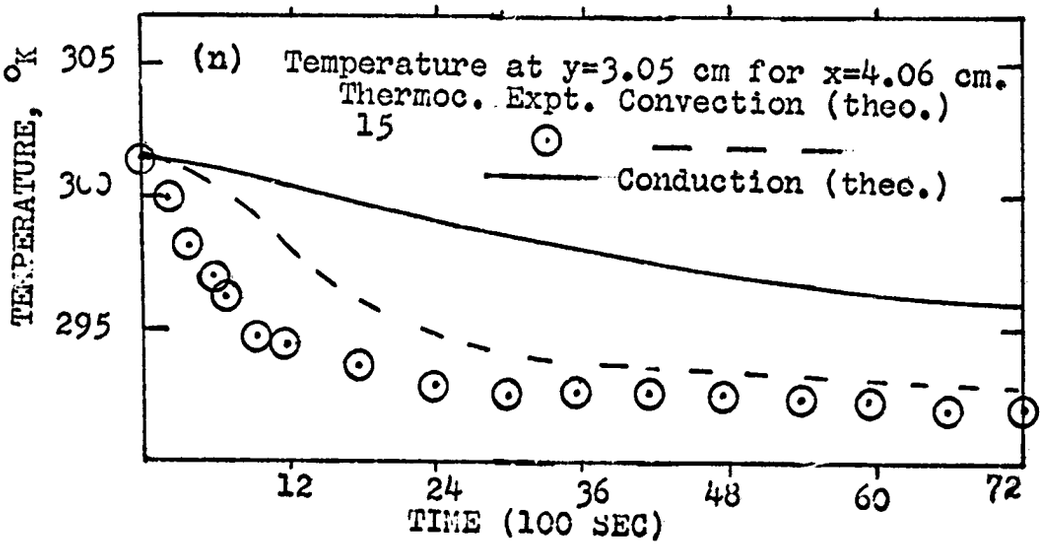

FIGURE 13 (contd). RUN 15: $\alpha = 60^{\circ}$; $T_a = 301.49\ ^{\circ}K$

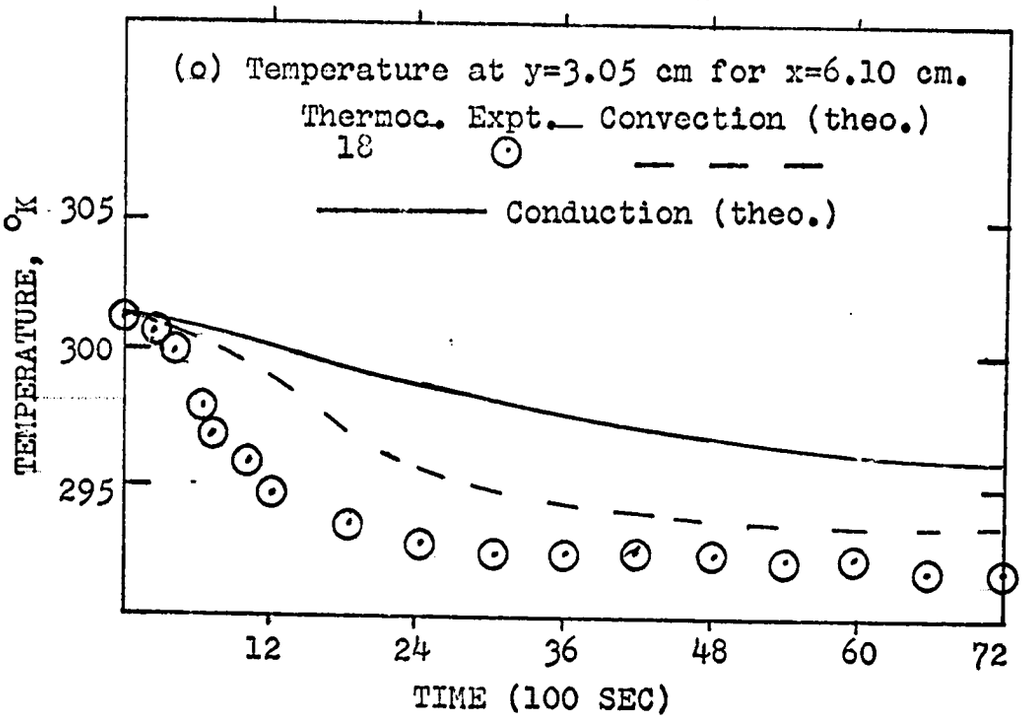

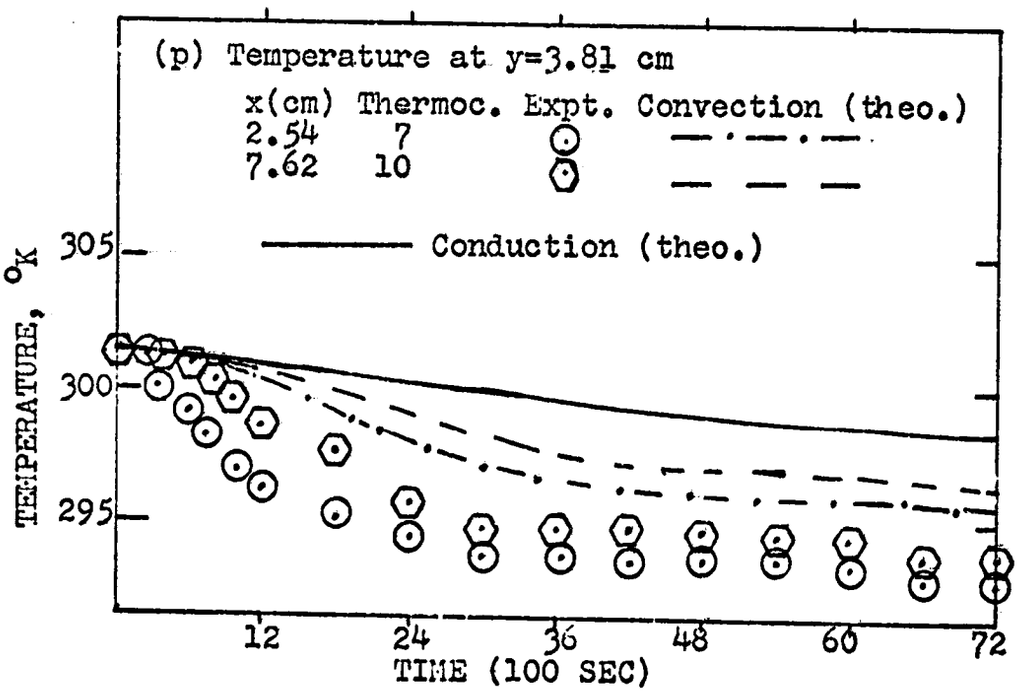

CONCLUSIONS AND RECOMMENDATIONS

The following conclusions were drawm from this study:

1. When the test cell was sitting on the horizontal plane with angle $\alpha = 0^{\circ}$, the heat transfer mode was by conduction, not convection.

2. Good agreement was obtained between the pure-conduction model and the experimental runs made at $\alpha = 0^{\circ}$.

3. When conduction was the heat transfer mode, the shape of the solidification interface was planar, not curved. For all horizontal x- positions the solid-phase height was the same.

4. The temperature during conduction solidification was strongly a function of time and distance y from the cooled bottom plate. It had no strong dependence on the horizontal x-direction when the containing side walls acted as insulators. It was found that one-dimensional transient conduction model in the y-direction predicted the phase change as well as did transient two-dimensional model that included the x-direction. This finding supports the findings in a previous transient one-dimensional conduction phase change study made by these investigators (Reference 13).

5. In solidification by conduction, in which the side walls approximate insulators, the extra minor accuracy obtained by using a transient two-dimensional model was not

worth the large differential in cost in computer time from a one-dimensional transient solution. A uni-dimensional transient solution would do as well and still save computer time.

6. The phase-change process was the controlling process. Whether the heat transfer mode was by conduction or convection, the actual values of phase-change enthalpy change, solidification temperature, density, specific heat and thermal conductivity at the interface seemed to control the accuracy of prediction of experimental data by theoretical models. More accurate values must be found for these properties at the interface where some of them experience discontinuities and sudden jumps. In the theoretical calculations, the interface was found to act as a pseudo-insulator between the two phases present.

7. With the container of the test material inclined at an angle, we found that convective effects became important.

8. Convection increased the heat transfer rate and caused a faster overall cooling of the test cell and its contents. Two indications of the magnitude of convective effects in the cell were how much below the conduction temperature the cell had been cooled at any given time, and the shape of the solidification interface. With convection present, and cooling occurring from below, the interface

became shaped slightly like an elongated S-curve with the up branch near the vertical wall passing through the origin of the angle of pivot, the flat (or inflexion) part near the half-way mark between the two side walls. The shortest height of solid occurred near the far side wall.

9. We could not get a complete solution of the full velocity equation by finite difference methods because of stability restrictions imposed by the solution procedure. Approximate velocity profiles were substituted into the temperature equation. The profiles involved a single circulation flow symmetric in the vertical y-direction but off-centered in the horizontal x-direction.

10. Convection caused the temperature profile to depend strongly on both horizontal and vertical directions (unlike conduction) even when the side walls were insulated. The maximum deviation in temperature between two points in the same horizontal plane at a given vertical distance from the cold plate seemed to depend more strongly on the temperature difference between the ambient and the freezing interface than on the angle of inclination. The angle of inclination, however, had significant effect on the overall heat transfer process.

11. Solid-solid phase transition may take place during solidification and the physical properties of the system should be modified to account for this.

12. The theoretical calculations used in this study to investigate natural convection are first approximations and clearly delineate the trend and significance of convection. With the availability of a much faster computer with a much larger memory bank than the computer available to us, one may finally use small enough time steps and space increments that would yield velocities higher or equal to those predicted analytically and still stay in the stable regime of finite difference solutions. In such a case, one could estimate more accurately the shape and magnitude of the velocities and come up with better gravity level approximations in the velocity equations.

13. Many theoretical methods used in the literature could not stand up to the test in predicting actual experimental data. These theoretical solutions were obtained under certain conditions and with physical properties that could not be duplicated easily in the laboratory.

14. Perhaps, a better approach to phase-change thermal control would be to use polymers that undergo solid-solid transition with high enthalpy change. Thus, the phase-change material could stay solid or amorphous within the range of its temperature of operation. Thus, better packaging would result. Materials that melt or solidify are more difficult to package in the liquid phase and more difficult to predict as to performance because of convective and other

effects.

15. Another approach to the thermal control problem with materials that go from liquids to solids and vice versa would be to come up with empirical effective thermal properties that incorporate convective and conduction heat transfer with phase change. For instance, such a procedure could take into consideration entrapped air pockets and voids in the solid phase, and heat transfer coefficients due to convection in the liquid phase.

We conclude that, with cooling occurring from below, gravity-induced convection is important in the solidification of n-hexadecane when the cooling is not oriented perpendicular to the direction of gravity. Heat transfer rate is, in general, increased.

NOMENCLATURE

Text	Computer	
B	A1	Constant (Eq.24c) — cm/sec
c		Constant (Eq.15) — $sec-^oK/cm$
c_p	CPL,CPP,CPS	Specific heat — $cal/(gm-^oK)$
c^*_{pS}	CP	Effective specific hest of solid phase (Eq.38) — $cal/(gm-^oK)$
$d,\bar{d}$	ROL,ROP,ROS	Density — gm/cm^3
D_i	D(I)	Coefficients in polynomial fit, $f(t) = D_1+D_2t+D_3t^2+..+D_it^{i-1}$ of cold plate temperature — $^oK/(sec^{i-1})$
e_i		Difference in temperatures recorded by the same thermocouple at the same time in a pair of experimental runs made under identical conditions - ^oK
$\bar{e}$		Sample mean of e_i in a sample of size n — ^oK
f(t)	T(I,1)	Temperature of cold plate — ^oK
g		Acceleration due to normal gravity cm/sec^2
G_1-G_{11}	G1-G11	Coefficients defined in Eq.30 and Eq.31
h	AHO,AHI	Height of the liquid phase of the test material (y direction) — cm
h_p	AHP	Thickness of walls of test cell — cm
H_f	HF	Latent heat of solidification - cal/gm

Text	Computer	
k	AK,PK,SK	Thermal conductivity – watt/(cm-^{o}K), cal/(cm-sec-^{o}K)
	K	Degree of polynomial fit f(t) of cold-plate temperature
m_e		True mean of e_i — ^{o}K
M	M	Number of finite-difference space nodes in the coordinate x direction
N	N	Number of finite-difference space nodes in the coordinate y direction
NS(i)	NS(I)	Number of finite-difference space nodes in the solid phase in the y direction
p,P		Pressure
q		Characteristic number (Eq.14) — cm^{-2}
Q		Fraction of normal gravity (Eq.47)
R_a		Rayleigh number (Eq.47)
s		Sample standard deviation of e_i in sample of size n (Eq.45) — ^{o}K
t	TIME,TSE	Time — sec
Δt	DELT	Finite-difference time increment – sec
T	T, TO	Temperature — ^{o}K
T_a	TA	Ambient (room and initial) temperature — ^{o}K
T_f	TF	Equilibrium solidification temperature of test material — ^{o}K
u	UX	Coordinate-x component of velocity - cm/sec
v	VY	Coordinate-y component of velocity - cm/sec

Text	Computer	
W	AL	Width of cell cavity (x direction) — cm
x	XA,XP	Abscissae in a Cartesian coordinate system — cm
Δx	DELX	Finite-difference space increment in the coordinate-x direction — cm
X(x)		Function defined by Eq.18 to Eq.22 — cm/sec
y	Y	Ordinate in a Cartesian coordinate system — cm
Δy	DELY	Finite-difference space increment in the coordinate-y direction — cm
α		Angle of inclination of the test cell measured anticlockwise from the horizontal plane — degrees
β		Coefficient in equation of state for density: $d_L = d_{Lo} + \beta T$ — $gm/(cm^3\text{-}^oK)$
γ	BB	Constant (Eq.23) — cm^{-1}
λ	ALA,ASA	Thermal diffusivity — cm^2/sec
ν		Kinematic viscosity — cm^2/sec
ω		Vorticity (Eq.10) — sec^{-1}
φ	PHI	Stream function (Eq.9) — cm^2/sec
π	PI	Constant — 3.14159266

Subscripts	Subindices	
i	I	Identifying number for finite-difference node in the x direction
j	J	Identifying number for finite-difference node in the y direction

Subscripts

L	——	Liquid phase of test material
P		Plexiglas, material of walls of test cell
S		Solid phase of test material

Superscript

'	Implies "evaluated at a new time" (Eq.32 to Eq.34)

LITERATURE CITED

1. Carslaw, H. S., and Jaeger, J. C., Conduction of Heat in Solids: Oxford Univ. Press, 2nd ed., pp. 282-296 (1959).

2. Stefan, J., "Uber die Theorie der Eisbildung insbesondere uber die Eisbildung in Polarmere," Annalen der Physik und Chemie, v. 42, p. 269 (1891).

3. Danckwerts, P. V., "Unsteady-state Diffusion or Heat Conduction with Moving Boundary," Trans. Faraday Soc., v. 46, p. 701 (1950).

4. Booth, F., "A Note on the Theory of Surface Diffusion Reactions," Trans. Faraday Soc. (London), v. 44, p. 796 (1948).

5. Kreith, F., and Romie, F. E., "A Study of the Thermal Diffusion Equation with Boundary Conditions Corresponding to Solidification or Melting of Materials Initially at the Fusion Temperature," Proc. Phys. Soc., v. 68, p. 277 (1955)

6. Chao, C. C., and Weiner, J. H., "Heat Conduction in Semi-Infinite Solid in Contact with Linearly Increasing Mass of Fluid," Quarterly of Applied Math, v. 14, p. 214 (1956).

7. Chambers, L. G., "A Variational Principle for the Conduction of Heat," Quarterly Jour. of Mech. and Applied Math, v. 9, p. 234 (1956).

8. Biot, M. A., and Daughaday, H., "Variational Analysis of Ablation," Jour. Aerospace Sciences, v. 29, p. 227 (1962).

9. Goodman, T. R., "The Heat-Balance Integral and Its Application to Problems Involving a Change of Phase," Trans. A. S. M. E., v. 80, p. 335 (1958).

10. Poots, G., "An Approximate Treatment of Heat Conduction Problem Involving a Two-Dimensional Solidification Front," Int. Jour. Heat and Mass Transfer, v. 5, p. 339 (1962).

11. Dusinberre, G. M., "Numerical Methods for Transient Heat Flow," Trans. A. S. M. E., v. 67, p. 703 (1945).

12. Fujado, P. R., Melting of a Finite Paraffin Slab, Thesis No. T-1215, Colorado School of Mines, Golden, Colorado (1968).

13. Ukanwa, A. O., Stermole, F. J., and Golden, J. O., "Phase Change Solidification Dynamics," Jour. of Spacecraft and Rockets, v. 8, no. 2, pp. 193-196, (Feb., 1971).

14. Miller, M. L., "Transient One-Dimensional Heat-Conduction Analysis for Heterogeneous Structures Including an Ablating Surface," A. S. M. E. Paper No. 59-HT-22 (1959).

15. Ehrlich, L. W., "A Numerical Method of Solving a Heat Flow Problem with Moving Boundary," Jour. Assoc. Computing Machinery, v. 5, no. 2, pp. 161-176 (1958).

16. Shlosinger, A. P., and Bentilla, E. W., Thermal Control by Use of Fusible Materials, Interim Report NSL65-16, Contract NAS8-11163, Northrop Corporation, Hawthorne, California (1965).

17. Bentilla, E. W., Sterrett, K. F., and Karre, L. E., Thermal Control by Use of Fusible Materials, Final Report NSL65-16-1, Contract NAS8-11163, Northrop Corporation, Hawthorne, California (1966).

18. Bannister, T. C., and Bentilla, E. W.,"Study on Thermal Control by Use of Fusible Materials," Inst. Environmental Sci., Ann. Tech. Mtg. Proc. pp. 593-607 (1966).

19. Grodzka, P. G., and Fan, C., Thermal Control by Freezing and Melting, Interim Report HREC-1123-1, LMSC/HRECA 791342, Contract NAS8-21123, Lockheed Missiles and Space Co., (1968).

20. Chambre, P. L., "On the Dynamics of Phase Growth," Quarterly Jour. of Mech. and Applied Math, v. 9, p. 224 (1956).

21. Muehlbauer, J. C., and Sunderland, J. E., "Heat Conduction with Freezing and Melting," Applied Mechanics Review, v. 18, no. 12, pp. 951-959 (1965).

22. Rohsenow, and Choi, Heat, Mass, and Momentum Transfer: Prentice-Hall, Inc., Englewood Cliffs, N. J. (1961).

23. Schlichting, H., Boundary Layer Theory: MacGraw-Hill Book Co., N. Y., N. Y. (1966).

24. Longwell, P. A., Mechanics of Fluid Flow, MacGraw-Hill Book Co., N. Y., N. Y. (1960).

25. Bird, R. B., Stewart, W. E., and Lightfoot, E. N., Transport Phenomena: John Wiley & Sons, Inc., New York (1960).

26. Wilkes, J. O., and Churchill, S. W., "The Finite-Difference Computation of Natural Convection in a Rectangular Enclosure," A. I. Ch. E. Jour., v. 12, no. 1, pp. 161-166 (1966).

27. Peaceman, D. W., and Rachford, H. H., "The Numerical Solution of Parabolic and Elliptic Differential Equations," Jour. Soc. Indust. Appl. Math., v. 3, no. 1, pp. 28-41 (March 1955).

28. Chandrasekhar, S., Hydrodynamic and Hydromagnetic Stability: Clarendon Press, Oxford, England (1961).

29. Pellew, A., and Southwell, R. V., "On Maintained Convective Motion in a Fluid Heated from Below," Proceedings of Roy. Soc. (London), ser. A, v. 176, pp. 312-343 (July 1940).

30. Leontev, A. I., Kirdyashkin, A. G., "The Theory of the Convective Heat Transfer for the Vertical Flow of Fluid," Int. Heat Transfer Conference, v. 1, pp. 216-229 (August 1966).

31. Bain, R. L., The Effect of Gravity-Induced Free Convection upon the Melting Phenomena of a Finite Paraffin Slab for Thermal Control, Thesis No. T-1319, Colorado School of Mines, Golden, Colorado (1970).

32. Perry, J. H., Chilton, C. H., and Kirkpatrick, S. D., Chemical Engineer's Handbook: McGraw-Hill Book Co., 4th Edition, Ch. 23, p. 54 (1963).

33. Maxwell, J. B., A Handbook of Hydrocarbons: Van Nostrand, Co., Inc., p. 161 (1950).

34. The Bristol Company, Wide-Strip Dynamaster Pyrometer Using Series L10 Amplifier, A Division of American Chain and Cable Co., Waterbury, Connecticut 06720.

35. Chemical Rubber Company, CRC Lab Apparatus, The Chemical Rubber Co., Cleveland, Ohio, p. 20 (1969).

36. Eastman Organic Chemicals, A Division of Eastman Kodak Company, Rochester, 3, New York.

APPENDIX A

The experimental data for the report is given in the following reference:

Ukanwa, A. O., "Thermal Modeling of Phase Change Solidification in Thermal Control Devices Including Natural Convection Effects," Thesis No. T1422, Colorado School of Mines, Golden, Colorado, 1971

APPENDIX B

FORTRAN IV Computer Program "CONDET.F4" for solving either the conduction model or the combined conduction-convection model of solidification heat transfer.

This program was actually run on a P.D.P-10 digital computer via a time-sharing teletype.

Instructions For The Use of "CONDET.F4"

A. For program execution:

6=INPUT DEVICE 7=OUTPUT DEVICE

B. INPUT DEVICE (OR INPUT FILE)

The cold-plate (bottom-plate) temperature is assumed to be a polynomial in time (t) for $0 \leq t \leq TB$, and constant thereafter at a temperature TC. Follow the following steps (in order) in reading in the input data:

1. Consult the section on nomenclature in this text for terms used in the computer program. Then read in:

2. Line 1 (or card 1): Ambient temperature (or initial uniform temperature, TA); equilibrium temperature of solidification (TF); final constant cold-plate temperature (TC); finite-difference time increment (DELT); space increment in the x-direction (DELX); space increment in the y-direction (DELY); all in that order. Use free-floating point format of FORMAT 2.

3. Line 2 (or card 2): Time at which cold-plate temp-

erature becomes constant (TB); time at which program execution should be terminated (TAU).Use free-floating point format (FORMAT 2).

4. Line 3 (or card 3): Degree of polynomial fit of cold-plate temperature (K); number of finite-difference nodes, in the x direction (M), in the y direction (N); an integer (NT) that is negative or zero for conduction-model solution but positive non-zero for the combined conduction-convection model solution. Use free-integer format (FORMAT 3).

5. Line 4 (or card 4): Coefficients (D(I)) of polynomial fit to cold-plate temperature. (See the section on nomenclature for the definition of D(I) or D_i). Use free-floating point format (FORMAT 2).

6. Line 5 (or card 5): Liquid-phase thermal conductivity (AK); solid-phase thermal conductivity (SK); liquid-phase density (ROL); solid-phase density (ROS); liquid-phase specific heat (CPL); solid-phase specific heat (CPS); latent heat of solidification (HF). Use free-floating point format (FORMAT 2).

7. Line 6 (or card 6): Properties of material of the wall of the test cell: thermal conductivity (PK); density (ROP); specific heat (CPP). Use free-floating point format (FORMAT 2).

8. Line 7 (or card 7): Initial height of test-cell

cavity (AHO); width of test-cell cavity (AL); thickness of test-cell walls (AHP). Use free-floating point format (FORMAT 2).

A sample input file looks like this:

```
301.49,290.6,269.83,1.0,0.254,0.127
362,0,7200.0
1,81,31,3
301.49,-0.0874
0.02036,0.00037,0.755,0.833,0.506,0.505,56.67
0.000496,1.155,0.35
3.81,10.16,1.27
```

Note that the listed input file is for the combined conduction-convection model, since NT=3 is positive and non-zero. Also, according to this file, the cold-plate temperature is linear with time (K=1) until t=TB=362.0 when it stays constant at TC=269.83.

C. OUTPUT FILE

This program will print out

1. The time at which a node in the y-direction solidifies, the node itself and its horizontal location.

2. The temperature profile and the stream function profile of the entire test cell every 60 time steps. It starts with the cold plate (J=1), prints out all horizontal (I) values and then goes to J=2, and so on.

3. Adequate headings are printed to identify what is being printed out.

The print-out may be modified from the general format given in this program to any desirable format by changing lines 64 to 78 of CONDET.F4 as needed.

```
C            ************
C            *          *
C            *          *
C            *   [illegible]   *
C            *          *
C            *          *
C            ************
C  [illegible] - [illegible] FOR SOLIDIFICATION
C  [illegible]
      [illegible] T( [illegible] ),[illegible] ),[illegible] ),[illegible] ),S(1[illegible])
    2 F[illegible](7F)
      F[illegible]
      F[illegible] (1[illegible],2))
      F[illegible](/[illegible] =[illegible],3/)
      F[illegible]1.,2)
    7 RE[illegible] T[illegible],TF,T[illegible],DELT,[illegible], ELY
      RE[illegible]
      RE[illegible]
    1 K[illegible]=[illegible]
      R[illegible] ( (I),I=1,[illegible])
      R[illegible] S[illegible]L,[illegible]
      R[illegible]
      RE[illegible] A[illegible],AL,[illegible]
   1[illegible] F[illegible]=[illegible]626
      T[illegible]=[illegible]
      J[illegible]=[illegible]
      A[illegible]=[illegible]/([illegible])
      G[illegible]=1.[illegible]T*(1.[illegible]/([illegible]ELX**2)+1.[illegible]/([illegible]ELY**2))
    2 G[illegible]/([illegible]EL[illegible]**2)
      G[illegible]/([illegible]EL[illegible]**2)
      C[illegible]=[illegible]*DELY
      [illegible]
      G[illegible]=[illegible]T*([illegible]/([illegible]EL[illegible]**2)+A[illegible]/[illegible]ELY+[illegible])/C1
   2[illegible] G[illegible]/([illegible]*([illegible]X**2))
      G[illegible]=2.[illegible]T*[illegible]/(C[illegible]Y)
      G7=[illegible]/(A[illegible])
      A[illegible]=-2.[illegible]A/[illegible]
      R[illegible]=(1[illegible]/17.[illegible])**[illegible].5
   3[illegible] AL[illegible]=1.[illegible]*AL
      A[illegible]=[illegible]*AL
      AL[illegible]=[illegible]*AL
      [illegible] I=1,[illegible]
      D[illegible] J=[illegible]
      F[illegible](I,J)=[illegible]
   3[illegible] T(I,J)=TA
      D[illegible] I=[illegible]
      [illegible](I)=1
   3[illegible] C[illegible]
      [illegible]I=[illegible]
      [illegible]I=[illegible]
      [illegible]C=[illegible]
   4[illegible] T[illegible]=T[illegible]+DELT
      T[illegible]=T[illegible]-DELT
   4[illegible] IF([illegible]),[illegible]
      C[illegible]=[illegible]/(TF-T([illegible],1))
      A[illegible]/([illegible])
      G[illegible]=[illegible]T*(1.[illegible]/([illegible]X**2)+1.[illegible]/([illegible]Y**2)
      G[illegible]/([illegible]EL[illegible]**2)
    5 G[illegible]/([illegible]**2)
      [illegible] I=[illegible]
```

```
      [illegible]
      [illegible]
      I[illegible],[illegible], [illegible]
      [illegible]
      [illegible]
 [illegible] F[illegible]                    [illegible] HEIGHT [illegible]
      [illegible]
 [illegible] F[illegible],1[illegible])
      [illegible]
 [illegible] [illegible] I=1,
      [illegible] J=1,
 [illegible] T[illegible](I,J)
      IF([illegible] 7)
 [illegible] [illegible](7, ) [illegible]
      [illegible](7,67)
 67   F[illegible]'TEMPERATURE PROFILE'/)
      [illegible] J=1,
 [illegible] [illegible](7,[illegible]) (T(I,J),I=1, ),
      [illegible](7,7[illegible])
 71   F[illegible]'[illegible]STI[illegible]'/)
      [illegible] J=1,
 73   [illegible](7,[illegible]) ([illegible](I,J),I=1, )
      J[illegible]=
 75   IF([illegible].GE.T[illegible])GO TO [illegible]74
      [illegible]
 77   IF([illegible].[illegible].TA[illegible])GO TO [illegible]5
 7[illegible]  J[illegible]
      [illegible] I=2, I
      IF([illegible](I).GE. I)[illegible] TO [illegible]72
 [illegible]  C[illegible]
      J=1
      [illegible] I=1,
      IF([illegible].[illegible],T[illegible])G[illegible]
 [illegible]  C[illegible]= [illegible](I)
      D[illegible] L=1,[illegible]
      LL= I-L
      C[illegible]=[illegible]*[illegible]+[illegible](LL)
 [illegible]9 C[illegible]
      T(I,J)=C[illegible]
      G[illegible]
 92   T(I,J)=T[illegible]
 93   C[illegible]
      J=
      D[illegible] I=[illegible]
 [illegible] T(I,[illegible])=[illegible]*T[illegible](I,J)+[illegible]*(T[illegible](I-1,J)+T[illegible](I+1,J))+[illegible]*T[illegible](I,J-1)+G7*TA
      D[illegible] I=2, I
      I[illegible]= [illegible](I)
      IF(I[illegible].LT.2)[illegible] TO [illegible]
      D[illegible] J=2,I[illegible]
      T(I,J)=T[illegible](I,J)*[illegible]+[illegible]*(T[illegible](I-1,J)+T[illegible](I+1,J))+[illegible]35*(T[illegible](I,J-1)+T[illegible](I,
     1J+1))
 1[illegible] C[illegible]
      I[illegible]= [illegible](I)
      IF(I[illegible].LT.2)[illegible] TO [illegible]
      I=[illegible]
      D[illegible] J=2,I
 1[illegible] T(I,J)=[illegible]*T[illegible](I,J)+[illegible]*T[illegible](I+1,J)*2.[illegible]+[illegible]35*(T[illegible](I,J-1)+T[illegible](I,J+1))
 1[illegible] I[illegible]= [illegible]
      I[illegible].LT.2)[illegible]114
      I=
```

```
      [illegible]
 11[illegible] T(I,[illegible])=[illegible](I,[illegible] [illegible]*T[illegible](I-[illegible],J)*[illegible], +[illegible]*(T (I,J-1)+T (I,J+1))
 1[illegible]  J[illegible]=[illegible])+1
      I=
      [illegible],[illegible]=[illegible],[illegible]
 117  T(I,[illegible])=T (I,[illegible])*[illegible]+[illegible]*T[illegible](I+[illegible],J)*[illegible], +[illegible]*(T (I,J+1)+T[illegible](I,J-1))
      I=
      [illegible]=[illegible])+[illegible]
      [illegible] J=[illegible], I
 12[illegible] T([illegible],J)=T (I,J)*[illegible]+[illegible]*T[illegible](I-[illegible],J)*[illegible], +[illegible]*(T[illegible](I,J-1)+T[illegible](I,J+1))
      [illegible] I=[illegible], [illegible]
      K[illegible]=[illegible](I)+1
      [illegible] J=[illegible], I
 12[illegible] T(I,J)=[illegible]*T (I,J)+[illegible]*(T[illegible](I,J+1)+T[illegible](I,J-1))+[illegible]*(T[illegible](I-1,J)+T[illegible](I+
     21,J))
      T([illegible], )=[illegible]*T (1, )+[illegible]*[illegible](1, I)+2,[illegible]*T[illegible](2, )+[illegible]*TA
      T( , )=[illegible]*T ( , )+[illegible]*[illegible]( , I)+2,[illegible]*T[illegible]( I, )+[illegible]*TA
      IF( [illegible])4[illegible],43,1[illegible]
 13[illegible] D[illegible] 1[illegible]7 I=2, I
      K[illegible]=[illegible](I)+1
      I[illegible]=I-[illegible]
      [illegible]=[illegible](I[illegible])
      X[illegible]=[illegible]*[illegible]
 1[illegible] D[illegible] [illegible]7 J=[illegible], I
      IF([illegible]) [illegible] 14
      [illegible]=[illegible]([illegible](I))
      A[illegible]=[illegible]*(P[illegible]I-[illegible], )
      G[illegible] T[illegible] 1[illegible]
 1[illegible] A[illegible]=[illegible]
 141  JL=J-[illegible]
      P[illegible]=[illegible](JL)
      Y=[illegible]*([illegible]JL+[illegible],[illegible])
      [illegible]=Y/[illegible]
 14[illegible] IF([illegible].GT.AL[illegible])[illegible] T[illegible] 15[illegible]
      X[illegible]=[illegible]
      AL =[illegible]1
      A =-[illegible]*[illegible] I/[illegible]
      DF1=[illegible]*F1
 15[illegible] D[illegible]=[illegible]*[illegible]I/A[illegible]
      P[illegible]I(I,J)=-[illegible]*[illegible]*[illegible]*SI[illegible]([illegible]1)*SI[illegible](DF1)/PI
      U[illegible]=[illegible]*[illegible]([illegible]1)*[illegible]([illegible]1)
      V[illegible]=[illegible]*[illegible]([illegible]1)*SI[illegible]([illegible])
      G[illegible] T[illegible] 16[illegible]
 155  X[illegible]=[illegible]-A[illegible]+AL3
      A[illegible]=-[illegible]*[illegible]
      AL =[illegible]3
      D[illegible]=[illegible]/A[illegible]I
      D[illegible]=[illegible]*[illegible]/[illegible]I
 16[illegible] D[illegible]=[illegible]*(AL[illegible]-[illegible])/A[illegible]I
      P[illegible]I(I,J)=-[illegible]*A[illegible]I*([illegible]F-[illegible]*([illegible]F**3)+([illegible]F**4))*(1.[illegible]-(SINH(DD[illegible])+SINH(DD
     3))/[illegible]I[illegible]([illegible]L))
      U[illegible]=A[illegible]*([illegible], -[illegible],[illegible]*(DF**2)+4,[illegible]*([illegible]F**3))*(1. -(SI[illegible](DD )+SI[illegible](DD))/SI[illegible]
     [illegible]([illegible]L))
 16[illegible] V[illegible]=[illegible]*([illegible]F-[illegible], [illegible]*([illegible]F**2)+([illegible]F**4))*([illegible]( ) )-[illegible](DD))/SINH(DDL)
 16[illegible] [illegible]=[illegible]*(T (I,J+1)-T[illegible](I,J-1))/DELY
      [illegible]=[illegible]*(T[illegible](I+1,J)-T (I-1,J))/DELX
      T[illegible]=[illegible]*([illegible]*[illegible]*[illegible]2)
      T(I,J)=T(I,J)-T[illegible]
 17[illegible] [illegible]
      G[illegible] T[illegible] 43
```

APPENDIX C: OTHER THEORETICAL CONSIDERATIONS

If one attempts to solve the vorticity equation (Eq.11) or the velocity equations (Eq.8) by central-difference methods, one finds that the following stability requirements must be satisfied:

$$1 - 2\nu\Delta t(1/(\Delta x)^2 + 1/(\Delta y)^2) \geq 0 \qquad \text{(C-1)}$$

$$|u(i,j)| \leq 2\nu/\Delta x \qquad \text{(C-2)}$$

$$|v(i,j)| \leq 2\nu/\Delta y \qquad \text{(C-3)}$$

When the vorticity or the velocity equations are solved conjointly with the temperature equation (Eq.5), the conditions of Equation (C-1) to Equation (C-3) must be satisfied conjointly with the conditions of Equation (39) and Equations (41). The most restrictive conditions are used to evaluate maximum time increment (Δt) and velocities allowable by stability requirements.

For our test material, $\nu > \lambda_L$; hence, Equation (C-1) rather than Equation (39) would determine Δt_{max}, but the allowable maximum velocities would be determined by Equation (41) rather than by Equation (C-2) or Equation (C-3).

At the first time step, every term except the gravity term in Equation (11) or Equations (8) would be zero. Thus, from Equations (8), the velocities obtained at the first time step would be:

$$u'(i,j) = -\frac{\beta g \Delta t}{\bar{d}_L}\left(T(i,j) - \bar{T} \right) \sin\alpha \qquad \text{(C-4)}$$

$$v'(i,j) = -\frac{\beta g \Delta t}{\bar{d}_L} \left(T(i,j) - \bar{T} \right) \cos \alpha \qquad (C\text{-}5)$$

The values given by Equations (C-4) and (C-5) must satisfy the conditions for stability given by Equations (41), (C-2), and (C-3). But, with experimentally-observed values, the temperature difference, $T(i,j)-\bar{T}$, is such that the stability requirements of Equations (41), (C-2), and (C-3) are violated even for $\Delta t \leq 0.05$ sec and $\Delta x = 0.0635$ cm. It is very hard to complete stable computer solutions for values smaller than these. Yet, in order to get stable solutions of the velocity and the temperature equations at the very first time step, one needs a time-step size much smaller than 0.05 sec. Even with such small time steps, it would get more difficult to satisfy the stability requirements as the velocities would increase with subsequent time steps. This was the problem that forced us to use approximate velocity profiles for our study in stead of solving the complete velocity equations by finite-difference methods.